

SOLID ACID CATALYSTS:
APPLICATIONS AND CHARACTERIZATION

By

NICHOLAS E. KOB

A DISSERTATION PRESENTED TO THE GRADUATE SCHOOL
OF THE UNIVERSITY OF FLORIDA IN PARTIAL FULFILLMENT
OF THE REQUIREMENTS FOR THE DEGREE OF
DOCTOR OF PHILOSOPHY

UNIVERSITY OF FLORIDA

1996

ACKNOWLEDGMENTS

My journey through graduate school has been like a roller coaster ride, a few twists, drops, and turns, but as a whole a incredibly enjoyable and unforgettable experience that I would like to do over and over if I could. As is the case with a roller coaster ride, my life has consisted of separate turns, parts if you will, that have defined who I am today. My undergraduate years spent in California were a time of unsure life and career goals. These years will always be remembered as my fondest years due to my friends and experiences at Disneyland and my two best friends Bob "turbo" Peterson and Steve "the chicken" Okabe. I want to thank Bob and Steve for all of their friendship and guidance. I will never forget our times in the apartment, over the line, and working out, I wish I could do it all over again.

From California fate took me to Illinois where the second part of my life began at Illinois State University. Here I made new friends and really learned chemistry for the first time. My professor Dr. J. House was not only a mentor but a wonderful person and friend. If all the other people in the world were like him the world would be a much better place. The friends I made included five people with whom I would spend the rest of my graduate school career with: Troy Halverson, Dave Kage, Scott Kassel, Rich Burton, and Eugene Wagner. Where did all the time go? I will never forget Femley Hall, The Pub, dollar import night and Rockys lunches.

After receiving my masters, I chose to go to University of Florida to obtain my Ph.D., but I almost chose otherwise. My professor here, Dr. Russell Drago, is the brightest person I have ever met, it is no wonder he is a famous chemist. Thanks Doc for all the guidance in chemistry, you taught me chemistry and made it fun, but you need to work on playing "slow" tennis. The transition to the south was easy because "the ISU crew" all came together. I still cannot believe that they accepted all of us. These past three years have flown by, and I can't bear to think of how my life will change without the "ISU crew" around. The past five years have been the most fun and enlightening of my life. I will never forget visiting UF with Dave, the "Nicki incident", the parties, softball and football teams, and all the Drago group. I would wish you all luck, but after spending all this time with you I realize that you don't need it. Never loose touch and never forget the times we had cause I never will.

The one constant through all the chapters of my life has been my family. This dissertation is dedicated to my Mom and Dad, and I am so proud of how hard Kim is working towards her goal, all those fights as kids taught you how to fight for what you want. A special thanks to Grandpa Kob who I know is looking down on me, you were right going for my Ph.D. was the right move.

I am sure my future holds more of the same roller coaster type turns, and bumps, but with Jennie everything will work out fine. I would like to thank Jennie for all of her support through all the uncertainty.

TABLE OF CONTENTS

| | <u>page</u> |
|---|-------------|
| ACKNOWLEDGMENTS | iv |
| LIST OF TABLES | vi |
| LIST OF FIGURES | vii |
| ABSTRACT | viii |
| CHAPTERS | |
| 1 GENERAL INTRODUCTION TO SOLID ACID CATALYSIS | 1 |
| Why Solid Acids are Important | 1 |
| Types of Solid Acids and the Source of Their Acidity..... | 2 |
| Methods of Determining the Strength of Solid Acids..... | 5 |
| Hydrocarbon Conversion Mechanisms Using Solid Acid Catalysts..... | 12 |
| Surface Science Methods..... | 18 |
| Overview of Proceeding Chapters..... | 22 |
| 2 ACIDITY AND REACTIVITY OF SULFATED ZIRCONIA..... | 24 |
| Introduction..... | 24 |
| Experimental..... | 27 |
| Results and Discussion..... | 29 |
| Conclusion..... | 37 |
| 3 CHARACTERIZATION OF THE ACIDITY OF SG- AlCl_3 | 42 |
| Introduction..... | 42 |
| Experimental..... | 44 |
| Results and Discussion..... | 46 |
| Conclusion..... | 53 |

| | | |
|--------------------------|---|-----|
| 4 | SYNTHESIS OF CAPROLACTAM USING SG-W..... | 62 |
| | Introduction..... | 62 |
| | Experimental..... | 63 |
| | Results and Discussion..... | 65 |
| | Conclusion..... | 80 |
| 5 | HYDROGENATION OF BENZENE USING SG-W-Pt..... | 91 |
| | Introduction..... | 91 |
| | Experimental..... | 92 |
| | Results and Discussion..... | 93 |
| | Conclusion..... | 97 |
| 6 | SYNTHESIS AND CHARACTERIZATION OF SG-WS..... | 100 |
| | Introduction..... | 100 |
| | Experimental..... | 101 |
| | Results and Discussion..... | 103 |
| | Conclusion..... | 109 |
| 7 | SOLID ACID ALKYLATION OF ISOBUTANE..... | 114 |
| | Introduction..... | 114 |
| | Experimental..... | 115 |
| | Results and Discussion..... | 117 |
| | Conclusion..... | 127 |
| 8 | GENERAL CONCLUSION..... | 133 |
| APPENDICES | | |
| A | CAL-AD PROCEDURE FOR SOLID ACID ANALYSIS..... | 137 |
| B | GAS CHROMATOGRAPHIC METHODS OF ANALYSIS..... | 141 |
| C | CAL-AD DATA FOR SOLID ACID CATALYSTS..... | 143 |
| REFERENCES..... | | 147 |
| BIOGRAPHICAL SKETCH..... | | 155 |

LIST OF TABLES

| <u>Table</u> | <u>page</u> |
|--|-------------|
| 2-1 Cal-ad Analysis of Sulfated Zirconia (SZ)..... | 32 |
| 2-2 ΔH_1 Values for Other Solid Acid Catalysts..... | 33 |
| 3-1 BET Analysis for Davison Silica Gel and SG- $AlCl_3$ | 47 |
| 3-2 Strength of Solid Acids..... | 50 |
| 3-3 ^{13}C Acetone Shifts on Solid Acids..... | 52 |
| 4-1 XPS Intensity Ratios W_{4f}/Si_{2p} of Prepared Catalysts..... | 69 |
| 4-2 Cal-Ad Analysis of Solid Acids..... | 73 |
| 4-3 Effect of Oxime Solvent on Amount of Carbon on Used SG-W's After 20 hrs..... | 75 |
| 4-4 Cal-Ad Analysis of Fresh and Regenerated SG-W Catalysts..... | 77 |
| 4-5 BET Analysis for Different Silica Gels Used..... | 78 |
| 6-1A Cal-Ad Analysis for SG-WS Catalyst..... | 104 |
| 6-1B ΔH_1 Values for Various Solid Acids..... | 104 |
| 6-2 BET Analysis of SG-W, and SG-WS Catalysts..... | 106 |
| 6-3 XPS Peak Positions and Peak Area's for SG-WS-Pt Catalyst..... | 107 |
| 7-1A Cal-Ad Analysis for SG-WS Catalyst..... | 118 |
| 7-1B ΔH_1 Values for Various Solid Acids..... | 119 |
| 7-2 TON for Alkylation of Isobutane With 2 Butene for Solid Acids..... | 120 |
| 7-3 Solid Acid Catalysts RON..... | 122 |

| | | |
|-----|---|-----|
| 7-4 | Cal-Ad Analysis of Ramp Regenerated SG-WS Catalyst..... | 125 |
| 7-5 | Regenerated and Resulfated SG-WS Catalyst..... | 126 |

LIST OF FIGURES

| <u>Figure</u> | <u>page</u> |
|---|-------------|
| 1-1 Bronsted Acid Sites on a Metal Halide Acid Catalyst..... | 2 |
| 1-2 Zeolite Bronsted Acidity..... | 3 |
| 1-3 Example of Bronsted Acidity Generation on Mixed Oxides..... | 4 |
| 1-4 Generation of Carbenium Ion..... | 13 |
| 1-5 Oxidation of Alkane to form a Carbenium Ion..... | 14 |
| 1-6 Loss of Proton from Carbenium Ion..... | 14 |
| 1-7 Hydride Shift in Carbenium Ions..... | 15 |
| 1-8 Methyl Shift in Carbenium Ion..... | 15 |
| 1-9 Hydride Abstraction by Carbenium Ion..... | 15 |
| 1-10 Addition of Carbenium to Olefin..... | 16 |
| 1-11 β Scission of Carbenium Ion..... | 16 |
| 1-12 Alkylation of Isobutane..... | 17 |
| 2-1 Pyridine Adsorption on Sulfated Zirconia..... | 39 |
| 2-2 $-\Delta H_{\text{ads}}$ for Sulfated Zirconia..... | 40 |
| 2-3 Calorimetric Titration of Sulfated Zirconias..... | 41 |
| 3-1 SG- AlCl_3 Catalyst..... | 54 |
| 3-2 ^{27}Al NMR Spectrum of SG- AlCl_3 | 55 |

| | | |
|-----|---|-----|
| 3-3 | ^{15}N NMR Spectrum of Pyridine on SG- AlCl_2 | 56 |
| 3-4 | ^{31}P NMR Spectrum of TMP on SG- AlCl_2 | 57 |
| 3-5 | ^1H NMR Spectrum of SG- AlCl_2 | 58 |
| 3-6 | SG- AlCl_2 Calorimetric Titrations..... | 59 |
| 3-7 | Calorimetric Titration of Used SG- AlCl_2 | 60 |
| 3-8 | ^{13}C NMR of Acetone on SG- AlCl_2 | 61 |
| 4-1 | SEM of SG-W..... | 82 |
| 4-2 | SG-W Tungsten 4f XPS..... | 83 |
| 4-3 | Infrared Spectrum of SG-W..... | 84 |
| 4-4 | Powder XRD of SG-W..... | 85 |
| 4-5 | Caprolactam Synthesis on SG-W Using Benzene Solvent..... | 86 |
| 4-6 | Effect of Solvent on Caprolactam Selectivity..... | 87 |
| 4-7 | Effect of Carbon Deposits on Caprolactam Selectivity..... | 88 |
| 4-8 | SEM of Used SG-W Catalyst..... | 89 |
| 4-9 | Analysis of Different Silicas..... | 90 |
| 5-1 | Benzene Hydrogenation on SG-W-Pt..... | 98 |
| 5-2 | Effect of Sulfur on Benzene Hydrogenation..... | 99 |
| 6-1 | SEM of SG-WS Catalyst..... | 110 |
| 6-2 | SG-WS Tungsten 4f XPS Spectrum..... | 111 |
| 6-3 | EPR Spectrum of Hydrogen Treated SG-WS and SG-WS-Pt..... | 112 |
| 6-4 | Heptane Conversion Using SG-WS and SG-WS-Pt..... | 113 |
| 7-1 | Alkylation of Isobutane Using Solid Acids..... | 128 |

| | |
|---|-----|
| 7-2 Proton Distributions for Solid Acids..... | 129 |
| 7-3 Regeneration of Solid Acids in the Alkylation Reaction..... | 130 |
| 7-4 SEM at 10,000X Magnification of Fresh and Used SG-WS..... | 131 |
| 7-5 SEM at 500X Magnification of Used SG-WS..... | 132 |

Abstract of Dissertation Presented to the Graduate School
of the University of Florida in Partial Fulfillment of the
Requirements for the Degree of Doctor of Philosophy

SOLID ACID CATALYSTS:
APPLICATIONS AND CHARACTERIZATION

By

NICHOLAS E. KOB

DECEMBER, 1996

Chairman: Dr. Russell S. Drago
Co-Chair: Dr. Vaneica Young
Major Department: Chemistry

Design and characterization of solid acid catalysts are essential due to environmental concerns with current commercial liquid acid processes based on HF and H₂SO₄. Solid acid catalyzed processes offer several advantages over liquid acids, most notable their potential to be regenerated. There currently exists no accurate method to evaluate the acidity of solid acids, resulting in the inability to successfully correlate acidity and reactivity. Such a correlation would provide researchers with a simple screening method when developing solid acid catalysts.

The development and characterization of several new solid acids, their activity in acid catalyzed reactions, and catalysts for the hydrogenation of benzene will be discussed. The acidity characterization of a aluminum chloride supported silica gel catalyst (SG-AlCl₃), and sulfated zirconia was performed. The SG-AlCl₃ catalyst was found to be a superacid with an acidity of 51 kcal/mole when titrated with pyridine, but sulfated zirconia was not found to be a superacid.

In particular, a silica supported tungsten oxide catalyst (SG-W), and an acid promoted SG-W catalyst, referred to as SG-WS, were developed and characterized. The SG-W catalyst was used for the production of caprolactam from cyclohexanone oxime in a flow reactor. A conversion of 99% of the oxime with over 90% selectivity to caprolactam was attained without significant deactivation for 40 hours. A thorough study of the deactivation and regeneration of the catalyst was performed, as well as the effects of reaction temperature, contact time, support, and cyclohexanone oxime delivery solvent on the conversion and selectivity.

The SG-WS catalyst was shown to be a strong acid, comparable to HZSM-5, and its activity for the alkylation of isobutane with 2-butene was studied. The SG-WS catalyst was shown to yield more turn overs per acid site than sulfated zirconia, HZSM-5, HY, and sulfuric acid. Extensive studies on the mechanism of deactivation and regeneration were performed on the SG-WS catalyst. From these studies and the acidity characterization, a correlation of the reactivity and acidity was established for the various solid acids tested.

CHAPTER 1 GENERAL INTRODUCTION TO SOLID ACID CATALYSIS

Why Solid Acids are Important

Every year millions of dollars worth of goods are manufactured with the use of acid catalysts.¹ Acid catalyzed reactions are the most important reactions involved in the rearrangement of hydrocarbons.² These reactions include the isomerization of alkanes, and alkenes, cracking, alkylation, synthesis of chemical intermediates and numerous other reactions. However, many of the current industrial processes are based on liquid acids such as HF and H₂SO₄. The use of liquid acids presents several environmental and safety problems.²

Liquid acids are harmful corrosive and potentially toxic substances making their use a safety risk to personnel. For example, HF, when used for the alkylation of isobutane with butene, has led to plant explosions.³ Other issues regarding liquid acids such as problems with storage, transportation and handling have been raised.⁴ In addition to the safety concerns, environmental problems such as disposal, and fundamental problems such as the costly separation of products from the liquid acid have led to the search for solid acids to replace the liquid acid catalysts.⁵ Solid acids alleviate many of the problems presented by liquid acids, which has made them a “hot” area of research for industry and academics.

Solid acids catalysts work on the same principle as liquid acids. They have the ability to donate hydrogen ions or protons, or accept electron pairs. Protons are released from ionizable hydroxyl groups in which the bond between oxygen and hydrogen is severed to yield O^- and H^+ . This ability to lend protons makes solid acids a viable alternative to liquid acids for hydrocarbon rearrangement reactions.

Types of Solid Acids and the Source of Their Acidity

Halogen Based Solid Acids

Metal halides complexed with certain compounds, such as supported on silica gel or alumina, exhibit strong acid characteristics. This has been evidenced by the isomerization of hydrocarbons at room temperature or below.⁶ In particular, $AlCl_3$, SbF_5 , and BF_3 , when supported on a porous solid support, are among the strongest solid acids known. These supported halide acids are binary acids (conjugate Bronsted-Lewis acids), and their acidity is attributed to the enhanced character of the Lewis and Bronsted sites of the support created by the coordination of the electron withdrawing metal halide to an adjacent oxygen atom as shown in Figure 1-1.

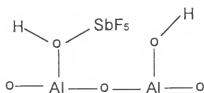


Figure 1-1: Bronsted Acid Sites on a Metal Halide Acid Catalyst.

Zeolites

Fundamentally, zeolites are metal oxide based solid acids, but due to their highly ordered structures, they are classified into their own group. Zeolites are highly crystalline hydrated aluminosilicates that have a uniform pore structure whose size and shape depends on many preparation conditions.⁷ The structure of zeolites consists of a three-dimensional framework of SiO_4 and AlO_4 tetrahedra linked by their corners, each of which contains a silicon or aluminum atom in the center. The number of cations (hydrogen for acid zeolites) is determined by the number of AlO_4 tetrahedra included in the framework. This arises from the substitution of Al^{+3} for Si^{+4} creating a negative charge which is compensated for by a cation.

Most industrial applications of zeolites are acid catalyzed reactions, such as the cracking of hydrocarbons. This means that the activity results from Bronsted acid sites arising from hydroxyls within the zeolite pore structure as shown in Figure 1-2.

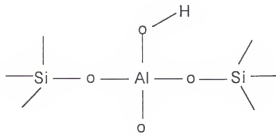


Figure 1-2: Zeolite Bronsted Acidity.

The proton is associated with the negatively charged framework oxygen linked to the aluminum tetrahedra. The protons have mobility along the framework and can be lost as water by dehydration at temperatures around 500°C . The strength of zeolite acid sites

differs from zeolite to zeolite and is linked to the bond angles, pore structure, and Si:Al ratio. It is generally accepted that the most acidic zeolite is HZSM-5. Other acidic zeolites with acidity less than HZSM-5 are Beta, faujasites (HY) and Mordenite.⁸

Mixed Oxide Solid Acids

It has been shown that the catalytic properties and acidity of oxide catalysts can be varied by addition of another oxide resulting in a mixed oxide catalyst.⁹ The generation of the new properties are attributed to interactions between the two oxides. A hypothesis regarding the generation of enhanced acidity of binary oxides has been proposed by Tanabe.^{9,10} According to the hypothesis, Bronsted acidity is generated by an excess of negative charge and Lewis acidity from an excess of positive charge resulting from the interaction of the binary oxides. The structure of the mixed oxides is pictured according to the following rules: 1) the coordination numbers of the two metal oxides are maintained when mixed; 2) The coordination number of oxygen of the major component metal oxide (the support) is retained. An example using tungsten oxide (WO_3) supported on silica (SiO_2) is shown in Figure 1-3.

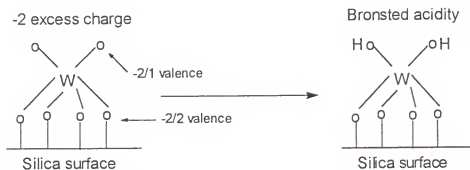


Figure 1-3: Example of Bronsted Acidity Generation on Mixed Oxides.

The six positive charges of tungsten are distributed to 6 bonds, giving a 6/6 valence to each bond. While for 4 of the oxygen atoms of tungsten the -2 charge is distributed to two bonds for a valence of -2/2 to each bond, for the other 2 oxygen atoms the -2 charge is distributed to 1 bond for a -2/1 valence to each bond. The charge difference as a result of mixing the metal oxides is $(6/6 - 2/2 - 2) \times 6 = -2$ excess charge. This causes the creation of Bronsted sites to accommodate the negative charge, as shown in Figure 1-3 results.

Methods of Determining the Strength of Solid Acids

The acid strength of solid acids is important to characterize for several reasons. First, reactions that are acid catalyzed differ in the required acid strength to catalyze the reaction. For example, low temperature alkylation of isobutane with an alkene requires a very strong acid to protonate the alkene due to the low reaction temperature. On the other hand dehydration of alcohols such as propanol requires a weak acid to catalyze the reaction. Therefore, if a rational catalyst selection is to be made, a characterization of the solid acids strength must be accurately determined. Second, not only the reactivity but also the selectivity of the acid catalyzed reaction is determined by the catalysts acid strength. For example, in the isomerization of heptane a strong acid is necessary to form the carbenium ion, but if too strong an acid catalyst is used, then cracking (taking heptane to lower alkanes) of the heptane will occur and the selectivity of the reaction for isomerization will decrease. In this case an accurate assessment of the strength of the acid catalyst is necessary if the desired product (iso-heptane) is to be made. Finally, during the course of a reaction, the acidic strength of the catalyst may change as a result of deactivation, causing a change in the reactivity and selectivity in the reaction. In this case

a accurate measurement of the catalyst before and after reaction will show that the loss of acidity caused the change in reactivity.

However, measurement of solid acid catalyst strength is elusive and not easily determined. Although solid acids are based upon the same principle as liquid acids, the ability to donate H^+ , their characterization is much more difficult. This difficulty arises for several reasons. Unlike liquid acids that possess homogeneous acid sites, solid acids have surfaces that are heterogeneous in their acidity. That is, not every acid site has the same strength on the surface of the solid acid. This presents a unique challenge in trying to determine the strength of a solid acid. The number of sites is just as important as the strength, for example if a certain acid strength is required for a reaction then the solid acid must not only posses this strength, but an appreciable number of acid sites with this strength. Further, quantification of the number and strength of acid sites present will aid in deactivation and regeneration studies. Unlike liquid acids, solid acids are able to surface stabilize adducts creating dispersion interactions which complicates the determination of the adduct strength. Given all these considerations, a solid acid analysis method must be able to quantify the number and strength of acid sites as well as addressing the problems associated with dispersion interactions of probe molecules.

To meet the need of determining solid acid strength, numerous analytical techniques have been used.¹¹ The most common technique employed is the use of acid base indicators. In this method, the strength of a solid acid is determined by its ability to change a neutral base adsorbed on the solid into its conjugate acid form,¹² during which a color change is observed. If a color change is observed, then at least some of the acid sites are assumed to have a pK_a value equal or greater than that of the indicator used.

The technique is based on the determination of an acids strength by reaction with probe bases and pKa. This technique is commonly referred to as the Hammett indicator method, and its acidity scale is based on the use of a Hammett acidity function (Ho) rather than pKa's. The definition of the acidity function is shown in Equation 1-1.

$$\text{(Equation 1-1)} \quad H_o = (pK_{BH^+}) - \log [BH^+]/[B]$$

A measurement of the distribution of acid sites on the catalyst is done by titration of the solid with a strong base using a series of Hammett color indicators. Despite its popularity as a method for determining solid catalyst acidity, several serious problems exist with the technique. First, the use of these indicator methods for liquid acids requires a very large excess of acid over indicator, and that the conjugate acid of the indicator exist as free ions. However, on a solid where acid sites are present in individual isolated sites, the interaction with a probe base is stoichiometric. When a deficit of base is added, the other non-interacting acid sites cannot help to stabilize the anion formed at the reaction site as liquid acids do. This results in the formation of tight ion pairs of the indicator and the acid site, thereby not meeting the criteria of a free ion. Also, this procedure assumes that equilibrium is attained at all times, which is not necessarily the case since the strongest sites may irreversibly bind the probe or they may become attached to nonacidic sites by surface stabilization. The method also does not distinguish between Bronsted and Lewis sites, present on the surface. Finally, this method does not quantify the number of acid sites, which is very important in the characterization of a solid acid. The Ho values obtained do not reflect the acid site strength, type, or number, as specified as being

required to accurately characterize a solid acid. The appeal of this technique undoubtedly comes from its ease and simplicity. However, the values obtained can only be used as a “quick” approximation of acidic strength.

Another commonly used method involves infrared spectroscopic studies of adsorbed basic probes.¹³ When the basic probe interacts with the solid acid an infrared shift occurs. This shift contains information about the type of adduct formed. For example, when pyridine is used as the probe it can be bound to the solid acid coordinately at 1440cm^{-1} or hydrogen bound at 1599 cm^{-1} or by proton transfer from a Bronsted site (pyridinium ion) at 1540 cm^{-1} . This method qualitatively determines the presence of Lewis and Bronsted acid sites. However, quantification of the number of sites is questionable due to the nature of the infrared experiment. Differentiation of the strength of solid acids is said to be determined by the magnitude of the infrared shift of the adsorbed probe.^{13a} For example, aluminum chloride, which is a strong acid, gives an acetonitrile CN adduct frequency of 2330cm^{-1} (uncomplexed acetonitrile CN is at 2266 cm^{-1}). A weak acid such as Zn^{+2} gives a CN shift of 2306 cm^{-1} . Differentiation of the strength of various solid acids is possible only when sufficiently large differences exist in the solid acids acidities as was the case above. Therefore, the infrared method is a very good quick method to get a approximate indication of the type and strength of sites present on the solid acid. However, this method does not allow accurate determination of either strength or number.

Solid acid acidity has also been measured using heat of adsorption and temperature programmed desorption of bases.¹⁴ Temperature programmed desorption (TPD) provides an acid strength distribution as a function of temperature through the determination of

base molecule desorption. By quantifying the amount of basic probe desorbing as a function of temperature, the number and strength of a distribution of acid sites is obtained for the solid catalyst. However, the numbers obtained are questionable because desorption channels for different probe molecules on solid acid catalysts are different. Therefore, it is claimed that no basic probe selectively probes only the acid site in the desorption measurement.

A new promising technique that has emerged is the use of nuclear magnetic resonance (NMR) to probe the acidity of solids.¹⁵ The technique follows the formation of chemical intermediates and products (carbenium ions) as a probe is adsorbed onto the solid acid catalyst and reaction takes place. This technique can be done at various temperatures using very small amounts of probe. A scale of relative acidity was constructed based on ^{13}C chemical shifts of acetone upon adduct formation.¹⁵ The advantage of this method is its ability to provide information not only about strength and number of acid sites but also about reaction products and intermediates that are formed. From these measurement mechanistic aspects of the reaction can be addressed. It is my belief that information from these types of measurements are best used as supplemental to other methods of solid acid characterization.

The application of calorimetry for solid acidity measurement by titrating the solid with a probe (liquid or gaseous) has been done.¹⁶ Measurement of the heat flow upon addition of a basic probe provides the surface site distribution by using the relationship between the differential adsorption heat and the quantity of base added. This technique has been adapted to microcalorimetry where small amounts of basic probe can be added in order to look at very small numbers of acid sites. This technique has the advantage of

allowing the simultaneous determination of the strength and number of acid sites present on the solid. This determination is based on the enthalpy of adduct formation, which is the appropriate measure of donor-acceptor bonding. However, in any calorimetric equilibria that involves gas-solid equilibria, the enthalpies contain contributions from a donor-acceptor interaction as well as a dispersion component. This dispersion component causes the measured enthalpy of donor-acceptor adduct formation to be larger than its true value. Many times these dispersion interactions contribute significantly to the measured enthalpy resulting in large errors in the measured enthalpy of adduct formation.¹⁷ Further, this error is not the same for different solid acid catalysts. That is, the dispersion contribution for adsorption of pyridine will differ from solid acid to solid acid. Many times the TPD or microcalorimetric measurements are done at elevated temperatures, which causes the equilibrium constants for the different strength acid sites to approach one another. This results in some of the basic probe going onto both the strong and weak sites, and hence an average enthalpy (strength) for both sites is found instead of the true value for the strongest site. For these reasons, the accurate characterization of solid acid acidity can not be acquired from this method.

The limitations for completely characterizing solid acid catalysts has led to the development of a new method of analysis. This method known as Cal-ad is based on enthalpies of interaction upon adduct formation.¹⁸ The method involves slurring a solid acid in a non-interacting solvent (cyclohexane) which is reacted with a known amount of added basic probe while stirring. After each injection of basic probe solution, the heat evolved is measured. This heat is then used to determine the enthalpy of adduct formation. In the cal-ad analysis, an adsorption isotherm is measured over the range of

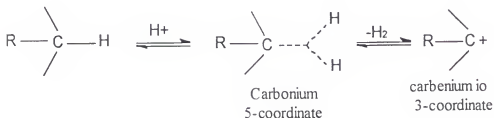
base additions used in the calorimetric titration. The combined calorimetric and adsorption data are analyzed to determine K 's (equilibrium constants), n 's (moles of site), and ΔH 's (enthalpies) for the solid acid catalyst. This method also allows for the determination of Bronsted and Lewis sites by varying the basic probe chosen. This is best accomplished by using pyridine (which will titrate both Lewis and Bronsted sites) and 2,6 lutidine (titrates Bronsted sites) in separate cal-ad analysis. Further, the cal-ad measurements are carried out in a hydrocarbon solvent (cyclohexane) whose molecules are close in molecular mass to those of the donor (pyridine) to cancel out the dispersion component. The enthalpies found are due exclusively to that of adduct formation and are accurate to ± 1 kcal/mole. The method can characterize fresh catalysts, evaluate deactivated catalysts, and monitor catalyst regeneration. This method is superior to the other techniques described for evaluating the acidity of solid acid catalysts and will be used in this dissertation for evaluation of solid acid catalysts. One criticism which could be raised with this technique is that measurements are made at temperatures which are usually well below those of catalytic reaction conditions. Therefore, one can argue that the characterization found using cal-ad is not representative of the surface of the catalyst at reaction temperatures. However, since no such method exists that can evaluate accurately the acidity of solid acid catalysts under reaction conditions, the cal-ad technique offers the best alternative. However, due to uncertainty with the error determination procedure used by the cal-ad program no errors in n or K are assigned, but the numbers reported are significant.

Hydrocarbon Conversion Mechanisms Using Solid Acid Catalysts

The most extensive use and potential application of solid acid catalysts is for petroleum-related hydrocarbon rearrangement reactions. Heterogeneous catalysts account for the production of the major part of petroleum and petrochemical products.¹⁹

Petrochemicals are organic compounds derived from natural gas or crude oils. The petrochemical field is a very diversified one. Several intermediates and chemicals from petroleum are used in specialized organic industries such as pharmaceuticals, pesticides, explosives, and fragrances.

It is generally agreed that acid-catalyzed hydrocarbon conversion reactions proceed by way of highly reactive, positively charged intermediates referred to as carbonium ions, and carbenium ions.²⁰ A carbonium ion is a 5 coordinate ion, while the carbenium ion is a 3 coordinate ion as shown in Figure 1-4. However, these terms are used interchangeably by most researchers and the term carbenium ion will be used in this dissertation.



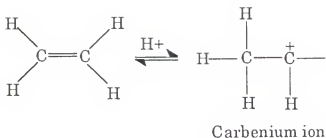


Figure 1-4: Generation of Carbenium and Carbonium Ions.

The stability of hydrocarbons, in particular alkanes, can be attributed to a number of factors, including their C-H and C-C bond strength and the absence of electron rich or deficient sites at which reactions can be initiated. Due to the difficulty of forming reactive cations, it was deemed that a “superacid” was necessary to perform such reactions. The development of superacid chemistry is due primarily to the pioneering work of Olah using liquid acids such as H_2SO_4 .²¹ Formally an acid is considered a superacid if its acidity exceeds that of sulfuric acid.

Organic substrates are protonated by “superacids” as shown in Figure 1-4. The overall reaction is formally a redox process, with the alkane acting initially as a base then eliminating a neutral molecule from the protonated species to give the carbenium ion. Once the carbenium ion is formed, there are a number of reaction pathways by which it can give rise to stable reaction products. The existence of carbenium ions as intermediates for solid acids has been controversial. However, they are accepted as a reasonable intermediate based on new NMR methods.¹⁵ Oxidation of alkanes also leads to the formation of carbenium ions as shown in Figure 1-5.



Figure 1-5: Oxidation of Alkane to Form a Carbenium Ion.

Carbenium ions undergo a variety of reactions which form the basis of isomerization, cracking, alkylation as well as many other reaction mechanisms, and also explain side reactions which accompany the main reaction pathway. The major reactions of carbonium and carbenium ions are described below.

1. Loss of a proton from an adjacent carbon atom (Figure1-6)

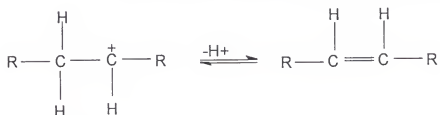


Figure 1-6: Loss of Proton From Carbenium Ion.

2. Internal rearrangement by a hydride ion shift. Such shifts occur rapidly and are a consequence of the difference in the stability of carbonium ions (Figure 1-7).



Figure 1-7: Hydride Shift in Carbenium Ions.

3. Internal rearrangement by migration of a methyl group (Figure 1-8).

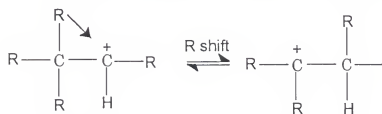


Figure 1-8: Methyl Shift in Carbenium Ion.

4. Removal of a hydride by another molecule (Figure 1-9).

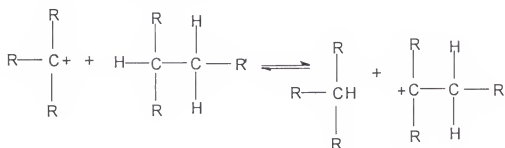


Figure 1-9: Hydride Abstraction by Carbenium Ion.

5. Addition of a carbenium ion to an olefin or arene (Figure 1-10).

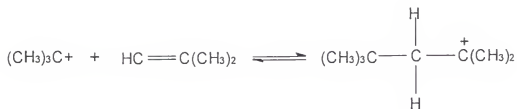
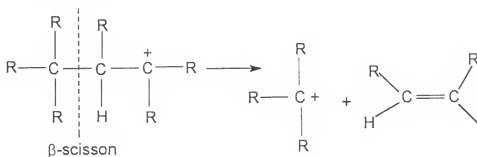


Figure 1-10: Addition of Carbenium to Olefin.

6. β - Scission of a carbenium ion to another carbonium ion and an olefin.

This reaction occurs most readily with ions capable of generating a tertiary cation on scission (Figure 1-11). Scission is β to the carbenium ion.

Figure 1-11: β -Scission of Carbenium Ion.

An example of the use of this carbenium ion chemistry theory to explain reaction products is shown for alkylation of isobutane in Figure 1-12. Notice that many the various types of carbenium ion rearrangements occur simultaneously resulting in a complex mixture of reaction products possible. It will be shown in proceeding chapters that the selectivity for certain reaction products can be controlled by a number of factors including catalyst acidity, reaction temperature, and reaction time.

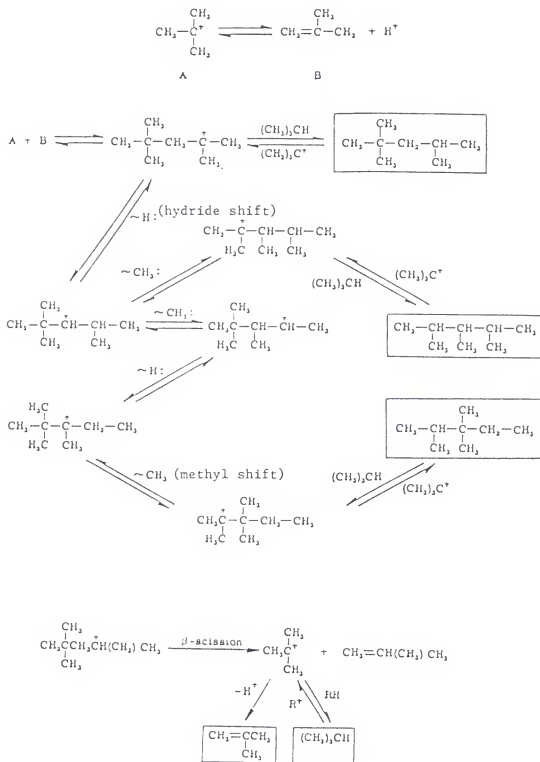


Figure 1-12 Alkylation of Isobutane

Surface Science Methods

X-Ray Diffraction

The x-rays produced in the diffraction experiment are monochromatic x-rays. A beam of electrons strikes a Cu metal target, and ionizes some of the Cu (1S, K shell) electrons. An electron in an outer shell immediately drops down to occupy the vacant 1S level, and the energy released in the transition is x-ray radiation. In the powder XRD experiment the x-rays strike a finely powdered sample, that ideally has crystals and lattice planes randomly arranged in every possible orientation. For each set of planes some crystals are orientated at the Bragg angle θ to the beam, and thus diffraction occurs for these crystals and planes. The Bragg approach is to regard crystals as built up in layer or planes such that each acts as a semi-transparent mirror. Some x-rays are reflected off the plane with the angle of reflection equal to the angle of incidence, others are transmitted to be subsequently reflected by succeeding planes. The perpendicular distance between pairs of adjacent planes is the d-spacing, and the angle of incidence is the Bragg angle θ . These parameters are related by Bragg's law shown in Equation 1-2.

(Equation 1-2)

$$n\lambda = 2d \sin \theta$$

The most important use of the powder XRD method for catalysis is in the identification of crystalline phases or compounds. Each crystalline phase has a characteristic powder pattern which can be used as a fingerprint for identification. The normal practice in comparing powder patterns for identification is to compare the d-spacing and relative intensities, and check that they match. Two samples may have the same d-spacing if their unit cell parameters are the same, but if different elements are

present then the intensities will differ. In catalysis crystallinity is not always a prerequisite for catalyst catalytic activity, although in some cases such as zeolites it is necessary.

Scanning Electron Microscopy

Electrons from an electron gun are focused onto a small spot of 50-100 angstroms in diameter on the sample. The electron beam is scanned systematically over the sample, both x-rays and secondary electrons are emitted by the sample. The former is used for chemical analysis, and the latter is used to build the sample image on a screen. SEM is a versatile technique which provides information regarding the catalysts topography, particle size, surface dispersion, and overall surface features. The SEM technique is based on reflection of an electron beam, therefore sample thickness is not a problem as it is in TEM. It is usually required that the catalyst sample is coated with a layer of metal (Au) to prevent the build up of charge on the surface of the sample. An added benefit to SEM is that when the sample is placed in the microscope and bombarded with electrons, x-rays are generated. The x-rays are characteristic emission spectra (EDS) of the elements present on the samples surface, and thus identification of surface species is possible for elements heavier than sodium.

X-Ray Photoelectric Spectroscopy

Photoelectron spectroscopy is based on the photoelectric effect. Photons from an aluminum X-Ray anode hits the sample and causes ionization to occur where the electron expelled from the sample has a certain amount of kinetic energy. Energy conservation requires that the kinetic energy is equal to the energy of the incident x-ray beam minus the binding energy of the electron from the sample as shown in Equation 1-3.

(Equation 1-3)

$$KE = h\nu - E_{\text{bind}}$$

Where $h\nu$ is the incident photon energy and E_{bind} is the binding energy of the electronic level considered. In conducting samples in electrical contact with the spectrometer a contact potential between the two is created and the binding energy is then equal to Equation 1-4:

(Equation 1-4)

$$E_{\text{bind}} = h\nu - KE - \phi_{\text{sp}}$$

where ϕ_{sp} is the work function of the spectrometer and is a constant. If the sample is an insulator, as some catalyst samples are, a positive charge develops on the sample because of its non-conducting nature and the binding energy is then equal to Equation 1-5:

(Equation 1-5)

$$E_{\text{bind}} = h\nu - KE - \phi_{\text{sp}} - E_c$$

where E_c is the positive charge that exists on the sample. The positive charge acts as an additional retarding potential and causes binding energy peaks to become charge shifted. The value of E_c is not constant and must be determined if E_{bind} is to be known. Two practices are commonly used to correct for charging, either the C1s binding energy peak which arises from contamination, and is known to be at 284.6 eV is used, or a peak from an element of known oxidation state in the sample itself is used. In catalyst samples, such as silica supported catalysts, the Si 2p may be used to correct for charging since it is known that the silica is present as SiO_2 .

Peak assignments in XPS are easily done with the aid of a binding energy table. However, several features that may occur in ones spectra will be explained in further detail. Peak intensities are more or less proportional to the concentration of the element on the samples surface, but it also depends on the elements cross section (probability of photoemission). Some electronic transitions do not give a singlet, but rather a doublet.

This is the case for any orbital that does not possess spherical symmetry. The doublet split is characterized by the quantum number j , which is equal to $l \pm s$, where $s = 1/2$. The magnitude of the spin-orbit splitting depends on the element itself.

Shake-up peaks may also be present, and are characteristic of certain elements. They are observed typically for the 2p transition levels of metals with unpaired d electrons (paramagnetic species). This satellite has practical applications as it relates to catalysis. It is a fingerprint of the oxidation state of the metal it arises from. For example Co^{+2} in CoO will have intense shake-up peaks, but Co^{+3} will not. Therefore, differentiation between Co^{+2} and Co^{+3} is readily made.

XPS as a technique is only a surface technique, and is sensitive only down to 3-6 nm from the samples surface. This is because electrons emitted from below this depth have large escape depths, and thus low probabilities of escaping into the vacuum before undergoing a collision. A vacuum of below 10^{-6} torr is required to avoid inelastic scattering of the photoelectrons inside the analyzer.

Since heterogeneous catalysis is a surface phenomenon, and catalytic activity is sensitive to the nature of the active species on the surface, XPS is a particularly useful technique for heterogeneous catalysis. Its main applications include determination of an active species oxidation state, support-overlayer dispersion, and correlation of these two parameters to catalytic activity. The deactivation or inability to fully regenerate a catalyst sample can be correlated with loss of dispersion or change in active species oxidation state.

Overview of Proceeding Chapters

This dissertation describes the development and characterization of several solid acid catalysts. The catalysts acidity are characterized using the cal-ad method, and NMR probe shifts, from these studies a scale of relative acidities was developed and compared to sulfuric acid. From this scale and comparison of catalytic activity a screening method was developed for solid acid alkylation of isobutane with butene catalysts. This screening method allows one a quick and inexpensive way to evaluate a catalyst. Screening methods for other reactions can also be developed by comparison of catalytic activity for a particular reaction to that of the cal-ad solid acid acidity scale.

The development of several new solid acids from supporting tungsten oxide on silica is described. A preparation method involving the controlled hydrolysis of WCl_6 with silica gel yielded a well dispersed acidic acid catalyst referred to as SG-W. It was found that SG-W catalyzed the Beckmann rearrangement of cyclohexanone oxime to caprolactam very effectively. The catalytic activity, deactivation, and regeneration of the catalyst was correlated to the dispersion and surface acid properties of the catalyst as determined by cal-ad. The addition of platinum to SG-W yielded hydrogenation activity which was studied using the benzene hydrogenation.

Addition of sulfate from sulfuric acid to SG-W yielded a catalyst referred to as SG-WS whose acidity was far in excess of SG-W. As a result of this enhanced acidity more difficult acid catalyzed reactions could be catalyzed using this SG-WS catalyst. In particular, the alkylation of isobutane with butene was studied. The activity of SG-WS and other solid acid catalysts was compared to that of sulfuric acid (the commercial catalyst). It was found that SG-WS yields more turn overs on a per acid site basis than

does sulfuric acid. In addition, it was found that of all the solid acids tested only SG-WS could be effectively regenerated. The deactivation and regeneration were guided by cal-ad analysis of the surface acid sites on SG-WS.

CHAPTER 2 ACIDITY AND REACTIVITY OF SULFATED ZIRCONIA

Introduction

Hino was the first to report that zirconium oxide modified with sulfate on the surface develops strong acidic properties and unique acid catalytic activity.²² Since the original report numerous studies using sulfated zirconia (SZ) as an acid catalyst have appeared. Its low temperature activity for isomerization of hydrocarbons is well documented, and has led to reports claiming that SZ is a solid superacid²³ or at least a very strong solid acid. The early assessment of acidity is in part based on the product distribution of paraffin isomerization with SZ catalysis giving products typical of that from catalysis by sulfuric acid and a mechanism that involves the formation of carbenium or carbonium ions. The formation of carbenium ions leading to isomerized paraffin products is analogous to the same type of reactions that proceed in concentrated sulfuric acid. This has led to claims that SZ is at least as strong an acid as concentrated sulfuric.

The direct measurement of the strength of a solid acid is much more elusive than measuring the strength of a liquid acid. Issues such as accessibility of sites and heterogeneity of the surface cause discrepancies in the different methods used to measure the acidity of solid acids.^{24,25} Not surprisingly, the measurement of the acid strength of

sulfated zirconia is the subject of many investigations producing varying results. Hammett indicators suggest a value of -14.5 to -16 on the H_0 scale, making SZ more acidic than 100% sulfuric acid.²⁴ The use of Hammett indicators are considered unreliable by most investigators for the accurate measurement of solid acidity.²⁶ H^1 NMR and Raman spectroscopic studies led to the conclusion that SZ has superacidic protons²⁷ and EPR studies²⁸ involving charge transfer complex formation using benzene as a probe have been interpreted to show that the acidity of SZ was greater than that of zeolite HY. Results from temperature programmed desorption of NH_3 ²⁹ and other bases were attributed to superacidic acid sites.³⁰ Recently microcalorimetric adsorption of gaseous NH_3 by solid SZ at 423 K was interpreted to involve very strong acid sites³¹ that catalyze the isomerization of butane.

In contrast to the above conclusions, numerous investigators have claimed that SZ is not superacidic. Temperature programmed desorption or methods based on desorption of weakly or strongly basic probes are reported to provide unreliable measures of acidity³² because desorption channels for different probe molecules on SZ are very different. It is claimed³³ that none of the probes selectively probe only the acid site in desorption measurements. These observations were interpreted to indicate^{32,33} that SZ and transition metal doped SZ's are not superacids. Infrared shifts of hydroxyl groups after benzene adsorption suggested that SZ acid sites are weaker than those found on HZSM-5³⁴. Another study reported that SZ is not really superacidic³⁵ based on its high temperature cracking activity. Changes in the NMR and FTIR upon adsorption of acetonitrile suggest that the acidity of SZ is similar to that of HY but less than that of HZSM-5 and is clearly not superacidic.³⁶ A recent report indicates that the activity of SZ for alkane reactions is

not related to acidity but is initiated by a one electron oxidation of the hydrocarbon by sulfate to form a carbocation.^{27,37} Surface binding is proposed to lead to a dramatic increase in the oxidizing ability of sulfate. The organic radical cation loses a proton and combines with the reduced sulfate radical to form a surface organic sulfate or alcohol. Transfer of a hydrogen atom from the organic radical cation leads to sulfite and the carbocation. Dehydrogenation of that alcohol can also generate alkenes which can be protonated to give a carbocation isomerization distribution in the products.

Doping of SZ with iron and manganese is reported to increase the activity of SZ for hydrocarbon cracking by increasing the solid's acidity.³⁹ On the other hand it has been claimed that the activity of SZ doped with Fe and Mn is due to redox active metal sites.^{26,35}

Since the discovery of SZ it has been reported that the acidic and catalytic properties depend on a number of preparative procedures including sulfation and the activation temperature. The proponents of superacidity often attribute results indicating SZ is not a superacid to differences in preparation. A detailed study of the preparation of SZ concluded that the sulfation procedure has no effect on the final SZ product.³⁸ It was further shown that the activation temperature affects the catalytic activity, but its effect on the acidity of SZ is not clear. Calcination of zirconia at 650°C produces a metastable tetragonal phase and a stable monoclinic phase. Sulfation is reported to crystallize ZrO₂ at 550°C and stabilize the tetragonal phase.

It is generally accepted that SZ contains only a small number of the most acidic sites and this complicates the assessment of the acidity of these sites. The low site

concentration in addition to perceived differences in preparative procedures have been used to rationalize differences in catalytic activity and measures of the acidity of SZ.

We report the use of results from a cal-ad titration of sulfated zirconia with pyridine to address this problem. Earlier research from this laboratory has reported that the cal-ad procedure determines the number (n_i), equilibrium constants (K_i), and strengths (ΔH_i , enthalpy) of different acid sites on solids.¹⁸ The subscripts (i) refer to the above quantities, where $i=1$ would be the first site describing the strongest sites, and $i=2$ the next site and so on. In the general area of donor-acceptor bonding, it has long been accepted that the appropriate measure of the strength of binding is the enthalpy of adduct formation. However, in any calorimetric or equilibrium measure that involves gas-solid equilibria, the enthalpies contain contributions from a donor-acceptor interaction as well as a dispersion component. The cal-ad measurements are carried out in a hydrocarbon solvent whose molecules are close in molecular mass to those of the donor¹⁸ to cancel out the dispersion component. This method is employed to measure the acidity of SZ, to compare it to other solid acids and to investigate the effects of preparative procedures and metal doping on the acidity.

Experimental

Catalyst Preparation

Zirconium sulfate was supplied by MEI in the form of sulfated $Zr(OH)_4$ precursor. This precursor was heated at different activation temperatures (600 °C and 300 °C) under dry air for 3 hours. The catalysts have a sulfur loading of 1.6 wt% which corresponds to

0.5 mmols of sulfur per gram of solid. Sulfated zirconia was doped with Pt by adding an aqueous solution of H_2PtCl_6 to the solid and evaporating to dryness. The loading of Pt after evaporation was 0.2 wt%. The Pt sulfated zirconia was activated at 600 °C in dry air for 3 hours. A SZ sample doped with iron and manganese was prepared according to a reported procedure.³⁹

Calorimetry and Cal-ad Analysis

The calorimetric titration was carried out as described previously.¹⁸ One gram of sulfated zirconia slurried in cyclohexane solution is reacted with pyridine while stirring. The cyclohexane and pyridine reagents used were distilled over P_2O_5 prior to use. After each injection of pyridine solution, the heat evolved is measured. This heat is then used to determine the enthalpy. In the cal-ad analysis an adsorption isotherm is measured over the range of base additions used in the calorimetric titration. The combined calorimetric and adsorption data are analyzed to produce K's (equilibrium constants), n's (mols of site), and ΔH 's (enthalpies).

UV-Visible Spectroscopy

Measurement of the free pyridine in solution in equilibrium with the sulfated zirconia in the calorimetric experiment was determined by UV-VIS as described previously¹⁸ using a Perkin-Elmer Lambda 6 UV/Vis spectrophotometer. Suprasil quartz cells were employed in the adsorption studies.

Alkylation of Isobutane with Butene

Alkylation of isobutane with butene was performed in a batch reactor. The batch reactor was filled to a total volume of 12 ml with a 50:1 volume ratio of liquid isobutane to liquid 2-butene. One gram of sulfated zirconia or 1 ml of concentrated sulfuric acid was placed into the batch reactor with a stir bar prior to filling with reactants. The reaction was carried out at 0°C with stirring for 30 minutes. Upon completion of the reaction the liquid product was filtered and the products were analyzed using gas chromatography. Pentane is added to the reaction products as an internal standard for gas chromatographic analysis.

Isomerization of Pentane

The isomerization of pentane was performed in a batch reactor using 1 gram of SZ and 3 ml of a 25% pentane solution in carbon tetrachloride. The reaction was stirred at 50 °C for the allotted time period and products were analyzed by gas chromatography.

Results and Discussion

Cal-ads Determination of Acidity

Figure 2-1 shows the results from adsorption measurements plotted as the moles adsorbed by the solid vs moles of pyridine added. Figure 2-2 shows the results from the calorimetric titration of SZ with pyridine, plotted as calories evolved, h' , vs moles of

pyridine added. For the first few injections of pyridine corresponding to less than 50 μmols , there is no free pyridine present in solution. The acid sites of the solid have totally complexed the pyridine. Dividing h' for these additions by the moles of pyridine added produces molarity weighted averages of the enthalpies of binding to the sites to which the pyridine coordinates. The sites involved in binding change for each addition as the strongest sites become saturated. The left axis of Figure 2-2 gives the average enthalpies for those additions in which 90% of the added pyridine is bound to the solid. The quantity of interest is the enthalpy of binding to the strongest site, not some average that is dependent on the magnitude of the equilibrium constants. This information can be provided by the full cal-ad analysis.

A dilute solution of pyridine was used in the calorimetric titration of SZ in order to avoid titration of all the strongest and some of the weaker acid sites with the first injection. A report has indicated that a very small concentration ($<70 \mu\text{mols/gram}$) of sites exist on SZ which are active catalytically but which deactivate very quickly.³¹ In our calorimetric titration the first injection of pyridine delivers 13 μmols of pyridine which is completely bound to the solid. With complete complexation of the first two additions of pyridine, we can divide h' by the moles added to get an average enthalpy of the sites titrated. The corresponding enthalpy for these 25 μmols of acid sites/ gram SZ is only -31 kcal/mol which is not superacidic. Since the average enthalpy of reaction for the first 13

μmol s of pyridine added is the same as that for the addition of the second injection of 12 more μmol s we can place an upper limit on the small amount of a very strong site that could be present. Furthermore, since the h' value for the first injection is 0.463 ± 0.029 calories, we can state that if superacidic sites are present (e.g. some with enthalpies above $50 \text{ kcal mole}^{-1}$) they would have to be present at concentrations of $2.5 \mu\text{mol}$ or less in order not to influence the average enthalpy of the first injection as compared to that of the second. An excess of 50 kcal/mole is a value we have chosen based on SGOAlCl_2 which is the strongest solid acid ($-\Delta H = 50 \text{ kcal mole}^{-1}$) studied by cal-ad to date.⁴⁰ This solid acid catalyzes low temperature cracking as well as the alkylation of isobutane and butane.

The above discussion indicated that average enthalpies result when h' is divided by the moles of base added and is typical of the literature procedures used to analyze gas-solid enthalpies and solution calorimetric data. Dividing h' by moles of base even at low base concentrations produces the enthalpy for the strongest site only if $K_1 \gg K_2$. Since n_2 is usually much larger than n_1 , the differences in K 's must be substantial to obtain an average enthalpy that is within 10% of that for site 1 by this approach. The average enthalpy problem is particularly critical in studies of gas solid equilibria at elevated temperatures. If the two K 's approach each other at elevated temperatures, average enthalpies will result. Unfortunately, there is no way to determine the extent of the averaging from enthalpy data alone. For example, the first two base additions in Figure 2-2 could be an average of 65-70% of $-40 \text{ kcal mole}^{-1}$ site and 30-35% of a $-13 \text{ kcal mole}^{-1}$ site. The average $-\Delta H$ would be 31 kcal/mole and a large error results by assuming the average is the strong site. As site 1 is saturated, the average $-\Delta H$ decreases to that of site 2 and this would give rise to a curve like that shown in Figure 2-2.

The full cal-ad analysis produces meaningful equilibrium constants, enthalpies and number of sites by simultaneously analyzing the data in Figures 1-2 and 2-2. Table 2-1 shows the ΔH , K and n values determined from the cal-ad analysis of SZ.

Table 2-1: Cal-Ad Analysis of Sulfated Zirconia (SZ)

| | |
|------------------------------------|------------------------------------|
| $K_1 = 7.5 \times 10^9$ l/mole | $K_2 = 3.0 \times 10^4$ l/mole |
| $n_1 = 2.45 \times 10^{-3}$ mole/g | $n_2 = 5.52 \times 10^{-5}$ mole/g |
| $\Delta H_1 = -31.2$ Kcal/mole | $\Delta H_2 = -25.8$ Kcal/mole |
| $\Delta S_1 = -59.5$ cal/deg | $\Delta S_2 = -66.1$ cal/deg |
| $\Delta G_1 = -13.46$ Kcal/mole | $\Delta G_2 = -6.1$ Kcal/mole |

Since $K_1 \gg K_2$ and the enthalpy of $-\Delta H_{ave}$ calculated from the first two injections of pyridine agrees with that of $-\Delta H_1$ from cal-ad, we conclude that if $K_1 \gg K_2$ then $-\Delta H_{ave}$ for the first few injections will be $-\Delta H_1$. The reported data for the $-\Delta H$ from the solid analysis of the calorimetric titration of pyridine with silica,¹⁸ and HZSM-5⁴¹ are summarized in Table 2-2. From these results one can place the acidity of the strongest sites as greater than silica gel, but less than those of HZSM-5. These results are consistent with those obtained by NMR and FTIR adsorption of acetonitrile,³⁶ and infrared adsorption of benzene.³⁴ Table 2-2 provides a scale of acidities of those solid acids which have been studied using the cal-ad technique.

The cal-ad procedure allows the determination of not only the relative strength but also the number of sites and their equilibrium constants for adsorption of a probe molecule which is information that is not obtained by using other common techniques of acidity characterization. The cal-ad determination of the enthalpy of the donor-acceptor

interaction of the solid acid with the basic probe pyridine supports the position that SZ is not a superacid and reinforces the suggested problems with other measurements suggesting superacidity.

Table 2-2: ΔH_1 Values for Other Solid Acid Catalysts

| Solid Acid | $-\Delta H_1$ (Kcal/mole) |
|----------------------|---------------------------|
| SiO ₂ | 12 |
| HZSM-5 | 41 |
| SG-AlCl ₃ | 51 |
| SZ | 30 |
| SZ-Pt | 30 |
| SZ-Fe-Mn | 26 |
| SZ-300°C calcination | 15 |

A study involving selective poisoning of the acid sites on SZ by NH₃ concluded that there are 70 $\mu\text{mole/g}$ of active acid sites³¹ in the solid. Our cal-ad analysis of n_1 sites plus n_2 sites gives us a total of 79 $\mu\text{mole/g}$ of acid sites. This is in excellent agreement considering different samples were measured in different laboratories using different techniques. This provides a confirmation of the cal-ad method.

Calorimetry using a gaseous probe molecule such as NH₃ is a common method used to analyze solid acid acidity.^{31,42} A recent report on the use of gaseous NH₃ calorimetry at 150°C showed that two or three types of sites were present on SZ. The strongest sites had a strength of 34- 39 kcal/mole, which is 3-9 kcal/mole higher than our

reported value. Measurements on silica⁴³ and carbonaceous solids⁴⁴ show that there is a contribution (about 10 kcal/mole) from non-specific dispersion force interactions when a gaseous probe is adsorbed on a solid. If one takes into account the 10 kcal/mole dispersion interactions in the gaseous NH_3 adsorption, then the results from cal-ad analysis agree quite well with the upper limit of strong acid sites found. The fact that the values are close at the lower limit is attributed to the effect of the high investigation temperature on the K's. At the higher temperature the K's approach one another and therefore site 1 is not being exclusively probed. The contribution from site 2 causes the measured enthalpy to be an average of site 1 and 2 and thus lower values are obtained.

The effect of activation temperature on the catalytic performance of SZ is widely documented.⁴⁵ In order to investigate the influence of the calcination temperatures on the acidity of SZ, a calorimetric titration of a sample calcined at 300 °C was carried out. Up to 13 μmoles , U.V. spectroscopy of the solution shows that all of the pyridine added is coordinated to the solid. Up to 90% is absorbed for additions in the range of 13 to 25 μmoles of pyridine. Since our main interest in these materials is the strength of the strongest acid sites, and since $-\Delta H_{\text{AVE}}$ is very low a full cal-ad analysis was not carried out. Instead, the calorimetric data are used to calculate the average enthalpy, h' divided by the moles of pyridine added, and the results are shown in Figure 2-3. Values of 15 kcal mole⁻¹ are obtained for the first 2 pyridine additions corresponding to 25 μmoles of pyridine added. Though this analysis does not give an accurate value for the strongest site, it does show that $-\Delta H_1$ is considerably less than 32 kcal/mole, and it is clear from this result that the calcination procedure greatly influences the acidity of SZ. At calcination temperatures

below 400 °C the SZ sample is amorphous. When the sample is activated at 500 °C, the SZ forms a tetragonal phase and the catalytic properties are greatly enhanced. SZ in the amorphous phase may contain adsorbed water coordinated to the acid sites and this causes the acidity of the sites to decrease.

The influence of 0.2 wt% Pt on the acidity of SZ activated at 600 °C was studied next. The calorimetric titration is shown in Figure 2-3. Again all of the added pyridine is adsorbed up to 25 μ moles of added pyridine and produces a $-\Delta H_{\text{AVG}}$ of 30.5 kcal mole⁻¹. Doping with platinum has had little effect on the acidity of the strongest sites of sulfated zirconia. The calorimetric titration curve for both sites is almost identical to SZ suggesting platinum doping does not modify the acidity of SZ. The effect of Pt addition to SZ is known to enhance the activity of the catalyst for hydrocarbon isomerization reactions.^{47,48} This could be due to the spill over effect of Pt when H₂ is used in the reactant feed. A similar increase in hydrocarbon isomerization activity is seen for Pt doped HZSM-5.⁴⁹

Relationships of Catalytic Activity and Acidity

We performed reactions with our sample of SZ which was activated at 600 °C to test the activity of the catalyst. As expected the catalyst isomerized pentane at 50 °C reaching 33% conversion of pentane after 30 hours. The catalyst activated at 300 °C had no activity for pentane isomerization. The decrease in the catalytic activity of samples calcined at 300 °C at the lower activation temperature may be due to the inability of the solid to stabilize the one electron transfer unless the tetragonal phase is present.

The description of SZ as having a small concentration of superacidic sites has often been invoked to explain the rapid deactivation of this catalyst. This explanation does not explain the catalytic reactivity of SZ in the isomerization of butane and pentane in recirculating reactors where the percent conversion is reported to increase at high temperatures with time on stream. Clearly this is inconsistent with a super acid mechanism in which coking deactivates the strongest acid sites and should result in decreased activity if the number of sites is small. Perhaps more disturbing is the fact that additions of Fe and Mn have been reported to enhance the activity of SZ 3 times^{39,46}. The addition of Pt to sulfated zirconia also increases its activity for hydrocarbon conversion reactions.^{47,48} As shown in Figure 2-3, these additions are not enhancing the acidity of the SZ. It has been reported that SZ undergoes a one-electron transfer mechanism rather than a traditional superacidic mechanism²⁷. This would account for the catalytic properties and the moderate acidity. Farcasiu and Davis^{35,37} report that the additions of Fe and Mn as well as Pt are aiding the reactions by modifying the one-electron acceptor ability of the sulfated zirconia catalyst.

The average enthalpy for the first two base additions of pyridine to Fe Mn SZ give an average enthalpy of 26 kcal mole⁻¹. Clearly the acidity is not increased and no new strong acid sites are evident. To the contrary, doping leads to a decrease in the average enthalpy of the strongest sites. If doping does not influence the equilibrium constants and the enthalpy for site 2, the ΔH_{ave} suggests that practically none of the strong acid sites for SZ remain in the iron-manganese doped sample.

When SZ activated at 600 °C was tested for alkylation activity, none was found. One ml of concentrated sulfuric acid at these conditions produce large amounts of

isooctane products. Alkylation of isobutane with butane is reported with SZ but in a flow reactor system at high temperatures and may involve a different mechanism for the reaction. Commercially, alkylation of isobutane is carried out at low temperatures using 100% sulfuric acid and a solid acid of comparable acidity should catalyze this reaction. The inability of SZ to perform this reaction at 0°C is further evidence that the acid sites are not superacidic.

The results of these catalytic studies with cal-ad analyzed catalysts emphasizes an important point. If super or strong acidity is to be inferred from catalytic isomerization activity it is essential to demonstrate that the reaction mechanism is indeed an acid catalyzed mechanism. Otherwise, correlations of reactivity with acidity will fail.

Conclusion

Our findings show that a significant amount of superacid sites does not exist on SZ or metal doped SZ. The calorimetric analysis indicates that the strongest acid sites on SZ are stronger than silica gel but weaker than HZSM-5. Furthermore, our results show that doping with platinum or iron and manganese does not increase the acidity of these materials.

The temperature of activation of SZ plays a role in determining both the acidity and the catalytic activity. The catalytic activity for hydrocarbon isomerization is well documented but the mechanism by which the transformation occurs is still in question. More research is necessary in this area to establish how SZ accomplishes the

transformations. It is the conclusion of this study that the mechanism is not based on the traditional carbenium ion mechanism because SZ is not a superacid. This example emphasizes the point that for correlations of the acid strength of catalysts with reactivity it is critical to be sure that the catalytic reactions proceed through a similar acid catalyzed mechanism for all catalysts being compared.

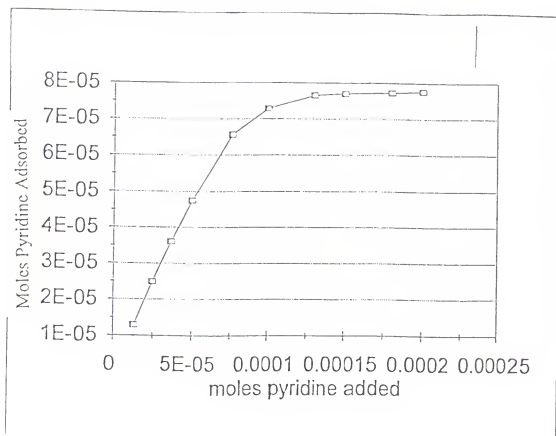


Figure 2-1 Pyridine Adsorption on Sulfated Zirconia

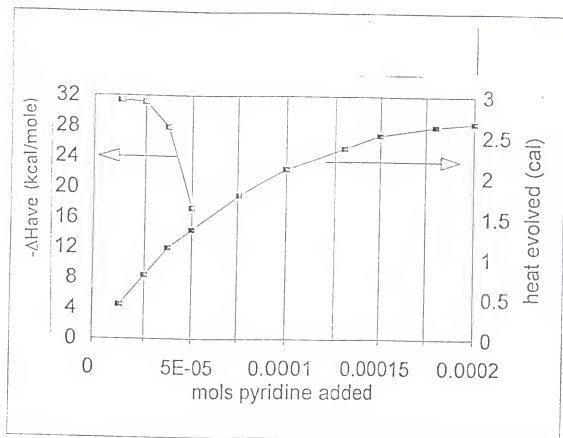


Figure 2-2 -ΔH_{ave} for Sulfated Zirconia

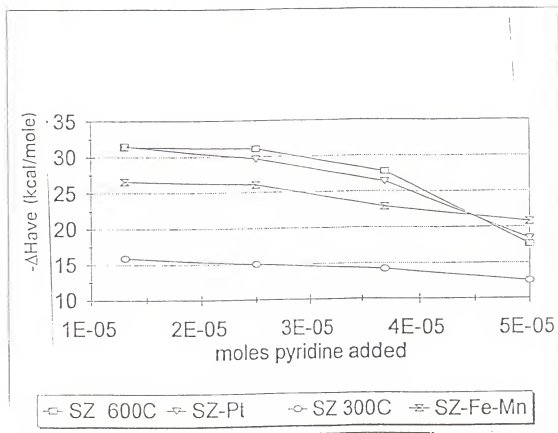


Figure 2-3 Calorimetric Titration of Sulfated Zirconias

CHAPTER 3 CHARACTERIZATION OF THE ACIDITY OF SG- AlCl_3

Introduction

Solid acid catalysts are widely used in major petroleum refining and petrochemical processes.⁵⁰⁻⁵² Reactions include cracking, isomerization, reforming, and hydrotreating. These catalysts also play a significant role in the synthesis of bulk and specialty chemicals.⁵³ The preparation and characterization of acidic heterogeneous solid catalysts have been the subject of many reports.^{1,2,54,55} These acid catalysts include a variety of structures such as zeolites, halide based acid catalysts, and oxide based acid catalysts. The acidity of the various solid acid catalysts are reported to vary greatly from “super” acids to weak acids.

Reactions occurring by acid catalyzed mechanisms vary in the strength of the acid required for reaction. The activity and selectivity of many acid catalyzed reactions is determined by the number, nature, and strength of the acid sites. For example alkylation of isobutane with butene to make isooctane requires a very strong acid catalyst. At present, liquid H_2SO_4 is used for this alkylation process. On the other hand, the dehydration of butanol is catalyzed by even weak acids.⁵⁶ As a result of these varying requirements, a considerable effort has been spent on developing a method to characterize the acidity of a solid acid.

A cal-ad method has been suggested as a procedure for characterizing solid acids.¹⁸ The method involves slurrying a solid acid in a non-interacting solvent and measuring the heat of interaction between the solid acid sites and known amounts of an added basic probe. This heat is combined with an adsorption measurement to provide a complete characterization of solid acidity in terms of K (equilibrium constant), n (moles of site), and ΔH (enthalpy) for the interaction. In the calorimetric titration, the dispersion component of the solid-donor interaction is minimized by slurrying the solid acid in a hydrocarbon solvent of molecular weight similar to that of the donor. Displacement of the hydrocarbon from the surface by coordination of the donor cancels out the dispersion component in the measured enthalpy.

Solid state NMR has been used for the structural characterization of solid acids and for the study of solid acidity.¹⁵ For example, ^{27}Al and ^{29}Si MAS NMR have been widely applied to study structures of solid acids such as zeolites.¹⁵ ^1H $\{^{27}\text{Al}\}$ double resonance experiments have been developed for isolating protons associated with aluminum from the bulk protons in zeolites. NMR studies of probe molecules adsorbed on solid acids also provides a wealth of information about the nature of the solids acidity. Probes such as trimethylphosphine can be used to differentiate Lewis and Bronsted sites present on the surface of the solid acid.^{15c} Acetone on the other hand, can be used as a probe to evaluate the acid strength of the solid regardless of the type of site. It was found that the ^{13}C chemical shift of the carbonyl carbon of acetone correlates well with the expected relative acid strength of zeolites.^{15a}

Drago has reported a silica supported aluminum chloride solid acid (SG-AlCl_2) that has been shown to perform isomerization and cracking of light paraffins at low

temperatures with activity far greater than any previously reported solid acid.⁴⁰ Given these observations this catalyst was claimed to be among the strongest Bronsted solid acids. This chapter reports improvements in the synthesis of SG-AlCl₂ and a more extensive characterization of its solid acid acidity. The acid strength of a variety of solid acids, including sulfated zirconia and HZSM-5 was investigated by heats of adsorption of pyridine using a calorimetry method. A similar calorimetry measurement was done using 2,6 lutidine as the probe to further establish that the strongest sites are Bronsted in nature. A number of multi-nuclear NMR experiments were performed to investigate the solid acidity of this catalyst. ¹⁵N and ³¹P NMR studies of adsorbed pyridine and trimethylphosphine provide unambiguous evidence for the presence of strong Bronsted sites on SG-AlCl₂. A ¹H {²⁷Al} spin echo double resonance experiment revealed that the Bronsted sites on SG-AlCl₂ have proton chemical shifts of 5.5 ppm, placing the acidity higher than that of sulfated zirconia and HZSM-5. ¹³C NMR of acetone clearly ranks SG-AlCl₂'s acidity close to superacidity, with less than 0.2 mmoles/g acetone loading, which is consistent with the results obtained by calorimetric analysis.

Experimental

Catalyst Preparation

SG-AlCl₂ catalyst preparation: Davison silica gel 80-200 mesh was pre-conditioned as follows. The silica was washed with 1M HCl followed by deionized water followed by 30% H₂O₂ followed by deionized water. The peroxide treatment produces the same material as described in previous reports but increases the strong acid functionality. After washing the silica was dried at 100°C overnight in vacuum. It is

critical to remove excess water without dehydrating the silanol functions. The silica is then refluxed in CCl_4 (dry) for 2 hours, after which time 0.0038 moles of aluminum chloride (anhydrous) per gram silica used is added to the stirring mixture. This mixture is allowed to react for 2 days under these conditions during which time the color of the solution will change to dark purple. The mixture is then filtered in a dry box where it is stored. The catalyst is moisture sensitive and thus any contact with moisture is to be avoided.

Acidity Measurements

Acidity measurements by calorimetry were carried out using one gram of catalyst slurried in cyclohexane (dried over P_2O_5 and distilled) with pyridine solution. Injections of known quantities of pyridine were made to the stirred catalyst in cyclohexane and the heat evolved from the reaction was measured after each injection. The calorimeter is equipped with a thermistor which is calibrated prior to each run. The measured heat evolved is then converted to an average enthalpy of sites titrated by determining the amount of pyridine on the solid. The complete cal-ad analysis is not carried out because small amounts of pyridinium chloride are formed complicating the spectral determination of the free pyridine in solution. As a result accurate enthalpies are measured but equilibrium constants are not accurately determined.

Samples of 0.4 g of SG-AlCl_3 was loaded into a shallow bed CAVERN under N_2 and evacuated to a final pressure of less than 10^{-4} torr for MAS NMR studies. ^1H , ^{13}C , ^{27}Al , and ^{31}P solid state NMR experiments were performed with magic angle spinning on a modified Chemagnetics CMX-300 Mhz spectrometer. ^1H and ^{13}C chemical shifts are reported relative to TMS, ^{15}N shifts relative to nitomethane, ^{27}Al shifts relative to 0.1 M

$\text{Al}(\text{H}_2\text{O})_6^{3+}$, and ^{31}P shifts relative to 85% H_3PO_4 . Chemagmetics probes were spun at 4 to 6.5 KHz, and 10 to 13 KHz.

Results/Discussion

Catalyst Characterization and Preparation

Important variables for the proper preparation of the SG- AlCl_2 catalyst include, silica pre conditioning, silica support surface area, solvent employed, as well as the amount and purity of Al_2Cl_6 reacted.⁴⁰ The preconditioning of the silica support is important because the Al_2Cl_6 reacts with the hydroxyl functionality cleaving the dimer and eliminating HCl when grafting to the support. It has been shown by back titration of the HCl evolved during the preparation that one Cl reacts for every one AlCl_3 used in the preparation. This is important to establish that no unreacted AlCl_3 remains. If the catalyst support is too dry then not enough hydroxyl functionality is present to fully react all the Al_2Cl_6 species, and SG- Al_2Cl_5 will form on the surface. The SG- Al_2Cl_5 on the surface gives rise to the penta coordinated aluminum species with ^{27}Al NMR peaks at 42 and 36 ppm. The strong Bronsted acid site on our SG- AlCl_2 catalyst is due to the 4 coordinate alumina species is shown in Figure 3-1. The solid state ^{27}Al NMR of 4 coordinate alumina has peaks at 65 ppm.

Silica gel conditioning can be monitored by TGA. Proper conditioning of the silica gel results in a surface with hydroxyl functionality that can be converted to about 4% water as measured by TGA. The unconditioned silica gel has about 8% water as measured by TGA. When the silica is dried at temperatures above 150°C much less than

4% water is generated from the hydroxyl functionality on the surface in the TGA experiment.

BET analysis for silica supports and the SG-AlCl₃ catalyst are shown in Table 3-1. Upon preparation the SG-AlCl₃ catalyst, the surface area and pore volume is reduced, consistent with grafting of the AlCl₃ on the surface. There is a 20% loss of surface area which indicates that the AlCl₃, which has a loading of 33 wt%, reacts with silica gel maintaining the solids structure and occupying Al sites over the silica gel surface. This produces a new material while maintaining most of silica gel's surface area.

Table 3-1: BET Analysis for Davison Silica Gel and SG-AlCl₃.

| Catalyst/Support | Surface Area (m ² /g) | Pore volume (cc/g) | Ave. Pore Size (Å) |
|----------------------|----------------------------------|--------------------|--------------------|
| Davison Silica | 265 | 1.1 | 175 |
| SG-AlCl ₃ | 215 | 0.76 | 140 |

Figure 3-2 shows the ²⁷Al spectrum of SG-AlCl₃ acquired in a 5 mm probe with a flip angle of less than 10° and has magic angle spinning speed (12,200 Hz). The spectrum shows two major isotropic peaks at -2 and 70 ppm. The 70 ppm resonance indicates the presence of tetrahedral aluminum, consistent with the grafting of AlCl₃ on the silica surface. The small peak at -2 ppm is indicative of octahedral aluminum, which is due to exposure to moisture during the sample preparation. The shoulder at 40 ppm indicates a small amount of penta-coordinated aluminum sites. The ²⁷Al spectrum differs substantially from those reported previously.⁵⁹⁻⁶⁰ In that report the most prominent peak is due to the penta coordinated site at 40 ppm. Also, in that report a peak at 85 ppm was reported, in

which aluminum is surrounded by 4 chlorines. This species at 85 ppm is absent on our catalyst. Others have also reported silica supported AlCl_3 catalysts^{59,60}, these preparations were done using silica which was not properly conditioned (too dry), causing the excess aluminum chloride to lead to 5 coordinate aluminum sites. Our catalyst prepared using pre conditioned silica results in predominantly 4 coordinate aluminum and titration of the HCl evolved during preparation shows that one mole of HCl is evolved per mole of AlCl_3 used in the preparation. When Al_2Cl_6 is reacted with silica dried at 300°C in air for 4 hours (a improperly conditioned silica), calorimetric titration with pyridine showed a less negative enthalpy (weaker acid) than when silica is conditioned properly. Weaker sites result because the hydroxyl clusters needed to form the Bronsted acid site as shown in Figure 3-1 are lost due to the excessive dehydration of the surface. Therefore, the use of appropriate synthesis conditions are necessary for generation of the tetrahedral aluminum sites, which are the strong Bronsted sites. ^{27}Al NMR provides a good tool for determining that the proper material has been synthesized. The proper material should have strong Bronsted acid sites associated with tetrahedral Al coordination, not 5 coordinate Al species.

Bronsted Acidity of SG- AlCl_2

^{15}N , ^{31}P , and ^1H MAS NMR were used to establish the Bronsted acidity of SG- AlCl_2 . Figure 3-3 shows the ^{15}N spectra of pyridine on a variety of solid acids. The spectra shown in Figure 3-3a and 3-3b were obtained on SG- AlCl_2 samples with pyridine loadings of 0.6 mmol/g and 1.3 mmol/g. Three isotropic peaks were observed on SG- AlCl_2 at -125, -147, and -185 ppm. The peak at -125 ppm is due to physisorbed or

weakly interacting pyridine on the catalyst surface based on the comparison of the lower loading and higher loading spectra. The peak at -185 ppm is assigned to the pyridine bound to the Bronsted acid sites. This assignment is consistent with a previous report, in which ^{15}N shift of -182.2 was observed for fully protonated pyridine by HCl pretreated silica-alumina. To further establish this assignment, pyridine ^{15}N was adsorbed onto a well characterized Bronsted solid acid HZSM-5. A resonance at -178 was observed, supporting our assignment of the -185 ppm peak on SG- AlCl_3 to Bronsted acid sites. The peak at -147 ppm in Figure 3-3 is due to pyridine interacting with Lewis acid sites on SG- AlCl_3 . Similar ^{15}N shifts were observed when pyridine was adsorbed onto pure AlCl_3 .

Figure 3-4 shows ^{31}P spectrum of trimethylphosphine (TMP) adsorbed on SG- AlCl_3 . The most important feature in this spectrum is the asymmetric doublet centered at -4 ppm. Lunsford^{15c} has observed a similar feature while studying the interaction of TMP with zeolite HY. The doublet pattern results from the scalar coupling of the protonated TMP by the Bronsted acid site on the catalyst. The measured scalar coupling constant (510 HZ) is very close to that observed on zeolite HY (550 Hz). The observation of scalar coupling provides unambiguous evidence for the existence of Bronsted sites on SG- AlCl_3 . The resonance at -43 ppm is due to TMP interacting with Lewis sites. We are presently unable to assign the other features in the spectrum, and further experimental work is under way to help assign the peaks.

^1H MAS NMR is valued for its ability to directly study Bronsted sites in solid acids like zeolites. However, strong homonuclear dipolar coupling between adjacent proton sites broadens ^1H spectra and thus limits the usefulness of the technique. A spin echo double resonance experiment allows the separation of protons dipolar coupled to the

aluminum. Figure 3-5 shows the application of the spin-echo double resonance to study SG-AlCl₂. Figure 3.5a, was acquired using a spin echo pulse sequence but without ²⁷Al irradiation during the τ period, shows a broad peak at 2.6 ppm assigned to the silanol protons on the silica surface. When a ²⁷Al field of 50 Hz was applied during the τ period, the proton signal associated with aluminum was destroyed (spectrum b). The difference spectrum (c) then shows the signal for the protons dipolar coupled to the aluminum, presumably the Bronsted sites (5.5 ppm) as proposed in Figure 3-1.

Acid Strength

The question of superacidity is one that has received much attention. A superacid is defined as having acidity greater than 100% H₂SO₄. Since one can not directly compare solid and solution acidity we propose the use of calorimetric titration with pyridine to correctly assign a $-\Delta H$ value for the strongest acid sites on sulfated zirconia and metal doped sulfated zirconia. Table 2 shows the $-\Delta H_1$ (the subscript refers to the first site which is the strongest site, if additional sites are described they will be assigned 2,3 and so on) for SG-AlCl₂ and other solid acids using pyridine as the basic probe and cyclohexane as the slurry solvent.

Table 3-2: Strength of Solid Acids

| Catalyst | $-\Delta H_1$ (kcal/mole) |
|-------------------------|---------------------------|
| SG-AlCl ₂ | 51 |
| Sulfated Zirconia | 31 |
| Fe-Mn Sulfated Zirconia | 26 |
| HZSM-5 | 41 |

The enthalpies for SG-AlCl₂ were calculated from pyridine additions of less than 25 µmoles/g of pyridine adsorbed onto SG-AlCl₂, and this amount of pyridine is fully complexed. The strength of the strongest acid sites on SG-AlCl₂ is much greater than those of other strong solid acids HZSM-5⁴¹ (the most acidic zeolite), sulfated zirconia,⁶² and metal doped sulfated zirconia.

A model of the strongest acid sites on SG-AlCl₂ is shown in Figure 3-1. The strong Bronsted acid strength of the proton is due to the formation of tetrahedral aluminum with electron withdrawing chlorine. To confirm that the strongest sites are Bronsted in nature, a calorimetric titration of SG-AlCl₂ was done using 2,6 lutidine as the basic probe in a cyclohexane slurry. Due to the steric effect of the methyl groups a reduced enthalpy from that of pyridine would be seen when interacting with Lewis sites. The experimental -ΔH₁ using 2,6 lutidine as the probe was found to be similar to that of using pyridine as the probe as shown in figure 3-6, establishing that the strongest sites are Bronsted.

It is proposed that the Bronsted sites are responsible for the bulk of the SG-AlCl₂ catalysts hydrocarbon isomerization activity. To test this hypothesis a sample of SG-AlCl₂ was used for butane isomerization until the activity dropped. This used catalyst sample was titrated calorimetrically using pyridine in the same manner as the fresh sample. Figure 3-7 shows that the used catalyst has a lower acidity as expected due to loss of the most acidic Bronsted sites. Titration of the used catalysts with 2,6 lutidine also shows a similar drop off in acidity.

Further evidence for strong acidity was provided by ^{13}C NMR of adsorbed acetone. Figure 3-8 shows ^{13}C MAS spectra of acetone on SG- AlCl_3 acquired at three different loadings. At lower loadings (Figure 3-8a, and 3-8b) ^{13}C shifts of acetone were observed at 243 and 241 ppm. It has been previously established that the ^{13}C shift of acetone is a good measure of the acid strength.¹⁵ The ^{13}C shifts of acetone on a variety of liquid and solid acids is shown in Table 3-3.

Table 3-3: ^{13}C Acetone Shifts on Solid Acids.

| Catalyst | ^{13}C acetone shift |
|------------------------------|-------------------------------|
| magic acid | 249 |
| 100% H_2SO_4 | 244 |
| HZSM-5 | 223 |
| HY | 218 |
| neat acetone | 205 |
| SG- AlCl_3 | 246 |

The acetone shift of SG- AlCl_3 clearly shows that it is a stronger acid than HZSM-5, as shown by calorimetric titration using pyridine, and that its acidity is about the same as that of 100% H_2SO_4 , making it a superacid. This would place the acidity of 100% H_2SO_4 on the calorimetric titration with pyridine in cyclohexane scale at approximately $-\Delta H_1 = 50$ kcal/mole. At higher acetone loadings (Figure 3-8c) upfield shifted resonances at 239 and 233 ppm are detected, indicating coordination of acetone with less acidic sites on the solid.

Stabilization of the SG-AlCl₃ catalyst is desired so that the deactivation by loss of HCl will not occur. Conditioned silica gel reacted with WCl₆ to form a tungsten oxide was used as the support for preparation of the SG-AlCl₃ catalyst. It was hypothesized that this would stabilize the acid sites, but the catalyst lost HCl as before. Another approach used was to react the SG-AlCl₃ catalyst with SO₃ vapors. It was thought that SO₃ would insert into the Al-Cl linkage, thereby stabilizing the acid sites. However, this approach did not work and HCl was still lost from the catalyst when N₂ was passed over it at 50°C.

Conclusion

Several points were established with this study. First, aluminum chloride supported on silica is the strongest solid acid known, and has acidity in excess of HZSM-5, sulfated zirconia and metal promoted sulfated zirconia. Second, the correct preparation of the SG-AlCl₃ catalyst requires that the hydration level of the silica be correct so that penta-coordinated aluminum structures are avoided. Third, the strongest sites which are responsible for the isomerization and cracking activity of the catalyst and these are Bronsted sites. Finally, the calorimetric titration provides a reliable characterization of the acid strength and complements NMR studies of solid acid catalysts.

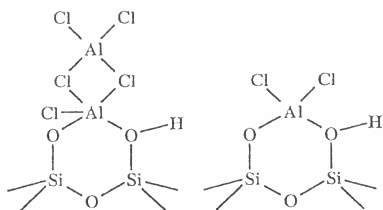


Figure 3-1 SG-AlCl₂ Catalyst

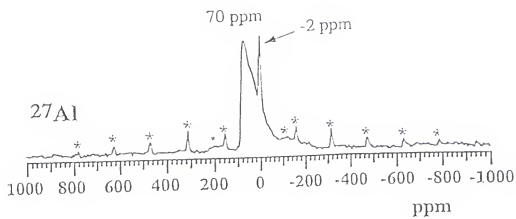


Figure 3-2 ^{27}Al NMR Spectrum of SG- AlCl_3

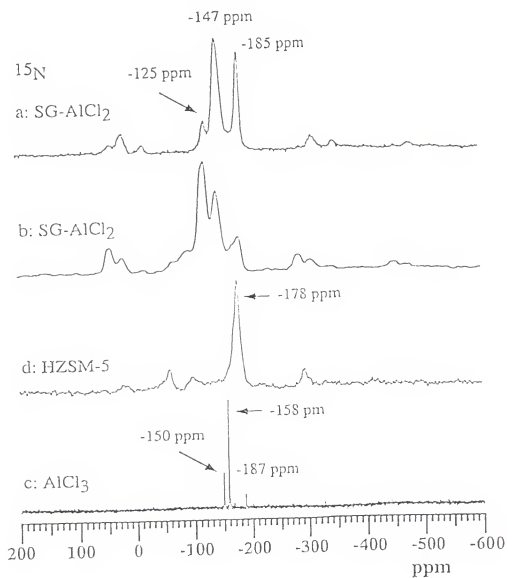


Figure 3-3 ^{15}N NMR Spectrum of Pyridine on SG- AlCl_2

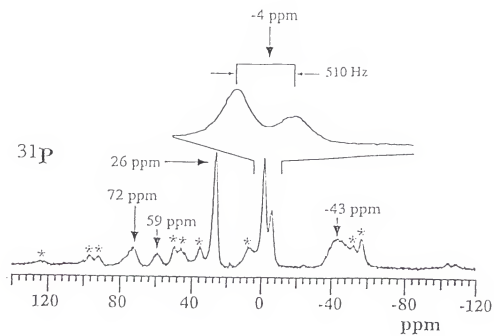


Figure 3-4 ^{31}P NMR Spectrum of TMP on SG-AlCl_2

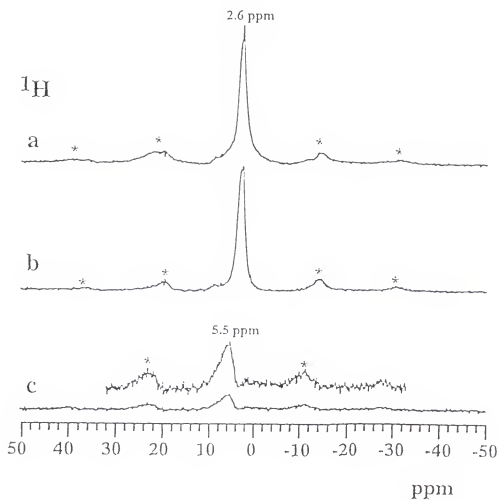


Figure 3-5 ^1H NMR Spectrum of SG- AlCl_2

Bronsted Acidity of AlCl_3

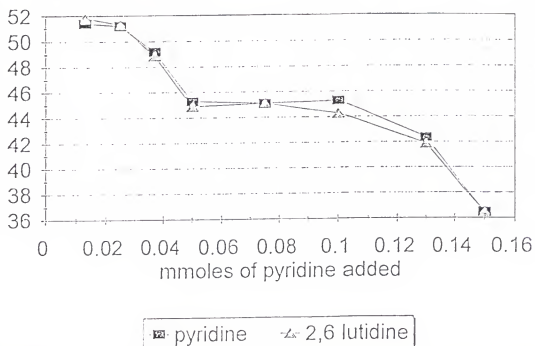


Figure 3-6 SG-AlCl_3 Calorimetric Titrations

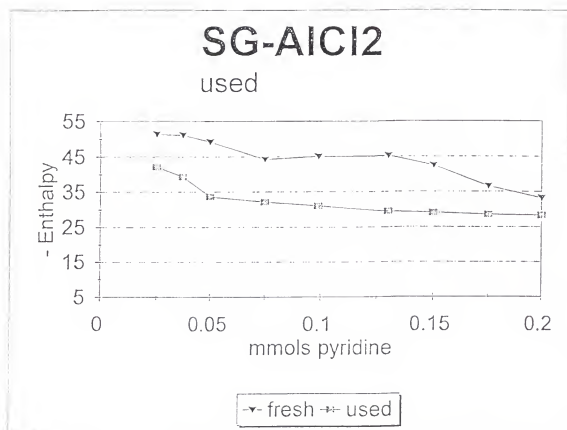


Figure 3-7 Calorimetric Titration of Used SG-AlCl₃

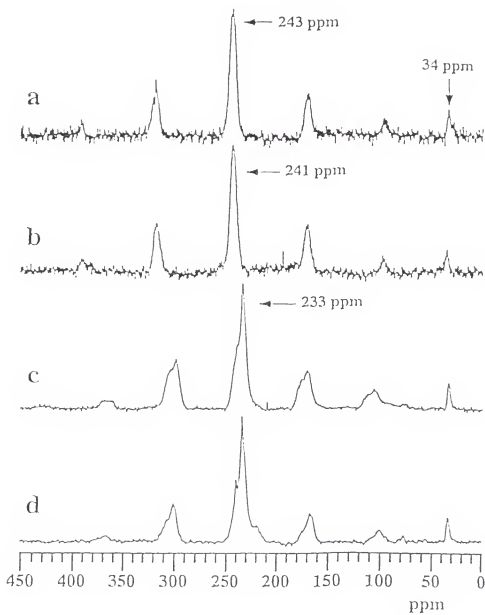


Figure 3-8 ^{13}C NMR of Acetone on SG-AlCl_3

CHAPTER 4

SYNTHESIS OF CAPROLACTAM USING SG-W

Introduction

Cyclohexanone oxime is an important chemical intermediate used for the production of ϵ -caprolactam, which is the monomer of Nylon 6. Commercially, it is synthesized by a liquid phase Beckman rearrangement of cyclohexanone oxime using a strong liquid acid such as sulfuric acid.⁶³ The commercial process uses stoichiometric amounts of sulfuric acid which results in the formation of large amounts of an ammonium sulfate by-product (1 -5 tons of ammonium sulfate produced per ton ϵ -caprolactam produced). Sulfuric acid has also come under environmental scrutiny in other processes such as alkylation of isobutane.⁶⁴ These considerations have led to interest in developing a solid acid catalyst that catalyzes the Beckmann rearrangement of cyclohexanone oxime in the gas phase. The use of a solid acid catalyst will eliminate the concerns with the current caprolactam production process.

Studies of the use of solid acid catalysts for the Beckmann rearrangement of cyclohexanone oxime to ϵ -caprolactam⁶⁵⁻⁶⁷ have been reported. Most of the previous studies reported rapidly declining selectivity's to ϵ -caprolactam with time on stream. The deactivation of the catalysts is attributed to coking.⁶⁵ The reaction calls for a strong not a super acid, becauseuse of a super acid results in the formation of other side products, and

cracking products. This has been shown in a study where strongly acidic aluminas yielded decreased caprolactam selectivity⁶⁵ compared to less acidic aluminas.

We have found that tungsten oxide supported on silica gel prepared by a controlled hydrolysis method is a strong acid. The controlled reaction and hydrolysis of tungsten hexachloride precursor with silica gel yields a catalyst that is acidic, well dispersed, and crystalline at low preparation temperatures. Other methods of supporting tungsten oxide on silica such as by thermal decomposition of ammonium tungstate^{53,69,70} require a high calcination temperature, which results in lower acidity and poorer dispersion.

In this paper we report a silica supported tungsten oxide catalyst that shows high activity for the vapor phase Beckmann rearrangement of cyclohexanone oxime to ϵ -caprolactam. Further, the catalyst activity did not substantially decline even after 40 hours. The effects of silica pore structure, reaction temperature, contact time, and cyclohexanone oxime carrier solvent were investigated.

Experimental

Catalyst Preparation

Several steps are employed for the preparation of the $\text{SiO}_2\text{-WO}_3$ (SG-W) catalyst. The first step is to properly condition silica gel which involves washing the silica gel (Davison 80-200 mesh) with 1M HCl, followed by deionized water, followed by 30% H_2O_2 , followed by deionized water. The washed silica is dried at 100°C overnight in vacuum and is allowed to stand exposed to the atmosphere for 1 day.

The conditioned silica is then refluxed for 2 hours in CCl_4 or CH_2Cl_2 solvent, and to this 0.0005 moles of tungsten (VI) chloride per gram of silica is added to the mixture.

The temperature is adjusted to 70°C, and this mixture is allowed to stir for 1 day. A color change is quickly apparent from blue to red to yellow which is characteristic of a change from tungsten hexachloride to the oxychloride to the oxide of tungsten. After 1 day the mixture is filtered, and the solid is washed with 1M HNO₃ followed by DI water. The yellow solid catalyst is dried and activated before use at 200°C in air.

Silica supported tungsten oxide was also prepared by thermal decomposition of ammonium tungstate at 500°C in air. A solution of ammonium tungstate corresponding to 10 wt.% WO₃ per gram silica was prepared in water. Silica gel was added to the solution and the water was evaporated. The resulting solid was calcined at 500°C in air to decompose the ammonium tungstate.

Reaction Conditions

Reaction of cyclohexanone oxime to ϵ -caprolactam was performed in a one time flow through reactor using the following conditions: 300°C, 0.5 grams of catalyst, 8 wt% cyclohexanone oxime in a solvent pumped into the reactor via syringe at 1 ml/hr with N₂ carrier gas flowing at 30 ml/min. Products were analyzed using gas chromatography and calibrated with known standards.

Surface Characterization

Raman spectroscopy was performed using a Dilor OMARS 89 spectrophotometer with a optical multichannel analyzer. Infrared studies were done by pressing KBr pellets and analyzed on a Nicolet model 5PC FTIR. Powder X-ray diffraction (XRD) studies were done using a Phillips X-ray diffractometer and a 2 θ range of 5 to 70 was obtained. X-ray photoelectric spectra (XPS) were obtained on a Kratos XSAM 800 spectrophotometer. Samples were mounted onto the adhesive side of aluminum tape and

scanned at 90 degrees using Al K α radiation. Scanning Electron Microscopy (SEM) analysis was done using a Joel 35C electron microscope with an acceleration voltage of 25 kv., studies were done using several magnifications.

Cal-ad Analysis of Solids

Calorimetric titrations were carried out as described previously.^{18,41} One gram of catalyst is slurried in cyclohexane solution and titrated calorimetricly with pyridine while stirring. The cyclohexane and pyridine reagents were distilled over P₂O₅ prior to use. After each injection of known amounts of pyridine solution, the heat evolved was measured. The heat is then used to determine the enthalpy. In the cal-ad process an adsorption isotherm is measured over the range of base additions used in the calorimetric titrations. The combined calorimetric titrations and adsorption data are analyzed to determine accurate K's (equilibrium constants), n's (moles of site), and ΔH 's (enthalpies).

UV-Visible Spectroscopy

Measurement of the free pyridine in solution in equilibrium with the solid in the calorimetric titration experiment was determined by UV-Visible spectroscopy as described previously.^{18,41} The UV-Visible spectroscopy of all sample was obtained using a Perkin-Elmer Lambda 6 UV-Vis spectrophotometer. Suprasil quartz cells were employed in the adsorption studies.

Results and Discussion

Catalyst Characterization

Most catalyst preparations involving tungsten oxide are made by using ammonium tungstate or other water soluble tungsten salts as the tungsten oxide precursor.⁷¹

Thermogravimetric analysis in this laboratory shows that a high temperature (500°C) is necessary to completely decompose the ammonium tungstate to tungsten oxide. At these elevated temperatures it is expected that the support (silica in this case) and tungsten oxide-hydroxide will become irreversibly dehydrated eliminating hydroxyl functionality, aggregating tungsten oxide species, and reducing the number of Bronsted acid sites.

The preparation described in this report provides a low temperature route to tungsten oxide on silica. The procedure involves a controlled reaction with tungsten hexachloride and the hydroxyl functionality of the silica support, followed by low temperature hydrolysis of the remaining chlorines. The low temperature synthesis results in a catalyst which retains more silica hydroxyl functionality and hydrates of tungsten oxide than thermal decomposition preparations. The hydrate of tungsten oxide is a "tungstic acid" ($\text{WO}_3 \cdot \text{H}_2\text{O}$) species, and a strong acid. The controlled hydrolysis uses the silica hydroxyl functionality as an anchoring site forming Si-O-W species.

The amount of hydration present on the silica surface is dependant on the temperature, time, and thermal pretreatment conditions of the silica. Therefore, the silica pretreatment is crucial to insure that the proper amount of hydroxyl functionality is attained. TGA analysis shows that a properly conditioned silica has 4.1% by weight water of hydration where as a unconditioned Davison silica has 8.6% by weight water of hydration.

The reaction of WCl_6 with silica gel makes it possible to apply a controlled amount of well dispersed tungsten to the surface of silica. The chemical reaction of WCl_6 with the silica surface results fromation of Si-O-W linkages, and the liberation of HCl gas.

When preconditioned silica is reacted with WCl_6 evolution of HCl indicates that the surface reaction is:



The use of a dry inert solvent prevents water from competing with the surface hydroxyl groups for hydrolysis of WCl_6 . The catalyst has also been prepared by a solid state reaction between the tungsten hexachloride and silica showing that the CCl_4 is not participating in the reaction.

Upon addition of WCl_6 to the silica- CCl_4 mixture the color changes from blue (WCl_6) to red (tungsten oxyhalide) to yellow ($\text{WO}_3 \cdot \text{H}_2\text{O}$) as intermediates form in the reaction of WCl_6 with silica's silanols. Collection and back titration of the HCl evolved from the preparation shows that 4 of the 6 chlorides have reacted with surface hydroxyls. This suggests that on average the anchoring species is $\text{W(OSi)}_4\text{Cl}_2$, and the 1M HNO_3 wash hydrolyzes the remaining chlorides. Washing with 1M HNO_3 will be shown to also facilitate the formation of crystalline tungsten oxide-hydroxide species on the surface of the silica. The result is a crystalline six coordinate silica tungsten oxide-hydroxide, $\text{W(OSi)}_4(\text{OH})_2$, which will be referred to as the SG-W catalyst.

SEM was used to investigate the tungsten oxide morphology, and dispersion over the silica surface. The catalyst as prepared consists of uniform size and shaped tungsten oxide clusters approximately 600 nm by 700 nm as viewed by SEM on the surface of silica as shown in Figure 4-1. The presence of clusters is consistent with our infrared analysis and a report using XPS.⁷³

The XPS spectrum of tungsten from the SG-W catalyst is shown in Figure 4-2 and is characteristic for WO_3 supported on silica.^{73,74} The broad nature of the spectrum was attributed to the presence of tungsten existing in non equivalent sites on the surface.⁷⁴ XPS intensity ratios have been shown to provide accurate information regarding overlayer-support dispersion⁷⁴ using Equation 4-2:

$$\text{(Equation 4-2)} \quad (I_p/I_s)_{\text{expt}} = (p/s)_b (\sigma_p/\sigma_s)$$

Where I_p is the intensity of the electrons from the promoter, I_s is the intensity of electrons from the support, $(p/s)_b$ is the bulk atomic ratio of the promoter and the support, and σ_p and σ_s are the Scholfield cross sections.⁷⁴ The model is used to predict XPS intensity ratios based on the bulk ratio of the metal and support. From this a theoretical value of 100% dispersion can be calculated and this value is an indication of the overlayer-support dispersion. XPS analysis of the intensity ratios of $\text{W}_{4f7/2}$ and Si_{2p} are shown in Table 1 and confirm the good dispersion of tungsten oxide on the silica. XPS atom ratios show the presence of 9.6 weight % tungsten oxide on the surface which compares favorably to the theoretical surface dispersion of 10.5 weight %. The slightly lower amount of tungsten oxide observed on the surface by XPS is likely due to the presence of tungsten oxide clusters as found by SEM. Using the Si 2p peak to correct the tungsten XPS spectrum for charging only tungsten VI is observed by XPS on the surface of the catalyst as evidenced by the $\text{W}_{4f7/2}$ peak at 35.4 eV. If tungsten (IV) was present a $\text{W}_{4f7/2}$ peak at 32.4 eV would also be observed and it is not observed.

An XPS spectrum of a sample prepared from thermal decomposition of ammonium tungstate is similar to that of the one shown in Figure 4-2 for the SG-W catalyst. However, the XPS intensity ratios of W 4f_{7/2} and Si 2p on the sample prepared by thermal decomposition of ammonium tungstate reveals a poorer dispersion as shown in Table 4-1. This poorer dispersion using a high temperature preparation is consistent with aggregation of surface species at high thermal treatments.

Table 4-1: XPS Intensity Ratios W_{4f}/Si_{2p} of Prepared Catalysts

| Catalyst Preparation | Theoretical dispersion | Experimental dispersion |
|--|------------------------|-------------------------|
| SG-W from WCl ₆ | 0.402 | 0.397 |
| From thermal decomposition of (NH ₄) ₂ WO ₄ | 0.402 | 0.266 |

The structure of the tungsten oxide species on the silica support was investigated using infrared and Raman analysis. Debate exists as to whether octahedral or tetrahedral coordination of tungsten is present on a tungsten oxide supported catalyst.⁷⁵ Crystalline WO₃ is an octahedrally coordinated and has a distorted ReO₃ structure. There are a great number of possible arrangements of these octahedra giving rise to both monoclinic and hexagonal forms of WO₃. Distortions of the ideal structure occur with introduction of waters of hydration and a large number of hydration levels are possible. The distortions occur by substitution of one of the axial octahedral oxygen's by H₂O. This leads to the formation of a terminal axial double bond opposite the H₂O which has double bond character and is designated W=O or the wolframyl species.

Tungsten is also known to exist in a tetrahedral arrangement as in Na_2WO_4 .

Preparation techniques or distortion during calcination causes supported tungsten oxide to adopt a tetrahedral geometry⁷⁶ which can be distorted. Li_6WO_6 which is octahedrally coordinated, changes when supported on silica and distorts to tetrahedral coordination.⁷⁶ Many studies have been done using Raman and infrared analysis on oxides of tungsten.⁷⁵⁻⁷⁷

The infrared spectra of our silica supported tungsten oxide catalyst has a band at about 950 cm^{-1} assigned to the $\text{W}=\text{O}$ stretching of the wolframyl species as shown in Figure 4-3. This band is detected near 1015 cm^{-1} in samples which are completely dry. This 1015 cm^{-1} band is not seen in our spectrum, indicating that after preparation and subsequent drying at 200°C in air not all of the associated waters of hydration are lost on SG-W. Indicating that the surface species is a tungsten oxide hydrate (hydroxide) or a $\text{WO}_3\cdot\text{H}_2\text{O}$ species. In addition to monomeric wolframyl species, cluster species of the type W_xO_y are possible. These species give rise to a band at about 700 cm^{-1} . It can be seen in Figure 1 that the catalyst as prepared does possess tungsten oxide clusters and confirms the SEM results. Upon increasing the tungsten oxide loading the band at 700 cm^{-1} increases in intensity. This is consistent with other reports which indicate the most active loading of tungsten oxide on a high surface area support is about 10%, which corresponds to a monolayer on a support with a surface area of approximately $300\text{ m}^2/\text{g}$.⁷¹ The band at about 800 cm^{-1} is associated with $\text{W}-\text{O}$ stretching mode in structures similar to $\text{WO}_3\cdot\text{H}_2\text{O}$, and correspond to structures where tungsten is in the octahedral environment.

Raman spectroscopy shows characteristic features for both tetrahedral and octahedral coordination of tungsten. The peaks centered at 680 cm^{-1} and 250 cm^{-1} are attributed to octahedral tungsten, specifically to $\text{WO}_3\cdot\text{H}_2\text{O}$ in which the ideal octahedron is

distorted.⁷⁸ In our spectrum a very weak peak is observed at 940 cm^{-1} which is assigned to tungsten in tetrahedral coordination.⁷⁶ Tungsten oxide coordinated in a tetrahedral environment is reported to exhibit a Raman band at about 930 cm^{-1} . This band can be shifted due to support interaction or by distortion of the ideal tetrahedron by association with water as discussed earlier. The Raman spectrum of SG-W compares well with the reported Raman spectra for $\text{WO}_3\cdot\text{H}_2\text{O}$ ^{76,78} and based on the Raman spectrum peak intensities it is concluded that only minor amounts of tetrahedral tungsten oxide are present. The major coordination of tungsten is octahedral on the SG-W catalyst.

Powder XRD analysis of SG-W and a solid prepared of WO_3 from thermal decomposition of $(\text{NH}_4)_2\text{WO}_4$ on silica are shown in Figure 4-4a and 4-4b. The diffractograms of both are characteristic of tungsten oxide, and their associated hydrates.⁷⁹ The crystallinity of SG-W is unexpected since in most cases high temperature calcination is required to impart crystallinity. Treating amorphous tungsten oxide clusters with a strong acid causes the clusters to become crystalline cluster species.⁸⁰ To confirm that the nitric acid wash was indeed causing crystallinity, a powder XRD pattern of a sample prepared by hydrolysis of WCl_6 without a HNO_3 wash was obtained. As shown in Figure 4-4c is this sample was amorphous.

A cal-ad analysis was carried out on the SG-W catalyst, a tungsten oxide supported silica prepared by thermal decomposition of ammonium tungstate, and silica gel¹⁸ and the results are shown in Table 4-2. Earlier research from this laboratory has reported that the cal-ad procedure determines the number(n_i), equilibrium constant (K_i), and strength (ΔH_i , enthalpy) of the donor acceptor interaction for different acid sites on solids.^{18,41} The procedure involves simultaneously analyzing the data from the calorimetric

titrations and adsorption experiments with a donor like pyridine.^{18,41} The subscripts (i) on the above quantities refer to sites involved, where $i=1$ would be the first site describing the strongest acid sites, and $i=2$ the next strongest site and so on. The cal-ad measurements are carried out in a non interacting hydrocarbon solvent whose molecules are close in molecular mass to those of the donor to cancel out any contribution of a dispersion component to the measured enthalpy. The cal-ad analysis procedure produces meaningful equilibrium constants, enthalpies, and number of sites by simultaneously analyzing the data from the calorimetric titrations with pyridine and the adsorption experiments.^{18,41} The results show that the second site enthalpies are the same within the experimental error of (± 1 kcal/mole), but the enthalpies of the first sites differ. The strength of the first site for the SG-W catalyst is more acidic. This could be due to the dehydration of the ammonium tungstate prepared catalyst acid sites caused by the high calcination temperature. Calorimetric titration of WO_3 (from Aldrich) and H_2WO_4 (from Aldrich) with pyridine were done since they are suspected to be the active species on the surface. The calorimetric titration without the adsorption analysis provides approximate enthalpies upon small additions of pyridine.⁴¹ If $K_1 \gg K_2$ then small amounts (<25 μ moles/g) of all the basic probe (pyridine) would be adsorbed onto the strongest ($-\Delta H_1$) site, and be fully complexed. This measured $-\Delta H_1$ is representative of the $-\Delta H_1$ that would be found by cal-ad analysis, and gives a accurate determination of the strength of the solid, but no indication of the n 's or K 's. WO_3 was found to have an enthalpy of 10 kcal/mole, H_2WO_4 had a enthalpy of 17 kcal/mole. Both ammonium tungstate and SG-W catalyst

preparations had stronger acidic sites indicating that support-tungsten oxide interactions are providing increased acidity.

Comparison of n_1 for the solid prepared from ammonium tungstate and the SG-W catalyst shows that the SG-W catalyst has a much larger n_1 . 0.5 mmoles of tungsten was used to prepare both catalysts, for SG-W all of the 0.5 mmoles is accounted for by n_1 and n_2 . The $-\Delta H_1$ and $-\Delta H_2$ for SG-W are greater than the value for silica gels strongest site showing that all the tungsten has gone to sites that have enhanced acidity (the tungsten is well dispersed). Whereas, for the solid prepared from ammonium tungstate only about 50% of the total tungsten has gone to sites that have enhanced acidity as compared to silica gel, which may be a reflection of the dispersion.

Table 4-2: Cal-Ad Analysis of Solid Acids

| Catalyst | $-\Delta H_1$ kcal/mole | K_1 l/mole | n_1 moles/g | $-\Delta H_2$ kcal/mole | K_2 l/mole | n_2 moles/g |
|---|----------------------------|-------------------|----------------------|----------------------------|-------------------|----------------------|
| silica | 12.6 | 1.7×10^4 | 8.6×10^{-4} | 5.3 | 3.2×10^2 | 8.6×10^{-4} |
| SG-W | 31.7 | 6.8×10^8 | 6.5×10^{-5} | 16.2 | 7.1×10^2 | 4.1×10^{-4} |
| $(\text{NH}_4)_2\text{WO}_4$ on silica | 27.4 | 1.2×10^9 | 1.6×10^{-5} | 17.8 | 5.8×10^3 | 2.4×10^{-4} |

Catalytic Studies for the Production of Caprolactam

Effect of solvent. Figure 4-5 shows the cyclohexanone oxime conversion and ϵ -caprolactam selectivity over the SG-W catalyst feeding a solution of 8 wt.% cyclohexanone oxime in benzene solvent. The other products produced are cyclohexanone and minor amounts of aniline which is consistent with other reports using solid acids for this reaction.⁶⁵ Initially, the selectivity was near 90% for ϵ -caprolactam but

declined to 78% after 10 hours and 60% after 25 hours. After 25 hours the catalyst which was initially yellow in color was visually coked (black in color) and was found to have 9.3 % coke and 1.1 % nitrogen. The cyclohexanone oxime conversion was 99% throughout the entire reaction time.

The catalyst was treated at 500°C for 8 hours in air to remove the coke (0.4% carbon and 0.0% nitrogen after regeneration), after which time the color was restored to yellow. The regenerated catalyst was retested at the same conditions. The conversion of the oxime was 99% the entire testing time of 20 hours, but the initial selectivity to ϵ -caprolactam initially at 85% dropped to 69% after 12 hours and to 53% after 20 hours. The regenerated catalyst came back to near the original activity as shown in Figure 4-6. This loss of activity is due to the loss of acid sites either during the high temperature regeneration or during the course of the reaction and will be discussed in greater detail in the deactivation section.

A sample of amorphous SG-W catalyst that was not HNO_3 washed was tested for caprolactam activity using a 8 wt% oxime in benzene solution, and 93% conversion with 70% selectivity to caprolactam was found which is poor compared to the 99% conversion and 90% selectivity to caprolactam of the HNO_3 washed SG-W catalyst at the same conditions. This shows that the crystallinity of the SG-W catalyst is a necessary condition to obtain high activity.

Deactivation is the main limitation for solid acid catalysts use in the Beckman rearrangement of cyclohexanone oxime to caprolactam. Thus, in order to try to extend the lifetime of the SG-W catalyst we investigated the effect of changing the solvent used

to deliver the cyclohexanone oxime while keeping all other conditions constant. The conversion of the oxime was 99% for all the solvents tested, but as shown in Figure 4-6 the solvent choice had an effect on the selectivity of the reaction for ϵ -caprolactam.

The use of methanol or acetonitrile as the cyclohexanone oxime solvent increased the selectivity of the tungsten oxide catalyst for caprolactam as compared to methylene chloride and benzene. A possible explanation for the solvents effect is its ability to increase the desorption rate of the caprolactam product decreasing the probability of the caprolactam opening to form polymer on the catalyst surface. The less basic solvents benzene or methylene chloride are not as effective in displacing caprolactam. This proposal should be manifested in the amount of coking for the different solvents. As shown in Table 4-3 the use of polar, more basic solvents acetonitrile and methanol resulted in the formation of the least amount of coke. The activity of this catalyst using methanol or acetonitrile as the oxime solvent is as good as any catalyst currently described in the literature.

Table 4-3: Effect of Oxime Solvent on Amount of Carbon on Used SG-W's After 20 hrs.

| Solvent | % Carbon on SG-W's surface |
|--------------------|----------------------------|
| Methanol | 4.6 |
| Acetonitrile | 4.4 |
| Benzene | 9.3 |
| Methylene chloride | 12 |

Methanol was used as the cyclohexanone oxime solvent while keeping all other conditions constant to investigate the catalysts lifetime and regeneration. The catalyst

lifetime was longer as shown in Figure 4-6, but coking still leads to a slow loss in selectivity. Upon removal of the coke by thermal treatment, the activity was 99% conversion of the oxime but only 88% selectivity to caprolactam. It appears as though the active sites on the catalyst are lost regardless of the solvent, and removal of carbon by thermal heating does not restore these sites.

Deactivation Mechanisms and Regeneration

The used catalysts contained carbon and nitrogen on the surface, while the fresh catalyst contained no nitrogen on its surface. The nitrogen suggests that the likely course of deactivation is from the polymerization of the caprolactam on the surface. The amount of nitrogen increased as the amount of carbon detected, and it increased with reaction time. This is a further indication of the presence of polymeric material on the surface. This polymerized caprolactam deactivated the active sites and led to the decrease in caprolactam selectivity. A study by Curtin⁶⁵ also reports the presence of polymerized caprolactam on the surface of their catalyst.

The Beckmann rearrangement mechanism requires acid sites. The loss of acid sites on the catalyst as a result of carbon formation during the reaction or during the regeneration process could lead to a lower activity. Cal-ad analysis of the fresh and used catalyst with regeneration confirms that acid sites are lost during reaction as shown in Table 4-4.

Table 4-4: Cal-Ad Analysis of Fresh and Regenerated SG-W Catalysts.

| Catalyst | $-\Delta H_1$ kcal/mole | K_1 l/mole | n_1 moles/g | $-\Delta H_2$ kcal/mole | K_2 l/mole | n_2 moles/g |
|---------------|----------------------------|-------------------|----------------------|----------------------------|-------------------|----------------------|
| SG-W fresh | 31.7 | 6.8×10^8 | 6.5×10^{-5} | 16.2 | 7.1×10^2 | 4.1×10^{-4} |
| SG-W used | 27.9 | 5.3×10^9 | 2.4×10^{-5} | 18.0 | 2.4×10^3 | 4.6×10^{-4} |

The ΔH_1 site in the regenerated catalyst is similar to that of the ΔH_1 site in the ammonium tungstate silica catalyst. This seems to indicate that the thermal removal of the carbon results in a surface that is similar to that achieved by thermal decomposition of ammonium tungstate, and the strongest sites are lost. High temperature regeneration results in an irreversible loss of acid sites by dehydration. Such an irreversible dehydration is known to occur with silica gel where silanol groups (Bronsted acid sites) are lost by high temperature treatments.⁸¹ It could be those strongest sites that are responsible for the very high initial selectivity to caprolactam. To further investigate this possibility a ammonium tungstate prepared catalyst of the same loading of tungsten was used with methanol as the solvent and all other conditions the same. After 10 hours the conversion of the oxime was 99% and the selectivity to caprolactam was 86% which is very close to the 88% selectivity found for the regenerated SG-W catalyst. Low temperature regeneration's were attempted but it was determined that in order to remove the carbon from the surface a regeneration temperature of 500°C is required. During the course of the reaction these strong acid sites on fresh SG-W sites become lost due to carbon and the

selectivity drops as a function of the carbon as shown in Figure 4-7. Upon regeneration these sites are not fully restored and hence the original selectivity is not achieved.

Another possibility is that during the course of the reaction or as a result of regeneration, agglomeration of active tungsten oxide has occurred. This possibility could also result in the loss of strong acid sites since fewer sites would be possible. SEM analysis of the used, and regenerated catalyst is shown in Figure 4-8, and it can be seen that aggregation has occurred. Therefore, it is proposed that the inability to completely regenerate the SG-W catalyst is a result of the inability to regenerate all the surface's strong acid sites.

Effect of Silica Pore Size

Using the same reaction conditions (methanol oxime solvent) the tungsten oxide catalyst made on a different silica gel support was studied. This new support (Fisher silica gel) has different surface characteristics and porosity than the Davison support, and Table 4-5 summarizes the support differences.

Table 4-5: BET Analysis for Different Silica Gels Used.

| Silica support | Surface Area (m^2/g) | Pore Volume (cc/g) | Ave. Pore Size (Å) |
|----------------|--|-------------------------------|--------------------|
| Davison | 265 | 1.1 | 175 |
| Fisher | 570 | 0.35 | 28 |

Consistent with others findings on the effect of support on caprolactam activity.⁶⁵ The support with smaller pores, Fisher, was inferior in selectivity to caprolactam with similar conversions of cyclohexanone oxime as compared to Davison supported tungsten (VI) oxide catalyst (SG-W) as shown in Figure 4-9. It is believed that the smaller pore

supports favor the formation of the smaller transition state side products (cyclohexanone and aniline)⁶⁵ leading to a drop in selectivity as the catalyst pores become smaller from carbon plugging. Smaller pores can also lead to longer retention times of the products on the solid.

Effect of Temperature and Feed Rate

The effect of temperature, oxime feed rate, and carrier gas flow rate were investigated by using methanol as the solvent for 8 wt% cyclohexanone oxime and other conditions constant. Increasing the N₂ carrier gas flow rate to 50 ml/min results in a drop in selectivity of caprolactam to 86% with 87% conversion of cyclohexanone oxime initially for 10 hours. When the N₂ flow rate was dropped to 10 ml/min the selectivity to caprolactam dropped to 82% for 10 hours of reaction with 99% cyclohexanone oxime conversion. The drop in the activity for caprolactam production when the flow rate is changed shows that the contact time of the gas phase oxime plays a significant role in the catalysis.

The variation of oxime feed rate was also investigated. It was found that doubling the feed rate to 2 ml/min results in a drop of cyclohexanone oxime conversion to 71%, but the selectivity to caprolactam remained at 90% after 10 hours. Halving the feed to 0.5 ml/min in methanol does not effect the conversion of cyclohexanone oxime or the selectivity to caprolactam for the first 10 hours of the reaction as compared to the feed rate of 1ml/min.

The effect of temperature on the reaction was carried out by varying the reaction temperature to 250°C, and 350°C. At 250°C the conversion of the oxime dropped to 50% (at 300°C conversion 99%) but the selectivity to caprolactam dropped only slightly to

89%. At 350°C the conversion of the oxime was still 99% but the selectivity to caprolactam drops to 74% after 10 hours compared to the selectivity's of over 90% at 300°C. Also, at the higher temperature the reaction products become noticeably yellow in color and some unidentified product peaks appear. The effect of temperature on caprolactam production over a solid acid was described in a report by Ushikubo⁶⁵ and our results are consistent with their findings.

Use of Supports Other Than Silica

The effect of changing the support used to react with WCl_6 was investigated by using alumina and titania as the supports. The same loading of tungsten was used to impregnate the alumina and titania while all other reaction conditions were kept constant. After ten hours of reaction the alumina supported catalyst had 94% conversion of cyclohexanone oxime but only 40% selectivity to caprolactam, and 54% selectivity to cyclohexanone (with silica 99% conversion oxime and 90% selectivity to caprolactam). The titania supported catalyst after 10 hours had 99% conversion of cyclohexanone oxime but only 27% selectivity to caprolactam, and 71% selectivity to cyclohexanone. These findings lead to the conclusion that silica is the best support for this application.

Conclusion

We have shown that controlled hydrolysis of WCl_6 leads to a superior preparation of tungsten (VI) oxide supported silica gel catalyst. A catalyst prepared in this way retains more Bronsted acidity and has a better dispersion than conventional methods. This catalyst was shown to have high activity for the Beckman rearrangement of cyclohexanone oxime to caprolactam which is a valuable chemical intermediate. The lifetime and

selectivity of the catalyst can be affected by changing the reactant solvent. The use of methanol as the reaction solvent results in the least amount of coke formation and the longest catalyst lifetime. Other variables such as reaction temperature, feed rate of cyclohexanone oxime and catalyst support were also shown to effect the activity for caprolactam production.



Figure 4-1 SEM of SG-W

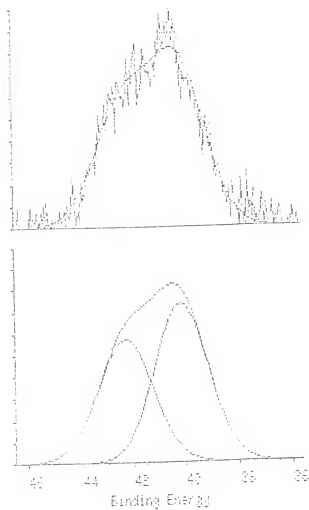


Figure 4-2 SG-W Tungsten 4f XPS

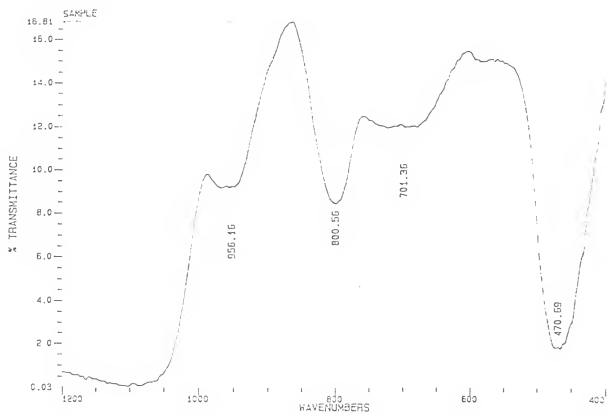
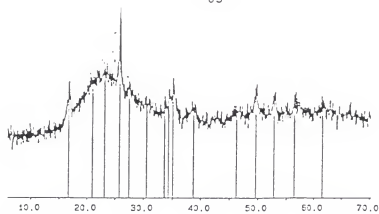
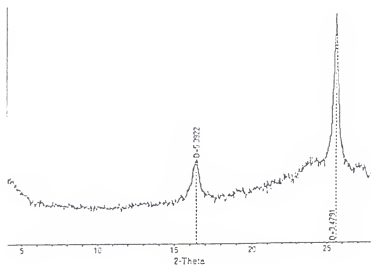


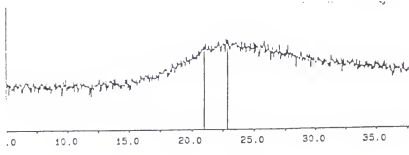
Figure 4-3 Infrared Spectrum of SG-W



(a)



(b)



(c)

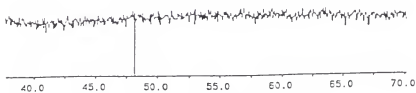


Figure 4-4 Powder XRD of SG-W

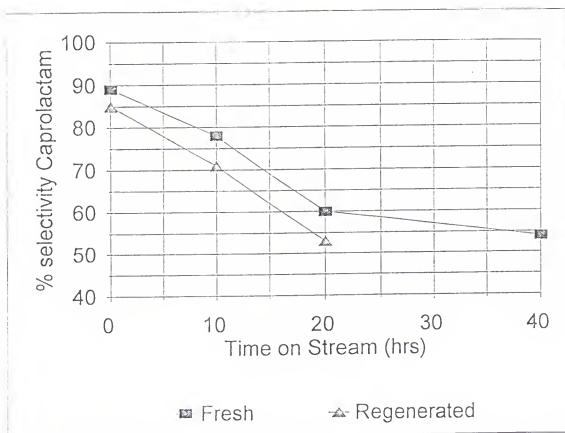


Figure 4-5 Caprolactam Synthesis on SG-W Using Benzene Solvent

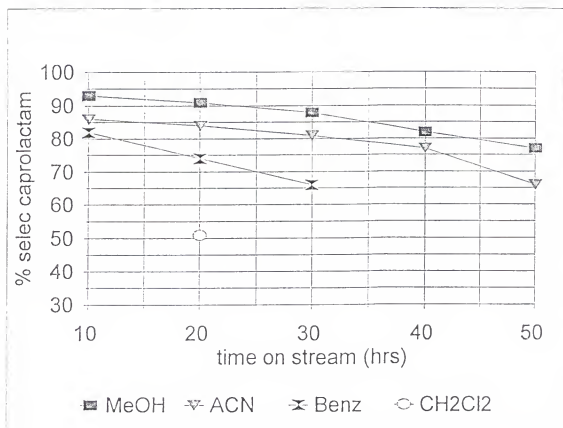


Figure 4-6 Effect of Solvent on Caprolactam Selectivity

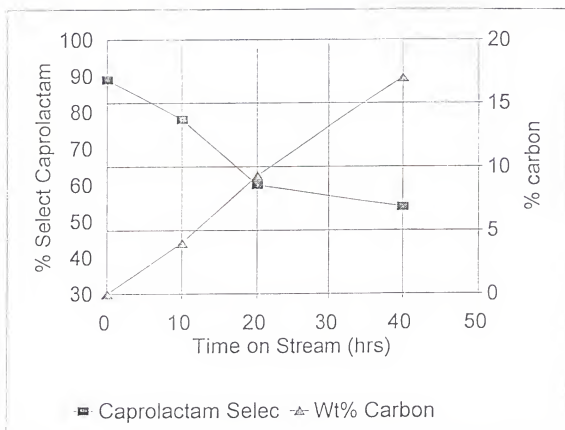


Figure 4-7 Effect of Carbon Deposits on Caprolactam Selectivity

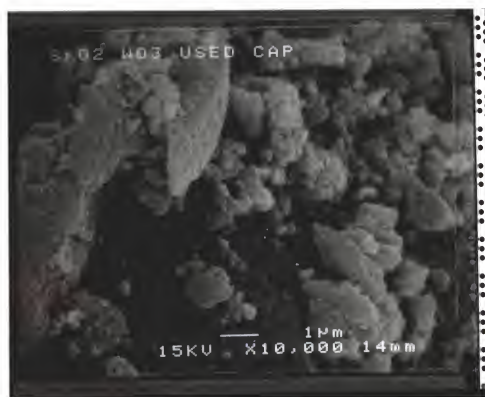


Figure 4-8 SEM of Used SG-W Catalyst

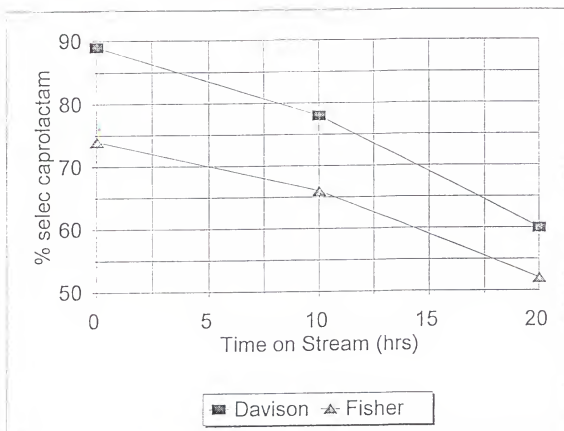


Figure 4-9 Analysis of Different Silicas

CHAPTER 5

HYDROGENATION OF BENZENE USING SG-W-Pt

Intorduction

Aromatics are being limited due to their effect in fuels on the formation of undesired emissions leading to health hazards.⁸² In order to meet the strict standards, refiners have been developing new hydrotreating catalysts. Benzene^{83,84} has been used as a model reactant for hydrogenation catalysts. The reaction mechanism for benzene hydrogenation is understood⁸⁵ and is assumed to be the mechanism for other aromatic hydrocarbon hydrogenations.

The use of acidic supports has been found to enhance hydrogenation rates over dispersed noble metal catalysts.⁸⁶ This is proposed to be due to noble metal - acidic support interactions, which leads to a enhanced activity as compared to the use of non-acidic supports. This increased activity is a result of spillover hydrogen and enhanced adsorption of the reactant onto the acidic sites.⁸⁷ Spillover is defined as the dissociative chemisorption of hydrogen on the noble metal, and the subsequent migration of atomic hydrogen to the surface of the support. As a result of spillover hydrogen from the noble metal site, the acidic support is able to perform hydrogenations which it otherwise would not be able to.

The application of hydrogenation catalysts is limited by their sulfur tolerance. Sulfur is known to poison noble metals catalysts and lead to significant deactivation.⁸⁸

Current commercial Pt/alumina catalysts normally require a severe hydrotreating pretreatment to reduce the sulfur concentration below 2 ppm.⁸⁹ It has been reported that the sulfur tolerance of a noble metal can be increased by using an acidic zeolite support.⁸⁸

We report the use of a silica supported tungsten oxide acid catalyst doped with platinum as a hydrogenation catalyst. This catalyst has unique hydrogen spillover properties due to the ease of formation of reduced tungsten oxide (H_xWO_x) sites from spillover hydrogen. Both the hydrogenation of benzene were carried out using this catalyst and its activity was compared to that of several other hydrogenation catalysts. In addition, its resistance to sulfur poisoning was investigated by using thiophene as a poison.

Experimental

Catalyst Preparation

The preparation of the silica supported tungsten oxide catalyst (SG-W)⁹⁰ and the silica supported tungsten oxide doped with platinum (SG-W-Pt) is done in a series of steps. Silica 80-200 mesh is conditioned as described in a previous report. The conditioned silica is refluxed in CCl_4 or CH_2Cl_2 solvent and 0.5 mmoles of tungsten hexachloride per gram of silica is added. The mixture is allowed to stir at 70°C overnight, then the solid is filtered off from the solvent. The resulting solid is washed with 1M HNO_3 and deionized water and a yellow solid is obtained which is the SG-W catalyst. To prepare the SG-W-Pt catalyst, the SG-W catalyst is impregnated with an aqueous solution of H_2PtCl_6 so that the resulting SG-W-Pt catalyst contains 0.2 wt% Pt.

The other catalysts used in this report were made by impregnating the supports with aqueous H_2PtCl_6 as to obtain the correct amount of Pt on the support.

Catalytic Testing and Surface Characterization

Catalytic hydrogenations were carried out using a flow reactor with 0.5 grams of catalyst, a feed of benzene supplied by a saturator at 70°C, H₂ carrier gas with a flow rate of 40 ml/min., and a reaction temperature varying from 25°C to 200°C. Poisoning studies were done by preparing solutions of benzene containing thiophene at the appropriate concentration for the reactant feed. Products were analyzed by gas chromatography and characterized with known standards.

SEM was performed on a Joel 35C electron microscope at several magnifications. X-ray photoelectric studies (XPS) were done using a Kratos XSAM 800 spectrophotometer. Samples were mounted on the adhesive side of sticky tape and scanned at 90 degrees. EPR spectra were collected at -77°C

Results and Discussion

SG-W-Pt Catalyst Characterization

SG-W has a BET surface area of 242 m²/g and SG-W-Pt has a surface area of 237m²/g, the starting Davison silica has a surface area of 265 m²/g. Only a small drop in surface area and pore volume has occurred as a result of preparation of the SG-W-Pt catalyst indicating that no significant pore blocking has occurred. This is a good indication that the dispersion of the active species on the silica is good since no significant loss of surface area or pore volume has occurred. SEM analysis confirms that the tungsten oxide is well dispersed and uniform throughout the sample. The approximate average dimensions of the rectangular shaped particles are 400 nm by 100 nm.

The catalyst undergoes a color change from green-yellow to deep blue when exposed to hydrogen (even at room temperature). The formation of non-stoichiometric oxides of tungsten (and molybdenum) as a result of partial reduction are known to cause the formation of “blue oxides”⁹¹ (H_xWO_{3-x} species) which are conductors. This is indirect evidence that the SG-W-Pt catalyst can activate and spillover hydrogen at room temperature. A sample of SG-W (no Pt added) does not undergo this color change when exposed to hydrogen even at elevated temperatures of 200°C. XPS analysis of the “blue oxide” and the untreated as prepared yellow-green SG-W-Pt catalyst was performed to ascertain any differences. The tungsten spectra are quite different, the hydrogen treated “blue oxide” SG-W-Pt catalyst shows the presence of two peaks for tungsten 4f_{7/2} while the yellow-green non hydrogen treated SG-W-Pt catalyst shows only one peak at 47.1 eV which corresponds to tungsten (VI) which is charge shifted. The SG-W-Pt catalyst hydrogen treated has peaks at 47.3 eV which corresponds to the same charge shifted peak observed for the non hydrogen treated sample, and one at 37.7 eV. The 37.7 eV peak corresponds to tungsten (VI) states which are not charge shifted to as great an extent. Since silica is an insulator any tungsten associated with the silica will be highly charge shifted resulting in the peak at 47.3 eV, which when charge corrected using the Si 2p peak, the W 4f_{7/2} peak is corrected to 36.2 eV matching the W (VI) literature value of 36.3 eV for tungsten oxide (WO₃).⁹² The other peak for the hydrogen treated sample could be the result of either a reduced form of tungsten, or less charge shifted tungsten species. It is not due to a reduced form of tungsten oxide because its binding energy does not match with any form of reduced tungsten oxide when charge corrected using the Si 2p

peak.⁹² The less charge shifted tungsten species on the sample is due to the formation H_xWO_{3-x} species which are conductors, which result in a less charge shifted species. By quantifying the amount of tungsten shifted and not shifted the percent tungsten associated with the Pt is found to be 43%. These we will show will be the sites responsible for the hydrogenation activity.

Catalytic Hydrogenation Activity

The activities for benzene hydrogenation using the platinum doped tungsten oxide catalyst (SG-W-Pt), the non platinum doped tungsten oxide catalyst (SG-W), and Pt doped on Silica are shown in Figure 5-1. Without the addition of platinum no activity is observed for benzene hydrogenation indicating that the tungsten oxide alone can not activate hydrogen. A much lower activity is found for the Pt on silica as compared to the SG-W-Pt catalyst which indicates that a interaction exists between the tungsten oxide and the hydrogen activated on the Pt. The high activity for the SG-W-Pt catalyst is attributed to the platinum activating the hydrogen and spilling it over to the tungsten oxide forming H_xWO_x species. This is evidenced by the change in color of the SG-W-Pt catalyst from green-yellow to deep blue. The formation of deep blue compounds from oxides of tungsten and molybdenum are known to occur due to the partial reduction of the oxide form its formal state of +6. In order to further confirm the presence of a partially reduced oxide state EPR experiments were conducted in which a sample of SG-W-Pt was treated with flowing H_2 at room temperature and its EPR signal was compared to that of SG-W-Pt untreated. The presence of a EPR signal with a approximate center field of 3300 Gauss, and a peak to peak width of 8 Gauss is detected for the H_2 treated sample indicating that a partial reduction of the tungsten oxide has occurred. The signal observed

is much similar to one found by other researchers for partially reduced tungsten oxide catalysts.⁹³

The activity of the SG-W-Pt for benzene hydrogenation is compared to other hydrogenation catalysts in Figure 5-1. The activity of the SG-W-Pt catalyst is as good or better than that of other catalysts for benzene hydrogenation (the only observed product is cyclohexane). To further investigate the potential of SG-W-Pt as a hydrogenation catalyst, the hydrogenation of tetrolin which has been shown to be a good industrial stimulant was performed. The SG-W-Pt catalyst was also active for hydrogenation of tetrolin.

In order for a hydrogenation catalyst to be considered commercially acceptable some tolerance to sulfur must be exhibited since sulfur is a contaminant in industrial feed streams. Thiophene has been shown to be a strong sulfur containing catalyst poison and a good stimulant for sulfur compounds found in industrial feed streams.⁸⁴ The SG-W-Pt catalyst was tested for its sulfur resistance by adding 200 ppm thiophene to a benzene feed and its activity was monitored as a function of time as shown in Figure 5-2. The resistance to sulfur was found to be about the same as that of Pt on alumina but far less resistant than for zeolite supported Pt catalysts. It has been found that zeolite supported Pt hydrogenation catalysts are very sulfur resistant, this resistance was attributed to the acidity of the zeolite support.⁸⁸ It is assumed that the sulfur poisons the Pt sites thereby reducing the catalysts ability to activate the hydrogen. It was speculated that the interaction of Pt with an acidic support somehow changes the Pt particles sulfur resistance. However, these findings suggest that acidity can not be the controlling factor since it has been found that SG-W has approximately the same acidity as zeolite HY as measured by

calorimetric titration with pyridine.⁹⁰ It is possible that the thiophene is poisoning the SG-W-Pt catalyst differently by somehow reducing the catalysts ability to not only activate hydrogen (on Pt) but also form the spillover species H_xWO_{3-x} . This would account for the great difference in sulfur resistance given the similar acidities of HY and SG-W.

Conclusion

A new silica supported tungsten oxide platinum (SG-W-Pt) catalyst is able to hydrogenate benzene and tetralin at low temperatures. It was shown that spillover hydrogen from the Pt sites onto the tungsten oxide sites results in the formation of a “blue oxide” H_xWO_{3-x} which is responsible for the activity. XPS studies found that 43% of the total tungsten associates with Pt, showing that spillover of hydrogen from the Pt is possible to tungsten oxides which are not directly next to the Pt site. The activity was shown to be superior to that of other commonly used hydrogenation catalysts. However, the addition of sulfur in the form of thiophene quickly deactivates SG-W-Pt's hydrogenation activity.

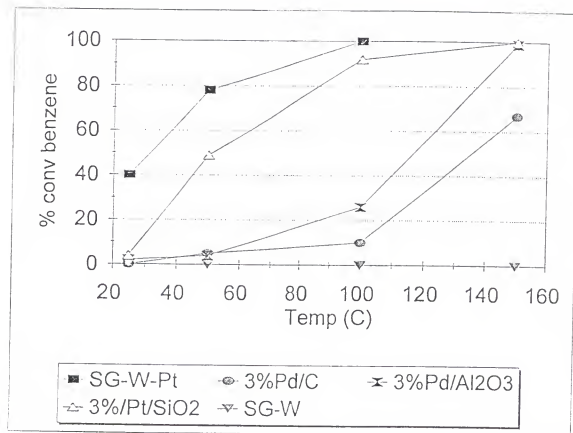


Figure 5-1 Benzene Hydrogenation on SG-W-Pt

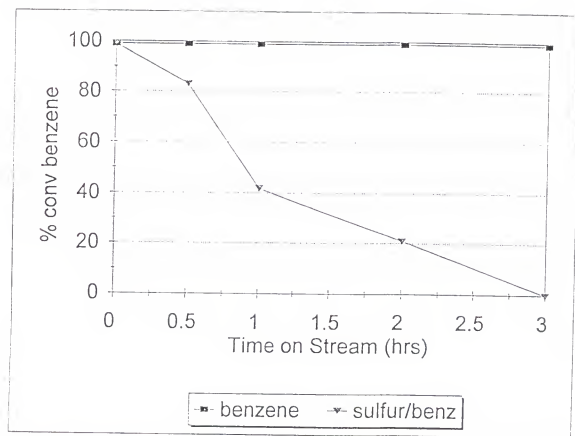


Figure 5-2 Effect of Sulfur on Benzene Hydrogenation

CHAPTER 6 SYNTHESIS AND CHARACTERIZATION OF SG-WS

Introduction

Design of new strong solid acid catalysts is essential due to environmental concerns with current acid catalysts such as H_2SO_4 , and for the production of high octane branched paraffins from linear paraffins.⁹⁴ The use of strong solid acid catalysts are active research areas for cracking, isomerization dehydration, alkylation, and other applications.⁹⁵ The importance and advantages of solid acid catalysts has been reported.⁹⁶ Currently, the strongest solid acids are halide based acids.⁴⁰ These acids although strong are air sensitive and deactivate by loss of HX (X is a halide) making them unable to be thermally regenerated in air. For these reasons the development of strong solid acid catalysts that are oxide based is desirable.

The cracking and isomerization of n-heptane is generally used as a test reaction to investigate solid acids⁹⁷ because it is a relatively difficult reaction to acid catalyze. The formation of carbocations are accepted to be the intermediates during the cracking, and isomerization of heptane.⁹⁸ A common connection between both cracking and isomerization products is the attack of a Bronsted acid site on a carbon-hydrogen bond to form a carbonium ion, which loses H_2 and leaves a carbenium ion on the surface.⁹⁹

Bifunctional catalysts combining hydrogenation-dehydrogenation, and Bronsted acid sites are used in hydrocarbon isomerization and cracking process. Such catalysts are

particularly useful for the isomerization of alkanes in order to enhance octane numbers. In contrast to most monofunctional catalysts a cooperation exists between the acid sites and the hydrogenation sites which leads to enhanced catalytic activity and high selectivity to isomerized products. Cracking takes place when branched alkylcarbenium ions are cleaved by β -scission. The distribution of hydrogenation and acid sites on the catalyst surface influences the activity and selectivity of hydrocarbon reactions.¹⁰⁰

In this study we report the synthesis of a new tungsten oxide sulfate promoted catalyst supported on silica (SG-WS catalyst), and a bifunctional SG-WS catalyst doped with platinum (SG-WS-Pt catalyst). The conversion of heptane was used as a test reaction to evaluate the catalysts activity and selectivity for hydrocarbon conversions. The preparation, surface structure, and acidity of the SG-WS and SG-WS-Pt catalyst was investigated.

Experimental

Cal-Ad Analysis of Solid Acids

The calorimetric titration procedure is described in previous reports.^{18,62} One gram of solid acid slurried in cyclohexane solution is reacted with pyridine while stirring. Pyridine and cyclohexane reagents were distilled over P_2O_5 prior to use. After each injection of small known concentrations of pyridine solution, the heat evolved was measured. This heat is then converted to an enthalpy. UV-visible spectroscopy is used to determine the amount of pyridine free in solution over the base additions used in the calorimetric titrations, and an adsorption isotherm is obtained. In the cal-ad analysis the

adsorption isotherm and calorimetric data are analyzed to produce K 's (equilibrium constants), n 's (moles of sites), and ΔH 's (enthalpies).

Catalyst Preparation

The $\text{SiO}_2\text{-WO}_3\text{-SO}_4$ (SG-WS) catalyst is prepared in a series of steps. First, the silica gel is conditioned to obtain the correct amount of hydration. The conditioning involves first washing the silica (Davison 80-200 mesh) with 1M HCl followed by deionized water followed by 30% H_2O_2 and then deionized water again. The washed silica is then dried at 100°C in vacuum overnight. Finally, the silica is allowed to stand out to the open atmosphere for 1 day. The conditioned silica is then refluxed for 2 hours in CCl_4 or CH_2Cl_2 solvent. To this 0.5 mmoles of WCl_6 per gram of silica is added, and the temperature is adjusted to 70°C. This mixture is stirred for one day and the color changes from blue to red to yellow. After one day, the solid is filtered off (this catalyst SG-W is described in a previous report⁹⁰) and washed with 1M HNO_3 followed by deionized water. The washed solid is dried at 100°C overnight in air. Finally, the dried solid is treated with 1M H_2SO_4 by adding the 1M H_2SO_4 (about 3ml per gram of solid) solution to a filter paper containing the solid, and is allowed to gravity filter. The resulting solid is the SG-WS catalyst and is dried at 200°C in air prior to use.

0.2 wt.% Pt was added to the SG-WS catalyst by impregnating SG-WS with a H_2PtCl_6 solution. The resulting catalyst was darker in color and quickly changed to blue when exposed to hydrogen indicating the formation of a $\text{H}_x\text{WO}_{3-x}$ species.

Reaction Conditions

The isomerization and cracking of heptane was done using a flow reactor system at 300°C, 1 gram of catalyst, 5 ml/min of carrier gas (either N₂ or H₂) saturated with a saturator of heptane at 70°C. Products were analyzed using gas chromatography with known standards.

Surface Science

Powder X-ray diffraction (XRD) studies were performed using a Phillips X-ray diffractometer and a 2 θ range of 5 to 70 was obtained. X-ray photoelectric spectra (XPS) were obtained on a Kratos XSAM 800 spectrophotometer. Samples were mounted onto the adhesive side of aluminum tape and scanned at 90 degrees, using Al K α radiation. Scanning Electron microscopy (SEM) analysis was done using a Joel 35C electron microscope with an acceleration voltage of 25 kv. EPR spectroscopy was done at room temperature and -77°C.

Results and Discussion

Characterization of Solid Acids

Previous research from this laboratory has reported that the cal-ad procedure accurately determines the number (n), equilibrium constants (K), and strengths (ΔH) of different acid sites on solid acids.^{18,62} The cal-ad analysis of SG-WS is shown in Table 6-1 as well as other ΔH_1 values for other solid acids as studied by cal-ad analysis using pyridine as the probe.

Table 6-1A: Cal-Ad Analysis for SG-WS Catalyst

| | |
|------------------------------------|------------------------------------|
| $n_1 = 1.7 \times 10^{-4}$ moles/g | $n_2 = 5.3 \times 10^{-4}$ moles/g |
| $K_1 = 7.5 \times 10^{10}$ | $K_2 = 1.2 \times 10^7$ |
| $-\Delta H_1 = 40.6$ kcal/mole | $-\Delta H_2 = 34.8$ kcal/mole |

Table 6-1B: $-\Delta H_1$ Values for Various Solid Acids.

| Catalyst | $-\Delta H_1$ (kcal/mole) |
|-------------------------------------|---------------------------|
| HZSM-5 ⁴¹ | 41 |
| HY | 32 |
| Sulfated Zirconia ⁶² | 31 |
| SG-AlCl ₃ ¹⁰¹ | 51 |
| SG-WS | 41 |
| SG-W ⁹⁰ | 30 |
| silica gel ¹⁸ | 12 |

The analysis shows that the acidity of the strongest sites on SG-WS (sulfated tungsten oxide catalyst) are stronger than those on sulfated zirconia, and HY, weaker than those on SG-AlCl₃ (aluminum chloride supported on silica gel catalyst⁴⁰), and about the same as those of HZSM-5.⁴¹ The ΔH_2 site of 33.9 kcal/mole agrees well with the value of 31.8 kcal/mole for the strongest site on SG-W⁹⁰ (tungsten oxide not sulfated) indicating that the second sites on SG-WS are the sites where the tungsten and sulfate are not associated, and that the strongest ΔH_1 sites are generated by sulfation of some tungsten oxide sites. A

total of 0.5 mmoles of tungsten oxide is applied in the preparation, and n_1 of SG-WS shows that only 34% of the tungsten oxide has formed the strong sulfated sites.

SEM was used to investigate the effects of sulfating on the morphology and dispersion of the SG-WS catalyst. By counting particles present at a constant magnification one can get an approximate idea of the surface dispersion of the tungsten oxide on the silica.¹⁰² SEM investigation of the SG-WS catalyst precursor SG-W⁹⁰ (SiO_2 - WO_3 no sulfate) as prepared shows mostly uniform size and rectangular or circular shaped tungsten oxide crystals of 100 nm by 400 nm as shown in Figure 6-1a. The magnification was 10,000x and approximately 350 particles are present in the frame. Upon sulfating of SG-W clustering of the tungsten oxide crystals is observed by SEM (Figure 6-1b), and they are no longer as uniform in size or shape as on SG-W. The crystals appear to be larger and more ellipsoidal in shape and have approximate average dimensions of 600 nm by 800 nm. The magnification is 10,000x and approximately 200 particles are present in the frame, the drop in particle number per frame is due to the clustering of the smaller particles that were present before sulfating. However, the dispersion of these clusters is uniform throughout the silica gel surface.

BET analysis for the solid acids and for Davison silica gel which is used to prepare SG-WS is shown in Table 6-2. The preparation of the SG-WS catalyst does not result in any significant loss of surface area or pore volume and indicates that little pore blocking has occurred during preparation and the tungsten oxide is dispersed on the surface.

Table 6-2: BET Analysis of SG-W, and SG-WS Catalysts

| Catalyst or Support | Surface Area (m ² /g) | Pore Volume (cc/g) |
|---------------------|----------------------------------|--------------------|
| Davison Silica | 265 | 1.1 |
| SG-W ¹⁰ | 242 | 0.96 |
| SG-WS | 231 | 0.92 |

Despite the morphological changes the structure of the SG-WS catalyst as observed by infrared and Raman analysis remains unchanged from that of SG-W which is distorted octahedral coordination of tungsten on the surface of silica.⁹⁰ Powder XRD analysis of SG-WS catalyst shows characteristic d spacing for crystalline WO₃ and its hydrates WO₃·H₂O.¹⁰³ From these results we conclude that the function of the sulfate is to enhance the acidity as no significant structural rearrangement of the tungsten oxide occurs.

The XPS spectrum shown in Figure 6-2 for tungsten is characteristic for WO₃ on silica, and the broad nature of the spectrum is attributed to tungsten existing in non equivalent surface sites.^{90,104} This could be due to the interaction of tungsten with sulfate or with the silica surface. Upon correcting the obtained spectra for charging using the Si 2p peak (Si 2p in the SG-WS catalyst was observed at 108.7 eV, the charge corrected value is 103.2 eV¹⁰⁵), XPS shows that no tungsten (IV) is present on the catalyst as prepared, only tungsten (VI) as evidenced by the charge corrected W_{4f7/2} peak position at 35.4 eV. and the absence of a charge corrected W_{4f7/2} peak at 32.5 eV.¹⁰⁵

The SG-WS-Pt catalyst shows the same infrared, and powder XRD spectrum, as that of SG-WS. Low temperature EPR of SG-WS shows no signal even when the catalyst is treated with H₂ at room temperature as shown in Figure 6-3a, which is expected for

diamagnetic tungsten (VI). However, when SG-WS-Pt is treated with H_2 at room temperature the color changes from green-yellow to blue which is due to the formation of H_xWO_{3-x} ($H_{0.12}WO_{2.88}$) species.¹⁰⁶ A signal is now observed in the low temperature EPR spectrum as shown in Figure 6-3b confirming that the tungsten (VI) has been partially reduced.¹⁰⁷ The mechanism of the formation of the H_xWO_{3-x} species is thought to be due to spillover hydrogen. Platinum is known to activate hydrogen^{108,109} by dissociating it on its surface. The hydrogen can then “spillover” to a surface adjacent to the platinum, in this case tungsten oxide forming H_xWO_{3-x} sites. Spillover hydrogen has been shown to be effective in enhancing hydrocarbon isomerization and cracking activity.¹⁰⁹

XPS of a SG-WS-Pt sample treated with hydrogen shows that the S2p and W4f peaks have been split into two charging components as shown in Table 6-3.

Table 6-3: XPS Peak Positions and Peak Area's for SG-WS-Pt Catalyst

| Catalyst | W 4f _{7/2} charging | W 4f _{7/2} less charging | S 2p charging | S 2p less charging | Si 2P |
|----------|---------------------------------|--------------------------------------|------------------|-----------------------|----------|
| SG-WS | 41.9 eV | ----- | 172.2 eV | ----- | 108.7 eV |
| SG-WS-Pt | 47.3 eV | 37.7 eV | 177.6 eV | 165.2 eV | 114.3 eV |

The more highly charged components are at 177.6 eV for S 2p and 47.3 eV for W4f_{7/2}. The less charged components are at 165.2 eV for S 2p and 37.7 eV for W4f_{7/2}. The non-charging value for W4f_{7/2} in pure WO₃ 36.3 eV. Only one peak is observed for Pt at 84.9 eV, and one peak for Si 2P at 114.3 eV (Pure SiO₂ has its XPS S 2p peak at 103.4 eV¹⁰⁵). Sulfated tungsten oxide on silica is an insulator so the sites not associated with platinum will be highly charge shifted.¹⁰² The SG-WS-Pt catalyst when treated with hydrogen forms species which are conductors,¹¹⁰ so the sulfur and tungsten atoms

associated with the Pt will not be charge shifted to as great an extent. From a quantitative analysis of the charged and not charged peak areas the number of sulfur and tungsten atoms associated with platinum can be found. It was found that 35% of the tungsten and 63% of the sulfur atoms are associated with the conducting platinum sites. This corresponds to 0.17 mmoles tungsten associated with the conducting sites. This number agrees well with the 0.17 mmoles of strong sites found by the cal-ad analysis indicating that the platinum may be deposited onto the strongest acid sites.

Heptane Isomerization and Cracking Reactions

The isomerization and cracking of heptane conversions and selectivity over SG-WS and SG-WS-Pt using N₂ and H₂ carrier gas is shown in Figure 6-4. The increased conversion of heptane for SG-WS-Pt using H₂ compared to N₂ shows that SG-WS-Pt is able to activate and spillover hydrogen at these temperatures and it appears that SG-WS is unable to activate hydrogen. The increased activity for acid catalysts due to spillover effects with platinum addition has been demonstrated¹⁰⁹ and the increased activity for heptane conversion for SG-WS-Pt is due to spillover hydrogen. The SG-WS and SG-WS-Pt catalysts both have high selectivity's to isomerization products as compared to HZSM-5 and sulfated zirconia when teated under the same conditions. The selectivity to isomerization or cracking is partially controlled by the rates of β -scission of the carbenium ion formed verses the rate of hydrogen transfer from the catalyst surface to the carbenium ion. It is possible that the rate of hydrogen transfer is faster on the tungsten based catalyst due to tungstens ability to go between WO₃ and H_xWO_{3-x} species. Although SG-WS does not effectively activate H₂, once the carbenium ion is formed the rate of surface hydrogen transfer along the may be fast. The H_xWO_{3-x} species could be an intermediate whereby the

transfer of hydrogen from the surface to the carbenium ion is fast and therefore little β -scission occurs. The selectivity to cracking or isomerization can also be partially controlled by the acid site strength, but HZSM-5 which has similar acidity was found to be selective to cracking products under the same conditions.

Carbon analysis of SG-WS and SG-WS-Pt after 2 hours of heptane reaction in hydrogen showed that the SG-WS has 2 wt.% carbon and SG-WS-Pt had 0 wt.% carbon. This is consistent with the hydrogen spillover activity of SG-WS-Pt which is known to aid in carbon removal.¹⁰⁸

Conclusion

A new solid acid catalyst SG-WS has been developed which has acidity equal to that of HZSM-5. SG-WS shows activity for isomerization of heptane with a high selectivity for isomerization products. Addition of Pt to SG-WS increases its heptane isomerization activity and extends its lifetime. The increased activity and extended lifetime were found to be linked to SG-WS-Pt's ability to activate hydrogen at low temperatures.



Figure 6-1 SEM of SG-WS Catalyst

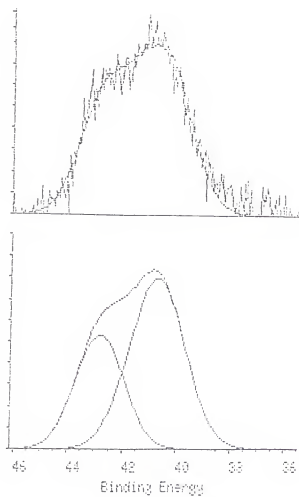


Figure 6-2 SG-WS Tungsten 4f XPS Spectrum

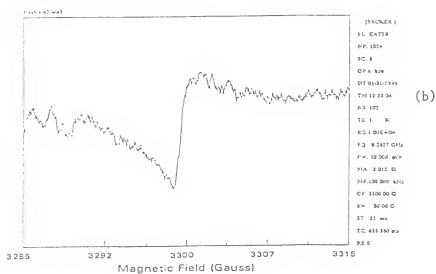
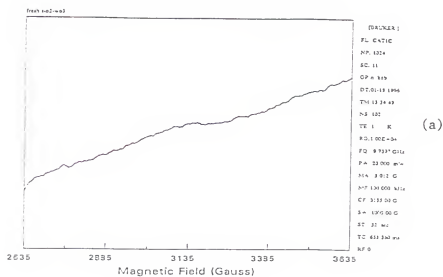


Figure 6-3 EPR Spectrum of Hydrogen Treated SG-WS and SG-WS-Pt

Heptane Conversion

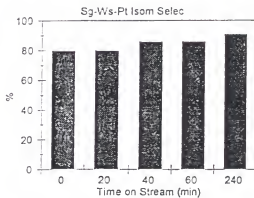
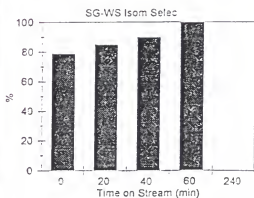
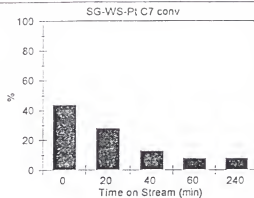
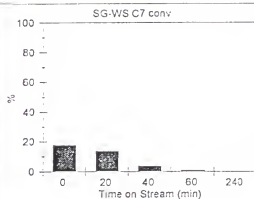
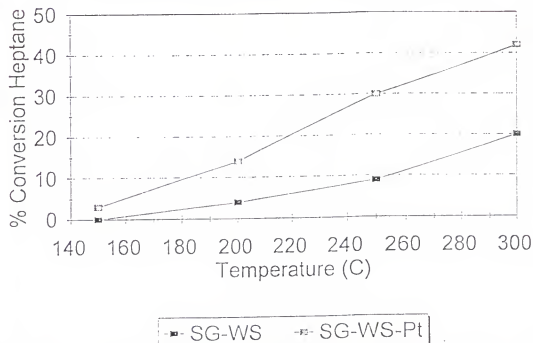


Figure 6-4 Heptane Conversion Using SG-WS and SG-WS-Pt

CHAPTER 7 SOLID ACID ALKYLATION OF ISOBUTANE

Introduction

High octane gasoline components have been produced for decades from alkylation of isobutane with butene. These processes have used either concentrated sulfuric acid (H_2SO_4) or hydrofluoric acid (HF) as the acid catalyst. The use of H_2SO_4 for the alkylation of isobutane with C4 olefins is described in a series of articles.¹¹¹ As a consequence of the clean air act emissions from automotive fuels will be regulated by the EPA and consequently refiners must meet new mandatory specifications on gasoline composition. The new standards translate into a reduction of aromatics which will cause a depletion in the octane rating of gasoline. Alkylation gasoline which is formed from low isoalkanes fits well into the new reformulated gasoline standards and has a high octane rating.¹¹² However, an increase in alkylation capacity is currently limited due to the use of HF and H_2SO_4 as the reaction catalysts which causes environmental problems. Therefore, there is a great incentive for developing solid acid catalysts that are environmentally friendly. In addition to being environmentally sound, solid acids offer several other advantages such as ease of product separation, potentially lower operating costs, and the potential to regenerate active sites.

Numerous types of acid catalysts have been investigated for the alkylation of isobutane with butene. The use of organochloroaluminum molten salts was found to be

effective for the alkylation of isobutane in a batch style process.¹¹³ However, molten salts lack many of the advantages that solid acids offer. Numerous researchers report the use of various solid acids for this reaction.¹¹⁴ Zeolites and zirconium sulfate in particular have been investigated for their potential application in alkylation process. Due to the difficulty of this reaction, many studies utilize a pressurized flow reactor system at high reaction temperatures.^{115,116} A solid acid that is capable of performing the reaction under conditions similar to that of the current process is more desirable.

In this study we report the use of a new solid acid which is a silica supported tungsten oxide promoted with sulfate (SG-WS). We report the investigation of this catalyst and other solid acids in a batch reactor system for the alkylation of isobutane with 2-butene. In particular, the activities, lifetimes, and regenerations of zeolites, supported metal halides, SG-WS, and zirconium sulfate catalysts were compared. The SG-WS catalyst gave the best results for alkylation in terms of its activity and ease of regeneration.

Experimental

Reaction Conditions

Alkylation of isobutane with 2-butene was performed in a batch reactor. The batch reactor was filled to a total volume of 12 ml with a 50:1 volume ratio of liquid isobutane to 2-butene. One gram of solid acid or one ml of concentrated sulfuric acid was placed into the batch reactor with a stir bar prior to filling with reactants. The reaction was carried out at 0°C with stirring for 30 minutes. Upon completion of the reaction the liquid products were filtered and analyzed using gas chromatography. Pentane was added

to the reaction products as the internal standard for the gas chromatography analysis. Carbon and sulfur analysis were performed by the C,H,N, and S method.

Calorimetric Titrations and Cal-ad Analysis

The cal-ad procedure is described in detail in previous reports and was used for all the systems described in this report.^{18,62} One gram of solid acid slurried in cyclohexane solution is reacted with pyridine while stirring. Pyridine and cyclohexane reagents were distilled over P_2O_5 prior to use. After each injection of known amounts of small concentrations of pyridine solution, the heat evolved was measured. UV-visible spectroscopy is used to determine the amount of pyridine free in solution in equilibrium with the solid acid. In the cal-ad analysis an adsorption isotherm is measured over the range of base additions used in the calorimetric titration. The combined calorimetric and adsorption data are analyzed to produce K 's (equilibrium constants), n 's (moles of site), and ΔH 's (enthalpies) for each site.

Catalyst Preparation

Solid acid catalysts used in this study were either prepared or purchased. Zeolite samples were purchased from PQ corporation in the proton form and were dried prior to each use. The SG- $AlCl_3$ catalyst preparation is described in a previous report.⁴⁰ Sulfated Zirconia was supplied by MEI corporation, it was calcined at $600^\circ C$ in air for 3 hours prior to use. The catalyst was found to have a sulfur loading of 1.6 weight % which corresponds to 0.5 mmol of sulfur per gram solid.

The SiO_2 - WO_3 - SO_4 (SG-WS) catalyst is prepared in a series of steps. First, the silica gel is conditioned to obtain the optimum level of hydration. The conditioning involves first washing the silica (Davison 80-200 mesh) with 1M HCl followed by

deionized water followed by 30% H_2O_2 and then deionized water again. The washed silica is then dried at 100°C in vacuum overnight. Finally, the silica is allowed to stand out to the open atmosphere for 1 day. The conditioned silica is then refluxed for 2 hours in CCl_4 or CH_2Cl_2 solvent. To this 0.5 mmoles of WCl_6 per gram of silica is added, and the temperature is adjusted to 70°C . This mixture is stirred for one day and the color changes from blue to red to yellow. After one day, the solid is filtered off (this catalyst SG-W is described in a previous report⁶⁰) and washed with 1M HNO_3 followed by deionized water. The washed solid is dried at 100°C overnight in air. Finally, the dried solid is treated with 1M H_2SO_4 (about 3ml H_2SO_4 per gram solid) by adding the 1M H_2SO_4 solution to a filter paper containing the solid and is allowed to gravity filter. The resulting solid is the SG-WS catalyst and is dried at 200°C in air prior to use.

Results and Discussion

Cal-ad Determination of Acidity of Solid Acids

The alkylation of isobutane with butene is a difficult reaction to acid catalyze. For this reason the acidity of various solid acid catalysts were investigated by cal-ad analysis using pyridine as the probe^{18,62}. Earlier research from this laboratory has reported that cal-ad analysis is an accurate method of evaluating a solid acids strength (ΔH_i , enthalpy), equilibrium constant (K_i), and number of sites (n_i).^{18,62} The (i) subscript refers to the number of sites, with the integer 1 assigned to the strongest site and 2 to the next strongest, and so on. The simultaneous analysis of both calorimetric and adsorption data provides an accurate determination of the thermodynamic parameters. The cal-ad measurements are carried out in a hydrocarbon solvent (cyclohexane) whose molecules are

close in molecular mass to that of the donor (pyridine) to cancel out any dispersion contribution to the measured enthalpy. A complete cal-ad analysis for the SG-WS solid acid in a cyclohexane slurry solution titrated with pyridine is shown in Table 7-1a.

Sulfur analysis of SG-WS shows that the 200°C air calcined treated catalyst has 1.6 wt.% sulfur. The tungsten sites which become sulfated are attributed to the strong ΔH_1 sites in the cal-ad analysis. It is interesting to note that the SG-WS value of ΔH_2 is approximately the same as that found for ΔH_1 on the SG-W catalyst (SG-WS without sulfation treatment shown in Table 1b), and the $-\Delta H_1$ value for sulfated silica is also approximately 32 kcal/mole. This indicates that upon sulfation of SG-W new strong acid sites are created which correspond to sulfated tungsten oxide sites on the surface of the silica. Shown in Table 7-1b are the ΔH_1 and n_1 values from cal-ad analysis for numerous solid acids, and an approximation of a ΔH_1 for H_2SO_4 based on these values and a report by Haw¹⁵ and Drago.¹¹⁹ These acids were used for the alkylation of isobutane with 2-butene in this report. One can see from these results that only SG- $AlCl_3$ has acid sites which are stronger than that of H_2SO_4 .

Table 7-1A: Cal-Ad Analysis for SG-WS Catalyst

| | |
|------------------------------------|------------------------------------|
| $n_1 = 1.7 \times 10^{-4}$ moles/g | $n_2 = 5.3 \times 10^{-4}$ moles/g |
| $K_1 = 7.5 \times 10^{16}$ l/mole | $K_2 = 1.2 \times 10^7$ l/mole |
| $-\Delta H_1 = 40.6$ kcal/mole | $-\Delta H_2 = 34.8$ kcal/mole |

Table 7-1B: $-\Delta H_1$ Values for Various Solid Acids.

| Catalyst | $-\Delta H_1$ (kcal/mole) | n_1 (moles) |
|---------------------------------|---------------------------|----------------------|
| HZSM-5 ⁴¹ | 41 | 4.8×10^{-5} |
| HY | 32 | 5.0×10^{-5} |
| Sulfated Zirconia ⁶² | 31 | 2.5×10^{-5} |
| SG-AlCl ₃ | 51 | 2.0×10^{-4} |
| SG-WS | 41 | 1.7×10^{-4} |
| SG-W ⁵⁰ | 30 | 6.5×10^{-5} |
| Beta | 35 | 5.0×10^{-5} |
| H ₂ SO ₄ | 50 | 0.018 (for 1 ml) |

Alkylation of Isobutane Using Solid Acids

Shown in Figure 7-1 is the amount of isooctane products (moles) found in the products liquids phase divided by the number of moles of an internal standard (pentane) using one gram of each catalyst and all other variables constant for the alkylation reaction. The activity is defined as the number of moles of isooctane produced divided by an internal standards moles. Since the goal of this research is to make isooctane this activity value will be used in subsequent comparisons as a indication of the extent of alkylation and to gauge the regeneration of the solid acids. Since cal-ad analysis revealed that one gram of each of the solids had different numbers of strong acid sites a comparison of the solid acids based on the number of strong acid sites was made. This was done by dividing the number of moles of isooctane produced by the number of strong acids sites for one gram of the strong acid catalyst yielding a turn over number (TON). Shown in Table 7-2 are the

TON for the various solid acids tested. It can be seen that the trend varies the same as the acidity as shown in Figure 7-1.

Table 7-2: TON for Alkylation of Isobutane With 2-Butene for Solid Acids.

| Catalyst | TON (moles iC ₈ /moles H ⁺) |
|------------------------|--|
| HZSM-5 | 2 |
| HY | 3 |
| sulfated zirconia (SZ) | 4 |
| SG-WS | 94 |
| zeolite Beta | 114 |
| SG-AlCl ₃ | 193 |

The differences in the alkylation activity for the various solid acids is attributed to several factors. First, the activity varies in the same manner as the acidity as measured by cal-ad analysis. However, one notable exception is HZSM-5 which should have a higher activity based on its measured acidity. Its low activity for isooctane production in HZSM-5 is attributed to diffusional constraints. This result is consistent with other researchers findings regarding the diffusional limited activity of HZSM-5 for alkylation of isobutane.¹²⁰ HY on the other hand has pores that should be large enough to accommodate isooctane production and desorption. However it is likely that the acidity of the acid sites on the surface are not strong enough to facilitate the reaction. This suggests that a $-\Delta H_1$ value of greater than 30 kcal/mole in the calorimetric titration with pyridine is necessary to catalyze

the alkylation of isobutane. This conclusion is supported by the fact that sulfated zirconia has a $-\Delta H_1$ of 31 and no diffusional constraints, and does not effectively catalyze the alkylation reaction. The use of zeolites and zirconium sulfate for use in the alkylation of isobutane with butene has been investigated,^{115,120} and the conclusions in those reports supports our finding that large pore acidic zeolites such as zeolite beta are the best zeolites and are better than zirconium sulfate.

Figure 7-1, and Table 7-2 show that the most effective solid acids for this reaction are SG-AlCl₃, SG-WS, and zeolite Beta. Since the activity of the other solid acids was minimal, no further investigations were done using these catalysts. Shown in Table 7-3 are the approximate RON (research octane number) calculated using the RON values shown at the bottom of Table 7-3. Also, shown in Table 7-3 are the TMP/DMH (trimethyl pentane/dimethyl hexane) ratios and the amount of 2-butene used by the catalysts. The TMP/DMH ratio is an indication of the quality of the alkylate since TMP has an octane value of 100 and DMH has an octane value of approximately 70. The TMP/DMH values of the solid acids are compared to that of concentrated sulfuric acids when tested under the same conditions as shown in Table 7-3. The low octane value for sulfuric acid in Table 7-3 is due to the long residence time for this catalyst, at shorter times a more favorable product distribution as well as octane number is found.¹¹³ All solid acids shown in Table 7-3 have similar RON and TMP/DMH ratios.

As expected, alkylation using 1ml of H₂SO₄ (approximately the same volume of 1 gram of solid acid) results in about 10 times more isooctane than the best solid acid (SG-AlCl₃). Therefore it would take about 10 grams of SG-AlCl₃ to get the same activity as 1 gram of H₂SO₄. By the same analogy it would take 29 grams of SG-WS to obtain the

same amount of isooctane produced by 1 g of H_2SO_4 . However, direct comparison in this way is not valid since the number (moles) of acid sites in 1 ml of H_2SO_4 (0.018 moles of H^+ considering only the first proton) is far greater than that on any of the solid acids. Calculated analysis shown in Table 7-1a for SG-WS only 1.7×10^{-4} moles of strong acid sites are present, which is 105 times less than 1 ml of H_2SO_4 . By the same comparison, SG- AlCl_3 has 90 times fewer strong acid sites. If one compares the acid catalysts by turn over number (TON), which is defined as the number of moles of isooctane produced in the reaction divided by the number of strong acid sites available then as shown in Table 7-2 the TON for SG- AlCl_3 is 193, for SG-WS it is 94, zeolite beta is 114, and for 1 ml H_2SO_4 it is 18.

Table 7-3 - Solid Acid Catalysts RON

| Catalyst | 2-butene used | TMP/DMH | RON |
|-------------------------|---------------|---------|-----|
| Beta | 84 | 3.0 | 93 |
| SG-WS | 80 | 2.5 | 92 |
| SG- AlCl_3 | 93 | 2.6 | 91 |
| H_2SO_4 | 99 | 2.8 | 92 |

*Values used to calculate RON³:

C6-C7 RON = 80, C9+ RON = 80, TMP RON = 100, DMH RON = 70

Shown in Figure 7-2 is the product distribution for the solid acids and concentrated sulfuric acid. It is clear from Figure 7-2 that both SG- AlCl_3 and

concentrated sulfuric acid undergo more side reactions. The extent of side reactions may be related to the number and strength of the acid sites which is greatest on these catalysts.

SG-AlCl₃ Deactivation and Regeneration

Reuse without regeneration of SG-AlCl₃ results in 43% of the original activity of the catalyst for the production of isooctane as shown in Figure 7-3. Carbon analysis reveals that after the first reaction 28% carbon is present on the surface despite little change in the catalyst color. This carbon was shown by mass spectrometry to be in the form of polymeric deposits which upon high temperature treatments became coke deposits evidenced by its black color. Subsequent uses of the catalyst without regeneration result in lower activities. Calorimetric titration of a used SG-AlCl₃ catalyst with pyridine shows loss of acid site strength from an initial $-\Delta H_1$ of 51 kcal/mole to a $-\Delta H_1$ of 39 kcal/mole which is due to loss of sites as a result of the reaction. The carbon deposits were found by mass spectra analysis to be polymeric carbon deposits which either cover or block access to the acid sites. Regeneration of this catalyst thermally is not possible due to the loss of HCl from the surface. Other methods of regeneration such as attempts to dissolve the polymer were ineffective. For this reason this catalyst, although highly active for alkylation, is not a good practical catalyst.

Zeolite Beta Deactivation and Regeneration

Reuse without regeneration of zeolite Beta results in 11% of the original activity of the unused catalyst for the production of isooctane as shown in Figure 7-3. Carbon analysis reveals that 4% carbon is present on the surface after one use. BET analysis of the used catalyst shows that the surface area has decreased from 720 m²/g to 408 m²/g which is consistent with carbon deposits blocking the pore openings. Two explanations

are possible for the deactivation of the catalyst. Either the acid sites are not accessible for the alkylation reaction once they become blocked by carbon or the isooctane is formed and its desorption through beta's pore channels is impeded by the carbon and hence more polymer is formed. A calorimetric titration of the used catalyst shows that $-\Delta H_1$ has dropped to 16 kcal/mole which is significantly lower than the original value of 36 kcal/mole. This indicates that the carbon is blocking access to the strongest acid sites, which are contained in the pores, since the basic probe pyridine (which is small) can not access them. Another study concluded that the formation of carbon (from polymerization) limits the formation of isooctane even on large pore zeolites due to diffusional constraints¹²⁰. Regeneration at temperatures below 500°C did not remove the carbon. When the catalyst was regenerated at 500°C in air for 12 hours about 1% carbon remained on the surface, but only 34% of the original activity for isooctane production was attained.

SG-WS Deactivation and Regeneration

Reuse of SG-WS without regeneration results in 32% of the original activity for isooctane production as shown in Figure 7-3, and 3% carbon is present on the surface after one alkylation run. Sulfur analysis shows that no sulfur has leached off the catalyst during the course of the reaction indicating that the reaction is surface catalyzed. Subsequent uses of the used catalyst result in lower isooctane production activities. Thermal regeneration of the SG-WS catalyst was done to remove the carbon from the surface. Unlike zeolite beta temperatures lower than 500°C were able to remove the carbon deposits from the surface of SG-WS. BET analysis of the used catalyst shows almost no reduction in pore volume from 0.92 cc/g to 0.88 cc/g, which indicates that the

carbon is not blocking the large pores. This could account for the ease of removal of the SG-WS carbon deposits compared to that of zeolite beta which has its carbon deposits in the pore structure.

Since the carbon is in the form of a polymer a low temperature regeneration was developed to allow the polymer to “unzip”. The following regeneration ramp was used. Upon regeneration using the ramp all the carbon is removed, and reuse of the catalyst regenerated with the ramp results in 34% of its original activity for isooctane production. Cal-ad analysis of the SG-WS catalyst directly after the ramp regeneration shown in Table 7-4 reveal that the strongest acid sites associated with $-\Delta H_1$ are lost by thermal regeneration, the strongest site left is the site associated with $-\Delta H_2$ from the original SG-WS catalyst. Sulfur analysis reveals that 63% of the sulfur is lost during the regeneration. Supporting the proposal that the strongest $-\Delta H_1$ sites are the ones associated with the sulfate-tungsten interaction and are mainly responsible for the alkylation activity.

Table 7-4: Cal-Ad Analysis of Ramp Regenerated SG-WS Catalyst.

| | |
|---|---|
| $n_1 = 2.7 \times 10^5 \text{ moles/g}$ | $n_2 = 2.8 \times 10^4 \text{ moles/g}$ |
| $K_1 = 4.0 \times 10^9 \text{ l/mole}$ | $K_2 = 4.7 \times 10^4 \text{ l/mole}$ |
| $-\Delta H_1 = 35.4 \text{ kcal/mole}$ | $-\Delta H_2 = 24.1 \text{ kcal/mole}$ |

A used SG-WS catalyst was regenerated by the thermal ramp and the sulfate was reapplied, in order to try to restore the strong acid sites lost during the regeneration.

Table 7-5 shows the cal-ad analysis of the SG-WS catalysts after regeneration and

reapplication of the sulfate. Comparison of n_1 in Table 7-5 with n_1 in Table 7-1a of the fresh SG-WS reveals that about 20% of the strongest sites have been reattained. The total number of sites reattained with a $-\Delta H$ of over 30 kcal/mole (the lower limit required for alkylation activity) is about 60%. The resulfated catalysts activity for isooctane production was 60% of the original catalyst, which agrees well with the number of sites recovered over -30 kcal/mole. Subsequent repetitions of reuses and regenerations (with sulfate readded) results in similar activities (about 60%) for isooctane production as compared to the original SG-WS catalyst. The original activity was not restored to the catalyst despite removal of the carbon deposits and resulfation. SEM analysis of the fresh and used catalyst with thermal regeneration shown in Figure 7-4 reveals that the morphology and dispersion of the sulfate-tungsten oxide clusters has been lost. At 10,000x magnification fewer particles are counted in some spots where other spots have the same or more particles than on the original SG-WS catalyst. This is an indication of a reordering of the surface active species during the reaction. Shown in Figure 7-5 is 500x magnification with the large particle being silica, and the small particles supported on them the tungsten oxide sulfate species. It is clear that some reordering has occurred as the uniformity of the dispersion is lost. Therefore, upon resulfation the surface is not restored to its initial state as shown in Table 7-5, and hence the activity is lower.

Table 7-5: Regenerated and Resulfated SG-WS Catalyst.

| | |
|------------------------------------|------------------------------------|
| $n_1 = 2.8 \times 10^{-5}$ moles/g | $n_2 = 3.1 \times 10^{-4}$ moles/g |
| $K_1 = 3.5 \times 10^{10}$ l/mole | $K_2 = 4.0 \times 10^5$ l/mole |
| $-\Delta H_1 = 41.1$ kcal/mole | $-\Delta H_2 = 32.9$ kcal/mole |

Conclusion

The use of solid acids to catalyze the alkylation of isobutane with 2-butene has been investigated. Both acidity and diffusional constraints influence the activity of a solid acid catalyst for alkylation. Of the solid acids studied SG-AlCl₃ shows the highest acidity and highest activity for alkylation. However this catalyst can not be regenerated thermally due to the loss of HCl from the surface. The SG-WS catalyst which consists of octahedral tungsten oxide associated with sulfate shows good activity and can be regenerated to about 60% of its original activity. Beta showed the highest activity of all the zeolites tested, but thermal regeneration did not restore its activity and the use of many zeolites for this reaction does not seem to be promising in the context tested due to diffusional problems and carbon pore blocking.

Cal-ad analysis of solid acids with pyridine is an effective method to characterize the acidic surface characteristics of solid acids. The alkylation of isobutane with 2-butene is an acid catalyzed reaction and the results of the calorimetric titrations correlate well with the activity of the solid acids for alkylation. Further, cal-ad and calorimetric analysis of the solid acids was shown to be an effective way to gauge the activity for alkylation of isobutane using solid acids and the regenerations of the acid sites associated with the reaction.

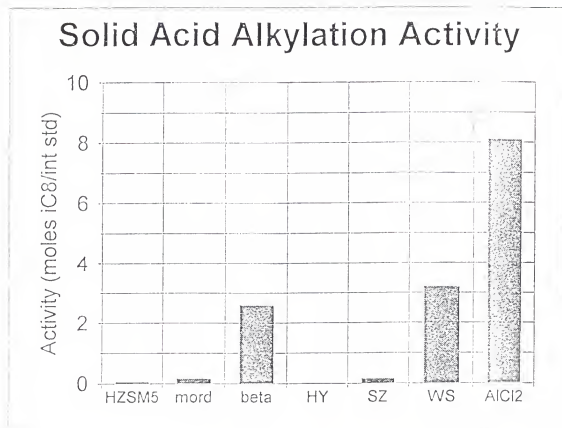


Figure 7-1 Alkylation of Isobutane Using Solid Acids

Alkylation Product Selectivity

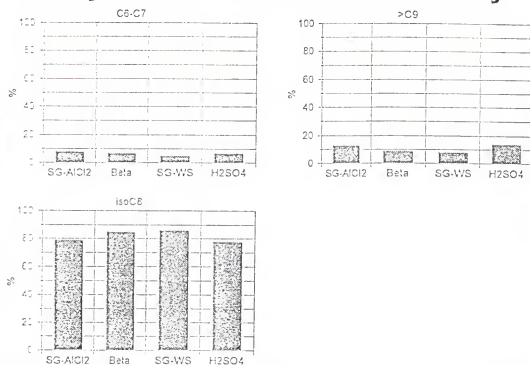


Figure 7-2 Proton Distributions for Solid Acids

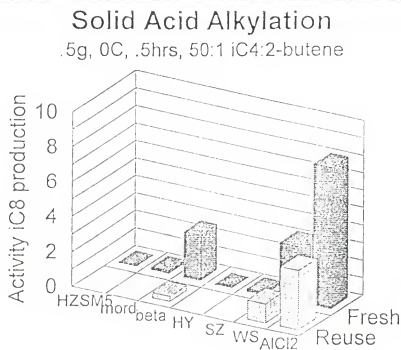


Figure 7-3 Regeneration of Solid Acids in the Alkylation Reaction

Fresh - see page 110



Used SG-WS Alkylation

Figure 7-4 SEM at 10,000X Magnification of Fresh and Used SG-WS



Figure 7-5 SEM at 500X Magnification of Used SG-WS

CHAPTER 8 GENERAL CONCLUSION

Conclusion on the Characterization and Useage of Solid Acid Catalysts

The characterization of the acidity of solid acid catalysts is a difficult task which involves characterizing not only the strength, but also the number of acid sites. Not all characterization techniques are able to perform such analysis. The cal-ad technique does provide meaningful n's (number of sites), K's (equilibrium constants), and ΔH 's (strengths) for solid acid catalysts. The characterization of several solid acid catalysts and a approximation for that of sulfuric acid has been accomplished. It was found that SG- AlCl_3 catalyst was indeed a "superacid" with a $-\Delta H = 51$ kcal/mole. Sulfated zirconia a popular acid catalyst in the current literature was found to be only a moderately strong acid with a $-\Delta H = 30$ kcal/mole. The hydrocarbon isomerization activity of sulfated zirconia was linked to its redox activity, and not to its acidity. This finding leads to the conclusion not all solid acid catalyzed reactions are necessarily controlled by the solid acids acidity. Other pathways, such as redox, may exist for solid acids to catalyze hydrocarbon rearrangement reactions.

A new solid acid catalyst SG-W was developed, and characterized. It was found that the SG-W catalyst consisted of six coordinate tungsten uniformly dispersed on the surface of silica. Cal-ad analysis determined that the SG-W was a moderate strength acid with a $-\Delta H = 30$ kcal/mole. The Beckmann rearrangement of cyclohexanone oxime to

caprolactam which is an industrially important reaction was found to be catalyzed by SG-W. The activity and selectivity of the reaction was better for SG-W than for any currently known solid acid catalyst. However, the catalyst was shown to be unregenerable to its initial activity. Cal-ad analysis and SEM showed that upon regeneration sintering of the tungsten oxide had occurred and acid sites were lost resulting in loss of activity when regenerated. Low temperature regeneration methods were not successful.

The addition of Pt to SG-W was investigated. It was found that when Pt was added SG-W showed the ability to activate hydrogen at low temperatures as evidenced by its color change and EPR spectrum. The hydrogenation of benzene, and tetralin activity of SG-W-Pt was studied and compared to other known hydrogenation catalysts. It was found that SG-W-Pt had activity comparable or better than other hydrogenation catalysts. However, SG-W-Pt was found to be poisoned and quickly deactivated when sulfur containing compounds are introduced into the feed.

In order to increase the acidity of the SG-W catalyst so that it could catalyze more difficult hydrocarbon rearrangement reactions it was treated with sulfate to produce the SG-WS catalyst. This SG-WS catalyst was found by cal-ad to have an acid strength equal to that of HZSM-5. Its activity for the alkylation of isobutane with butene to make isooctane was investigated and compared to other solid acids and that of the commercial sulfuric acid. It was found that most solid acids tested could not catalyze this reaction. The best catalysts tested were SG-AlCl₃, zeolite beta, and SG-WS with SG-AlCl₃ having the greatest activity. However, compared to the same amount of sulfuric acid by weight, it would take about 8 grams of SG-AlCl₃ and 20 grams of SG-WS to get the same activity of 1 gram of H₂SO₄. Comparison based on the number of acid sites however shows that

SG-AlCl₃, Beta, and SG-WS yield more turn overs (moles of isooctane produced/ moles of acid site) than H₂SO₄. The ability to regenerate SG-AlCl₃, beta, and SG-WS was extensively studied. It was found that SG-AlCl₃ could not be regenerated thermally or by other methods. Beta which deactivated by build up of polymeric carbon deposits also could not be regenerated back to its initial activity. SG-WS was found to be regenerable with a low temperature ramp and reapplication of lost sulfate sites resulting in a return of 60% of its original activity. Cal-ad and SEM were used to guide the regeneration and account for the loss of 40% of its activity.

The addition of Pt to SG-WS was investigated to ascertain its effects on hydrocarbon isomerization. It was found that Pt addition resulted in spillover hydrogen enhancing the isomerization activity of SG-WS for heptane isomerization. The activity and selectivity of the catalyst was compared to that of sulfated zirconia, and HZSM-5, with SG-WS-Pt showing a greater selectivity for isomerization over cracking.

Although this dissertation describes several old and new solid acids and their successful application to hydrocarbon rearrangement reactions. It is clear from the caproactam and alkylation results that they can not yet rival and may never rival the activity of liquid acids due to the number of acid sites available for reaction. The greatest advantage of solid acids is their potential to be regenerated which would make up for the lesser activity compared to liquid acids. However, as clearly shown in this report this advantage remains largely unattained to this date. As a result very few processes have replaced liquid acid catalysts with solid acids. If solid acids are to ever rival liquid acids the issues regarding deactivation and regeneration must be addressed. This dissertation has shown that cal-ad along with other techniques is an effective way to gauge a solid acid

catalysts deactivation and regeneration. Further study along these lines may result in a better regeneration method being developed. Another approach to the problem is to incorporate the active metal oxide into the structure as in a zeolite. Sol-gel synthesis is a means which can be used to accomplish this goal. However, the incorporation is difficult due to the many controlling factors associated with sol-gel synthesis.

APPENDIX A
CAL-AD PROCEDURE FOR SOLID ACID ANALYSIS

Cal-ad Procedure

1. Perform calorimetric experiment to obtain voltage deflections for known amounts of injected basic probe. Convert voltage deflections into heats using calorimetry spreadsheet.

In the column labeled "volts" place the values obtained from the calorimetric experiment.

In the inj V(ml) column are values for the injection volume delivered by the syringe used in the calorimetric experiment. The [pyridine] column shows the calculated concentration of basic probe used in the experiment. The heater constant is calculated from V(H), and V(R) values obtained in the calibration portion of the calorimetry experiment. Three reproducible experiments should be done and the average numbers from the runs used in subsequent evaluations.

2. Perform adsorption experiment to find the concentration of basic probe (pyridine) adsorbed onto the solid and free in solution for each known injection of basic probe.

Place the absorbance values obtained from the UV experiment into the adsorption template in order to calculate the moles of pyridine adsorbed onto the solid and pyridine free in solution. From the template values for X_m (moles pyridine adsorbed on solid/g) and C_{eq} (concentration of pyridine free in solution) are calculated. Three reproducible runs should be done and the average of numbers from the runs used in the fitting procedure described below.

3. In order to get first guesses for n (number of sites) and K (equilibrium constants) for each site on the solid acid Langmuir plots of C_{eq}/X_m versus C_{eq} are made. Each straight line portion of the curve is assumed to be a different site, and $1/\text{slope} = n$ (number of moles) for that site and the intercept times n (moles for that site) is equal to $1/K$ for that site. This analysis of each straight line portion is done to obtain n 's and K 's for each site, producing n_1, K_1 and n_2, K_2 etc.

4. If any absorbances in the UV adsorption experiment were below 0.01 then in order to obtain the concentration of free pyridine in solution and the moles pyridine adsorbed for these points one must use the Chronister template, which is a polynomial series. Place the guesses for n_i and K_i from the Langmuir plots into the template and vary the column labeled "[B]", the concentration of pyridine free in solution or C_{eq} , to obtain the best fit for the it and the moles pyridine adsorbed (X_m). The numbers found for the points below 0.01 absorbance will be used as their values in subsequent analysis, while for all points with an adsorbance above 0.01 the experimental values are used.

5. Take the absorbtion data only, and place it into the padfit prodgram to solve for n 's and K 's. For inital guesses for n 's and K 's, and the number of sites use numbers obtained from the Langmuir plots. If the numbers do not seem good you may go back to Chronister template to adjust the numbers for absorbances below 0.01.

6. Take the numbers obtained for concentration of pyridine free in solution (C_{eq}), moles pyridine adsorbed (X_m), and calorimetry heats (in calories) from cal experiment and place

them into the padfit program. The first initial guesses for n_i , K_i should be from the step 5 and calorimetry heats in calories from the calorimetric experiment. Keep adjusting guesses for n_i , K_i and $-\Delta H_i$ until the best fit is obtained.

7. Go back to the Chronister template use the new n_i and K_i values to calculate new values for $[B]$ or C_{eq} and moles pyridine adsorbed or X_m for the points with experimental adsorbance below 0.01.

8. In padfit use the revised n_i , K_i , C_{eq} , and X_m numbers and continue this process in steps 5, 6 and 7 until the best fit is reached.

APPENDIX B
GAS CHROMATOGRAPHIC METHODS OF ANALYSIS

Alkylation

35°C (hold for 10 min.) ----> ramp at 5°C/min. to 200°C -----> hold at 200°C for 10 min.

Isomerization of C7, C8, and C10

100°C (hold for 15 min.) -----> ramp at 25°C/min. to 200°C -----> hold at 200°C for 10 min.

Caprolactam

225°C isothermal

Isomerization of C5, and C4

70°C isothermal

Hydrogenation of benzene

100°C isothermal

Dehydration of propanol and butanol

70°C (hold for 9 min.) ----> ramp 15°C/min. to 200°C ---> hold at 200°C for 5 min.

APPENDIX C
CAL-AD DATA FOR SOLID ACID CATALYSTS

Cal-ad Data for SG-W Catalyst.

| <u>Concentration pyridine free in solution</u> | <u>Moles pyridine adsorbed</u> | <u>Heats (cal/mole)</u> |
|--|--------------------------------|-------------------------|
| 0.35×10^{-9} | 0.13×10^{-4} | 0.3946 |
| 0.80×10^{-9} | 0.25×10^{-4} | 0.7235 |
| 0.20×10^{-8} | 0.37×10^{-4} | 1.185 |
| 0.50×10^{-8} | 0.50×10^{-4} | 1.591 |
| 0.29×10^{-6} | 0.66×10^{-4} | 2.053 |
| 0.76×10^{-4} | 0.89×10^{-4} | 2.396 |
| 0.23×10^{-3} | 0.12×10^{-3} | 2.992 |
| 0.36×10^{-3} | 0.14×10^{-3} | 3.407 |
| 0.38×10^{-3} | 0.15×10^{-3} | 3.463 |
| 0.42×10^{-3} | 0.16×10^{-3} | 3.567 |
| 0.51×10^{-3} | 0.18×10^{-3} | 3.804 |
| 0.70×10^{-3} | 0.20×10^{-3} | 4.238 |

Cal-ad Data for SG-WS Catalyst

| Concentration pyridine free in solution | Moles pyridine adsorbed | Heats (cal/mole) |
|---|-------------------------|------------------|
| 0.12×10^{-11} | 0.13×10^{-4} | 0.5033 |
| 0.25×10^{-11} | 0.25×10^{-4} | 0.9613 |
| 0.32×10^{-11} | 0.37×10^{-4} | 1.178 |
| 0.59×10^{-11} | 0.50×10^{-4} | 1.868 |
| 0.11×10^{-10} | 0.76×10^{-4} | 2.616 |
| 0.21×10^{-10} | 0.10×10^{-3} | 3.663 |
| 0.45×10^{-10} | 0.13×10^{-3} | 4.716 |
| 0.94×10^{-10} | 0.14×10^{-3} | 5.465 |
| 0.19×10^{-8} | 0.17×10^{-3} | 6.477 |
| 0.66×10^{-8} | 0.19×10^{-3} | 7.359 |
| 0.12×10^{-7} | 0.24×10^{-3} | 8.332 |
| 0.24×10^{-7} | 0.31×10^{-3} | 11.47 |
| 0.88×10^{-7} | 0.40×10^{-3} | 15.69 |
| 0.24×10^{-6} | 0.57×10^{-3} | 20.74 |
| 0.30×10^{-5} | 0.68×10^{-3} | 24.96 |

Cal-ad Data for Sulfated Zirconia (SZ) Catalyst

| <u>Concentration pyridine free in solution</u> | <u>Moles pyridine adsorbed</u> | <u>Heats (cal/mole)</u> |
|--|--------------------------------|-------------------------|
| 0.16×10^{-9} | 0.13×10^{-4} | 0.4338 |
| 0.58×10^{-6} | 0.26×10^{-4} | 0.8508 |
| 0.94×10^{-5} | 0.36×10^{-4} | 1.132 |
| 0.25×10^{-4} | 0.47×10^{-4} | 1.254 |
| 0.10×10^{-3} | 0.65×10^{-4} | 1.682 |
| 0.27×10^{-3} | 0.73×10^{-4} | 1.945 |
| 0.73×10^{-3} | 0.77×10^{-4} | 2.066 |
| 0.10×10^{-2} | 0.78×10^{-4} | 2.248 |
| 0.12×10^{-2} | 0.78×10^{-4} | 2.287 |

LIST OF REFERENCES

1. Thomas, J. *Scientific American* **1991**, 112..
2. Misono, M.; Okuhara, J.; *Chemtech* **1993**, 23.
3. Sheckler, J.; Hammershamb, H.; Ross, L.; Comey, K. *Oil & Gas J.* **1994**, Aug 22, 49.
4. Scott, B. *Hydrocar. Proc.* **1992**, Oct., 77.
5. Arata, K. *Adv. Catal.* **1990**, 17, 165.
6. a) Kurosaki, A.; Okazaki, S. *Chem. Lett.* **1983**, 1741.
b) Howie, O.; Okazaki, S. *Chem. Lett.* **1986**, 1089.
7. Breck, D. Zeolite Molecular Sieves, Wiley, New York, 1974.
8. Dai, P. *Catal. Today* **1995**, 26, 3.
9. Tanabe, K.; Misono, M.; Ono, Y.; Hattori, H. Studies in Surface Science and Catalysis, Vol. 51, Elsevier Press, New York, 1989.
10. Tanabe, K.; Sumiyoshi, K.; Shibata, T.; Kiyora, T.; Kitahawa, J. *Bull Chem. Soc. Jpn.* **1974**, 47, 1064.
11. Kijaski, J.; Baiker, A. *Catal. Today* **1989**, 5, 1.
12. Bosman, H.; Kruissink, E.; Van der Spoel, J.; Van der Burk, F. *J. Catal.* **1994**, 148, 660.
13. a) Purcell, K.; Drago, R. *J. Am. Chem. Soc.* **1966**, 88, 1045.
b) Kataoka, T.; Dumesic, J. *J. Catal.* **1988**, 112, 66.
c) Parry E. *J. Catal.* **1963**, 2, 371.
14. a) Wang, G.; Itoh, H.; Hattori, H.; Tanabe, K. *J. Chem. Soc. Faraday Trans. I.* **1983**, 79, 1373.
b) Tsutsumi, K.; Koh, H.; Hagiwara, S.; Takahashi, H. *Bull. Chem. Soc. Jpn.* **1975**, 48, 3576.
c) Lin, C.; Hsu, C.; *J. Chem. Soc. Chem. Comm.* **1992**, 20, 1479.

15. a) Haw, J.; Nicholas, J.; Xu, T.; Beck, L. *Acc. Chem. Res.* **1996**, 29, 259.
b) Beck, L.; White, J.; Haw, J. *J. Am. Chem. Soc.* **1994**, 116, 9657.
c) Beck, L.; Haw, J. *J. Phys. Chem.* **1995**, 99, 1079.
d) Xu, T.; Haw, J. *J. Am. Chem. Soc.* **1994**, 116, 10188.
e) Chu, P.; Lunsford, J. *J. Phys. Chem.* **1991**, 95, 7362.
16. a) Carniti, P.; Gervasini, A.; Auroux, A. *J. Catal.* **1994**, 150, 274.
b) Gervasini, A.; Bellussi, G.; Fenyuesi, J.; Auroux, A. *J. Phys. Chem.* **1995**, 99, 5117.
17. Dumesic, J.; Cardona-Martinez, N. *J. Catal.* **1991**, 128, 23.
18. a) Lim, Y.; Drago, R.; Batich, M.; Wong, N.; Doan, P. *J. Am. Chem. Soc.* **1987**, 109, 169.
b) Chronister, C.; Drago, R. *J. Am. Chem. Soc.* **1993**, 115, 4793.
19. Matar, S.; Mirbach, M.; Tayim, H. Catalysis in Petrochemical Processes, Kluwer Academic Press, Holland, 1989.
20. a) Kazansky, V. *Acc. Chem. Res.* **1991**, 24, 379.
b) Kazansky, V.; Senchenya, J. *J. Catal.* **1989**, 119, 108.
21. Olah, G. *Angew. Chem. Ed. Engl.* **1995**, 34, 1393.
22. Hino, H.; Arata, K. *J. Chem. Soc. Chem. Commun.* **1980**, 851.
23. Davis, B.; Keogh, R.; Srinivasan, R. *Catal. Today* **1994**, 20, 219.
24. Guisnet, M., *Acc. Chem. Res.* **1990**, 23, 392.
25. Carniti, P.; Gervasini, A.; Auroux, A. *J. Catal.* **1994**, 150, 274.
26. Farcasiu, D.; Ghenciu, A.; Li, J. *J. Catal.* **1996**, preprint.
27. Riemer, T.; Spielbauer, D.; Hunger, M.; Mekheimer, G.; Knozinger, H., *J. Chem. Soc. Chem. Commun.* **1994**, 1181.
28. Chen, F.; Coudurier, G.; Joly, J.; Verdrine, J. *J. Catal.* **1993**, 143, 616.
29. Corma, A.; Fornes, V.; Juan-Rajadell, M.; Lopez-Nieto, J. *Appl. Catal.* **1994**, 116, 151.
30. Morterra, C.; Verrato, G.; Pinna, F.; Signoreto, M.; Strukul, G. *J. Catal.* **1994**, 149, 181.

31. Yaluris, G., Larson, R., Kobe, J., Gonzalez, M., Fogash, K., Dumesic, J., *J. Catal.*, **1996**, 158, 336.
32. Srinivasan, R., Keogh, R., Chenciu, A., Farcasiu, D., Davis, B. *J. Catal.* **1996**, 158, 502.
33. Wan, K., Khouw, C., Davis, M., *J. Catal.* **1996**, 158, 311.
34. Kustov, V., Kazansky, V., Figueras, F., Tichit, D. *J. Catal.* **1994**, 150, 143.
35. Cheung, T. K., d'Itri, J. L., Lange, J. L., Gates, B. C. *Catal. Lett.* **1995**, 31, 153.
36. Adevva, V., de Haan, W., Janchen, J., Lei, G., Schunemann, V., van de Ven, L., Sachtler, W., van Santen, R. *J. Catal.* **1995**, 151, 364.
37. Ghenciu, A., Farcasiu, D. *J. Chem. Soc. Chem. Commun.* **1996**, preprint.
38. Morterra, C., Cerrato, G., Pinna, F., Signoreto, M. *J. Catal.* **1995**, 157, 109.
39. Cheng, J., D' Itri, J., Gates, B. *J. Catal.* **1995**, 151, 464.
40. a) Getty, E., Drago, R. *J. Am. Chem. Soc.* **1988**, 110, 3312.
b) Getty, E., Drago, R. *Inorg. Chem.* **1990**, 29, 1186.
c) Drago, R., Petrosius, S., Chronister, C. *Inorg. Chem.* **1994**, 33, 367.
41. Drago, R.; Dias, S.; Torrealba, M. Submitted to *J. Am. Chem. Soc.*
42. a) Parrillo, D., Gorte, R., Farneth, W. *J. Am. Chem. Soc.* **1993**, 115, 12441.
b) Parillo D., Gorte, R. *Catal. Lett.* **1992**, 16, 17.
c) Ho, N. *J. Phys. Chem.* **1994**, 20, 5362.
43. Cardona-Martinex, N., Dumesic, J. *J. Catal.* **1991**, 128, 23.
44. Arnett, E., Hutchinson, B., Healy, M. *J. Am. Chem. Soc.* **1988**, 110, 5255.
45. a) Ward, D., Ko, E. *J. Catal.* **1994**, 150, 18.
b) Hino, M., Kobayashi, S., Arata, K. *J. Am. Chem. Soc.* **1979**, 101, 6439.
46. Jatia, A., Chang, C., MacLeod, J., Okubo, T., Davis, M. *Catal. Lett.* **1994**, 25, 21.
47. Hu, J., Vernkaesh, K., Tierney, J., Wender, I. *Appl. Catal A* **1994**, 114, L179.
48. Liu, H., Adevva, V., Lei, G., Sachtler, W. *J. Molec. Catal. A* **1995**, 100, 35.

49. Zhang, A., Nakamura, I., Aimuto, K., Fujimoto, K. *Ind. Eng. Chem. Res.* **1995**, 34, 1074.
50. Arata, K. Solid superacids vol 17; Academic Press: N.Y., 1990; p.165.
51. Pines, H. The Chemistry of Catalytic Hydrocarbon Conversion Academic Press: N.Y., 1981.
52. Matar, S.; Mirbach, M.; Tayim, H. Catalysis in Petrochemical Processes Kluwer Academic Publishers: Holland, 1989.
53. Ushikubo T.; Wada, K.; *J. Catal.* **1994**, 148, 138.
54. Tanabe, K.; Yamaguchi, T. Successful Design of Catalysts vol 144; Elsevier Scientific Publishers: Amsterdam, 1988; p 99.
55. Sommer J.; Hachoumy, M.; Garin, F. *J. Am. Chem. Soc.* **1995**, 117, 1135.
56. Grange P.; Guiu G. *J. Catal.* **1995**, 156, 132.
57. Drago, R.; Petrosius, S.; Kaufman, P. *New J. Chem.* **1994**, 18, 937.
58. Drago, R.; Petrosius, S.; Kaufman, P. *J. Molec. Catal. A* **1994**, 89, 317.
59. Maciel, G.; Sato, S. *J. Molec. Catal. A* **1995**, 101, 153.
60. Clark, J.; Martin, K.; Teasdale, A.; Barlow, S. Author's Preprint.
61. Gates, B.; Fuentes, G.; Boegel, J. *J. Catal.* **1982**, 78, 436.
62. Kob, N.; Drago, R. Submitted to *J. Phys. Chem.*
63. Ed. M. Howe-Grant Encyclopedia of Chemical Technology Wiley & Sons, NY, vol.4 p. 827.
64. Tabane, K *Catal. Rev.-Sci. Eng.*, **1993**, 35(4), 483.
65. a) Curtin, T., Mcmonagle, J., Ruwet, M., Hodnett, B. *J. Catal.*, **1993**, 142, 172.
b) Wada, K., Ushikubo, T. *J. Catal.* **1994**, 148, 138.
66. Armor, J. *J. Catal.* **1981**, 70, 72.
67. Curtin, T., McMonagle, J., Hodnett, B. *Catal. Lett.* **1993**, 17, 145.

68. Sudhakar Redy, J., Ravishanker, R., Sivasanker, S., Ratnasamy, P. *Catal. Lett.* **1993**, 17, 139.
69. Yamaguchi, T., Tanaka, Y., Tanabe, K. *J. Catal.* **1980**, 65, 442..
70. Gielgens, L., van Kampen, M., Broek, M., van Harkeveld, R., Ponc, V. *J. Catal.* **1993**, 154, 201..
71. Yamaguchi, T., Tanaka, YI, Tanabe, K. *J. Catal.* **1980**, 62, 442..
72. Fricke, R., Hanke, W., Ohimann, G. *J. Catal.* **1983**, 79, 1.
73. Kepert, D., *Progr. Inorg. Chem.* **1962**, 4, 199.
74. a) Biloen, P., Pott, G. *J. Catal.* **1973**, 30, 169.
b) Kerkhof, F., Moulign, J. *J. Phys. Chem.* **1979**, 83, 1612.
c) Scholfield, J. *J. Electron Spec. Relat. Phenom.* **1976**, 8, 129.
75. Van Roosmalen, A., Koster, D., Mol, J. *J. Phys. Chem.* **1980**, 84, 3075.
76. Wu, J., Shuben, L. *J. Phys. Chem.* **1995**, 99, 4566.
77. Thomas, R., Moulign, J., Medema, J., DeBeer, V. *J. Molec. Catal.* **1980**, 8, 161.
78. Desbat, D., Lassegues, J., Gerand, B., Figlarz, M., *J. Catal.* **1983**, 79, 215.
79. Miyake, J. *J. Appl. Phys.* **1984**, 55, 2752.
80. Greenwood, M.; Earnshaw, A. Chemistry of The Elements Pergamon Press, NY, 1984, p.1167.
81. Satterfield, C. Heterogeneous Catalysis in Industrial Practice McGraw-Hill, NY, 1991, p. 120.
82. Crow, P.; Williams, B. *Oil & Gas J.* **1989**, Jan 15.
83. Ioannides, T.; Verykios, X. *J. Catal.* **1993**, 143, 175.
84. Chou, J.; Haung, Y; Lin, T.; Chang, J. *Ind. Eng. Chem. Res.* **1995**, 34, 4277.
85. Lin, S.; Vannice, A. *J. Catal.* **1993**, 143, 539.
86. Lin, S.; Vannice, A. *J. Catal.* **1993**, 143, 563.
87. Chou, P.; Vannice, A. *J. Catal.* **1987**, 107, 129.

88. Barbier, J.; Lamy-Pitara, E.; Marecot, P.; Boitiaux, J.; Cosuns, J.; Verna, F. *Adv. Catal.* **1990**, *37*, 279.
89. Cooper, B.; Stanislaus, A.; Hannerup, P. *Hydroc. Proc.* **1993**, June.
90. Kob, N.; Drago, R. Submitted to *Ind. Eng. Chem. Res.*
91. Muller, M.; Mayer, M.; Kirckemeyer, E.; Diemann, E. *Angew. Chem. Int. Eng.* **1996**, *35*, 1206.
92. Wagner, C.; Riggs, W. Handbook of X-ray Photoelectric Spectra, Perkin Elmer, 1993.
93. Basiur, A.; Patwardhan, R.; Vyas, S. *J. Catal.* **1991**, *127*, 86.
94. Sheckler, J.; Hammershaimb, H.; Ross, L.; Romey, K., *Oil & Gas Journal*, **1994**, Aug 22, 49.
95. Tanabe, K., In Heterogeneous Catalysis by Novel Solid Strong Acids and Superacids Eds. Shapiro, B.L., Texas A&M University Press, College Station, TX, P. 71.
96. Verdre, T.C.; Auroux, A.; Boho, V.; Dejaifve, P.; Naccache, C.; Weirzchowski, P.; Dervane, E.; Nagy, J.; Gilson, J.; Van Hoff, C.; Van Den Berg, J.; Wolthoizen, J., *J. Catal.* **1974**, *59*, 248.
97. Corma, A.; Monton, J.; Orchilles, A. *Appl. Catal.* **1986**, *23*, 255.
98. Meusinger, J.; Corma, A. *J. Catal.* **1995**, *152*, 189.
99. Blomsma, E.; Martens, A.; Jacobs, P. *J. Catal.* **1995**, *155*, 141.
100. a) Guisnet, M.; Alvarez, F.; Giametto, G.; Perot, G. *Catal. Today* **1987**, *1*, 415.
b) Alvarez, F.; Riberio, F.; Giametto, G.; Chevalier, F.; Perot, G.; Guisnet, M., *Stud. Surf. Sci. Catal.* **1989**, *46*, 1339.
101. Kob, N.; Xu, T.; Drago, R.; Haw, J., Submitted to *J. Am. Chem. Soc.*
102. Drago, R.; Young, V.; Kob, N.; Singh, D.; Grunewald, R. Submitted *Microporous Materials*.
103. Miyake, J. *J. Appl. Phys.* **1984**, *55*, 2752.
104. Biloen, P.; Pott, G. *J. Catal.* **1973**, *30*, 169.

105. a) Biloen, P., Pott, G. *J. Catal.* **1973**, 30, 169.
b) Ng, K., Hercules, D. *J. Phys. Chem.* **1976**, 80, 2094.
106. a) Greenwood, N.; Ernschaw, G. In Chemistry of the Elements Pergaman Press, Oxford, P. 1174.
b) Cotton, F.; Wilkinson, G. In Advanced Inorganic Chemistry Wiley & Sons, NY, p. 807.
107. Barur, A., Patwardhan, S., Vyas, S. *J. Catal.* **1991**, 127, 86.
108. a) Conner W., Falconer, J. *Chem. Rev.* **1995**, 95, 759.
b) Parera, J., Traffano, E., Musso, J., Pieck, C., Studies in Surface Science and Catalysis: 17 Eds. Pajonk, G., Tiechner, S., Germain, J., Elsevier, Amsterdam, 1983 P. 101.
109. a) Zhang, A., Nakamara, I., Aimoto, K., Fujimoto, K., *Ind. Eng. Chem. Res.* **1995**, 34, 1074.
b) Hattori, H., Studies in Surface Science and Catalysis: 77 Eds. Pajonk, G., Tiechner, S., Germain, J., Elsevier, Amsterdam, 1995 P. 77.
110. Shen, P., Syed-Bokhari, J., Tseung, A.C. *J. Electro. Soc.* **1991**, 138, 2778.
111. a) Corma, A., Martinez, A. *Catal. Rev. Sci. Eng.* **1993**, 35, 483.
b) Albright, L., Spalding, M., Faunce, J., Eckert, R. *Ind. Eng. Chem. Res.* **1988**, 27, 381.
112. Sachtler, J., Hammershaimb, H., Ross, L., Comey, K. *Oil & Gas J.* **1994**, Aug 22, 49.
113. Ohgoshi, S., Kanni, J., Sagimoto, M. **1994**, US Patent 5,321,196.
114. Guo, C., Liao, S., Qian, L., Tanabe, K. *Appl. Catal. A* **1994**, 107, 239.
115. Unverricht, S., Ernst, S., Weitkamp, J. Studies in Surface Science and Catalysis, Vol.84, Elsevier Science, New York, p.1963.
116. Corma, A., Juan-Rajadell, J., Lopez-Nieto, J., Marteniz, A., Martinez, C. *Appl. Catal. A* **1994**, 111, 175.
117. Miyake, J. *J. Appl. Phys.* **1984**, 55, 2752.
118. Kerkhof, F., Moulign, J. *J. Phys. Chem.* **1979**, 83, 1612.
119. Kob, N.; Drago, R. Results to be Published.

120. Chu, Y., Chester, A. *Zeolites* **1986**, 6, 195.

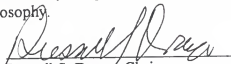
BIOGRAPHICAL SKETCH

Nicholas E. Kob III was born in Evanston, Illinois on August 28, 1969, to parents Nick and Kathy Kob. He attended Loara High School in Anaheim, California and graduated in June 1987. While in high school, Nick was a member of the national honors society, vice president of his senior class, and two time state wrestling finalist. In the Fall, of 1987 he began college at San Diego State University as a chemistry major. Here he became a member of Sigma Pi fraternity and was elected as an officer. After two years, he transferred to California State University Fullerton where he graduated under the direction of Dr. V. Willis in June 1991.


In Fall 1991 he began graduate school at Illinois State University. His thesis titled "The Use of Sonochemistry to Generate Coordination Reactions" was selected as outstanding masters thesis throughout the entire school. He graduated with a MS in chemistry under the direction of Dr. J. House in June 1993.

In Fall 1993 he began graduate school at the University of Florida to attain his doctorate in chemistry. His research focused on the development, characterization, and application of solid acid catalysts under the direction of Dr. Russell Drago and Dr. V. Young. Upon completion of his doctorate he plans to work for DuPont.


I certify that I have read this study and that in my opinion it conforms to acceptable standards of scholarly presentation and is fully adequate, in scope and quality, as a dissertation for the degree of Doctor of Philosophy.


Russell S. Drago, Chair
Graduate Research Professor of
Chemistry


I certify that I have read this study and that in my opinion it conforms to acceptable standards of scholarly presentation and is fully adequate, in scope and quality, as a dissertation for the degree of Doctor of Philosophy.


Vaneica Young, Cochair
Associate Professor of Chemistry

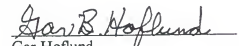
I certify that I have read this study and that in my opinion it conforms to acceptable standards of scholarly presentation and is fully adequate, in scope and quality, as a dissertation for the degree of Doctor of Philosophy.


Daniel R. Talham
Associate Professor of Chemistry

I certify that I have read this study and that in my opinion it conforms to acceptable standards of scholarly presentation and is fully adequate, in scope and quality, as a dissertation for the degree of Doctor of Philosophy.


Samuel Colgate
Professor of Chemistry

I certify that I have read this study and that in my opinion it conforms to acceptable standards of scholarly presentation and is fully adequate, in scope and quality, as a dissertation for the degree of Doctor of Philosophy.


Gar Hoflund
Professor of Chemical Engineering